In presenting the dissertation as a partial fulfillment of the requirements for an advanced degree from the Georgia Institute of Technology, I agree that the Library of the Institute shall make it available for inspection and circulation in accordance with its regulations governing materials of this type. I agree that permission to copy from, or to publish from, this dissertation may be granted by the professor under whose direction it was written, or, in his absence, by the Dean of the Graduate Division when such copying or publication is solely for scholarly purposes and does not involve potential financial gain. It is understood that any copying from, or publication of, this dissertation which involves potential financial gain will not be allowed without written permission.

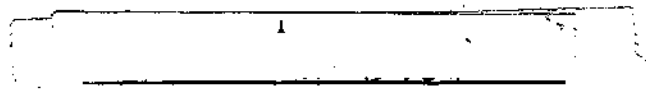

7/25/68

GENERALIZED POWER SPECTRAL DENSITY ANALYSIS WITH APPLICATION TO AIRCRAFT TAXIING PROBLEMS

A THESIS

Presented to

The Faculty of the Graduate Division

by

Robert Pang Chen

In Partial Fulfillment

of the Requirements for the Degree

Master of Science in Engineering Mechanics

Georgia Institute of Technology

June, 1969

GENERALIZED POWER SPECTRAL DENSITY ANALYSIS WITH

APPLICATION TO AIRCRAFT TAXIING PROBLEMS

Approved:

Chairman

Date approved by Chairman: May. 20, 1970

ACKNOWLEDGMENTS

The author wishes to thank Dr. Michael C. Bernard for his suggestion of the topic and his help throughout the preparation of this work. He also wishes to thank Dr. Charles E. S. Ueng and Dr. Wilton W. King for reading the manuscript.

TABLE OF CONTENTS

LIST OF ILLUSTRATIONS

SUMMARY

The dynamic responses of aircraft to random loadings have been studied in the light of power spectral methods for nearly 15 years by various researchers. H. Press and B. Mazelsky have applied the method to gust loads on airplanes in 1953. J. C. Houbolt did some pioneering work on taxiing using the same method in 1955. Their respective procedures are widely adopted by the aircraft industry.

It is generally accepted that the input spectra of either velocity components of a turbulent patch of air mass or roughness of a given runway are truly nonstationary phenomena. However, no attempt was made to treat the problems accordingly. The reasons for the lack of such studies are two-fold:

(i) The nonstationary power spectra are much more complex to handle than the stationary ones from mathematical and computational viewpoints. The interpretation of the resulting double frequency transfer functions are only understood for some simple spring-mass systems as reported by Y. K. Lin and J. B. Roberts around 1963 and 1965.

(ii) There are many unsettled questions with respect to the validity of the linear system assumption as applied to a multimodal elastic airplane which remain to be solved.

The present study presents a universal method of assessing both nonstationary and stationary roughnesses experienced by a given aircraft

during its taxiing operations. The generalized roughness spectrum is shown to be in agreement with the results obtained by Y. K. Lin, J. B. Roberts, and S. K. Srinivasan when different assumptions were made. It also reduces to the similar form for the one-runway-one-forward-speed case presently employed by the aircraft industry. The transfer function for the pitching motion was investigated in detail and it shows the trends found from the experimental results of G. J. Morris which were not explainable in the past. A logical explanation for such deviations is now available.

CHAPTER I

INTRODUCTION

The dynamic responses of airplanes to random loadings have been investigated in the light of power spectral density analysis for years. Liepmann [1],† Press and Mazelsky [2] have applied the methods to buffeting problem and gust loads, respectively, as early as 1952-3. The latter group cited the merits of power spectral analysis for gust response studies in the following manner:

> (1) Continuous turbulence can be described in analytical form by a power spectrum rather than by discrete gusts.
> (2) The load response of airplanes to continuous rough air can be evaluated.
> (3) The desirable response characteristics of an airplane for minimizing gust effects in continuous rough air will become amenable to analysis.

Equivalent statements are also applicable to airplanes taxiing on rough surfaces without reservations.

Fung [3] introduced the power spectral approach to dynamic loads problems and later [4] presented the first proven example in the aeronautical field to tackle the forcing function as a nonstationary process.* Bieber [5] and Lin [6] have also contributed to this relatively scarce branch of random processes through their works in missle structural loads and panel vibrations, respectively.

---

†Numbers in brackets refer to items in Literature Cited section.

*There are other nonstationary examples in earthquake problems by Bogodanoff, etc. [7] and Rosenbleuth, etc. [8].

Pioneering works in runway roughness studies by power spectral methods may be found in the publications of Walls, etc. [9] and Houbolt, etc. [10]. Much literature on the subject has appeared since the late 1950's and early 1960's. Most of it [11-14] was purely experimental in nature and the collected data therein did not substantiate the generally accepted assumption that the airplane is a linear time-invariant system. Other publications [15-19] concentrated on the development of roughness criteria or the quantitative evaluation of roughness spectra from various sites. It is also revealed that the increased ground speeds of current airplanes have extended the long wavelength end of the roughness spectra to approximately 500 feet and some of the existing roughness spectra are in error within this range due to the failure of removing the contamination from the slow varying gradients of the runways [17].

In view of all these unsolved difficulties, some investigators [20-23] have suggested treating the airplane taxiing problem as a deterministic process. They have obtained reliable results for some particular segments of certain given runways. However, these achievements cannot be extrapolated to formulate design criteria for new airplanes or to predict fatigue life for fleet operations owing to the fact that there is more than one runway to be considered. In order to account for the chance encounter of different runways with varying roughnesses, it is only reasonable to approach the problem in a probabilistic sense with power spectral techniques developed from random processes. The methodology for such a process is presented in Chapter II.

Since the transfer function is an integral part of the power spectral methods, and published experimental results [10-14] cited earlier have shown discrepancies with regard to the linear-time invariant system assumption, it is necessary to re-evaluate the analytical method used in the derivation of the transfer functions. The causes for the unsuccessful acquisition of a roughness amplitude and taxi speed insensitive transfer function [10,11,17] are given by:

1. The linear system assumption for the multimodal flexible structure.

2. The complex nonlinear characteristics of the landing gears.

In order to obtain a sound transfer function, a simplified airplane model with the essential degrees of freedom is developed from its linearized equations of motion. The linearization is deemed convenient in view of the fact that nonlinear systems in random vibrations have been expounded by different researchers [24-29] and standardized methods are available if needed. The derivation of the transfer functions is presented in Chapter III.

A more imminent need in the airplane taxiing problem, therefore, seems to be the development of a methodology that will account for the different levels of measured roughnesses in their existing format (i.e., power spectral densities or profile elevations together with a rational probability distribution for the arrival times of taxi events for the airplanes from past utilization records or prospective requirements. This information will require the treatment of the roughness inputs as a piece-wise stationary process with the current

stationary one-runway-one-taxi-speed analysis and any deterministic roughness approach included as special cases. It will also require the elimination of the pitfalls attributable to power spectral analysis, namely, (i) the inability to discern between a few high bumps and many low bumps of the same wavelength, (ii) the failure to indicate when the runway needs repair, (iii) no consideration of the juxtaposition or phasing of the individual bumps or depressions, (iv) the interactions between different roughnesses in a series of taxi events, (v) the landing roll-out and take-off run phases of airplane ground operations which are not amenable to constant speed analysis.

Thus, the task of establishing the aforementioned methodology is two-fold.

1. To find a realistic model that will accommodate the piecewise stationary roughnesses.

2. To ensure the direct incorporation of existing roughness power spectral densities into the model.

Chapter II is devoted to the detailed development of such a composite roughness input which may be described briefly as a sequence of nonstationary pulses. It must be pointed out at the beginning that treating the airplane taxiing problem as a nonstationary process is not without precedence [4] and the actual response of a vibratory system under stationary excitation will be nonstationary if one considers the transient part of the response as shown by Caughey and Stumpf [30], and Lin [6]. Kur'yanov [31] has suggested that it is often necessary, along with the analysis of stationary random processes, to perform a

frequency analysis of certain nonstationary processes such as might be termed "pseudostationary." It is therefore only fitting to treat both the excitation roughnesses and airplane responses as nonstationary processes, since the composite roughnesses are only piece-wise stationary, or pseudostationary. In the light of the above reasoning, it is logical to anticipate that the composite roughness input is a train of pulselike power spectral density related quantities, say autocorrelation functions, with random strength and shape for each constituent pulse obtained from the specific runway where the taxi event took place. It is interesting to find that Lin [32-34] has published a series of papers on nonstationary shot noise and the last [34] of which may be modified to describe exactly the process needed to specify the composite roughness input. The development for Stationary Strength and Nonhomogeneous Poisson Arrival Rate Pulses and Nonstationary Strength and Time Correlated Pulses of Chapter II follows closely Lin's work [34]. Other sections therein are either explanatory remarks on the justification of employing that particular random process in view of its resemblance to the physical phenomenon, or comparisons of the generalized results with published works and the limiting case of one-runway-one-speed taxiing.

CHAPTER II

ROUGHNESS INPUTS TREATED AS A SPECIAL CLASS OF NONSTATIONARY RANDOM PROCESSES

Philosophical Background

The methodology of representing a probable set of runway and/or taxiway roughnesses ranging from well-maintained airports to unprepared front-line airstrips as nonstationary random pulses may be understood by some insights arising from the actual aircraft operations and their omnipresent environmental disturbances. The philosophy that allows such a treatment is exemplified by a typical time history of the wing root bending moment of a conventional airplane as depicted in Figure 2.1.

Figure 2.1 illustrates all the significant load levels any aircraft may encounter repeatedly throughout its service life. The time axis has been extended schematically for the durations of disturbed motions either in air or on ground to demonstrate the inherent pulse-like randomness in the response. It is further stipulated that the atmospheric gust responses contribute to the total fatigue damage of the airframe only in a fashion described as G-A-G (ground-air-ground) cycles; hence, it is conveniently permissible to assume all the time periods other than ground operations quiescent.*

---

*See Houbolt [35] in employing the same argument for gust response studies.

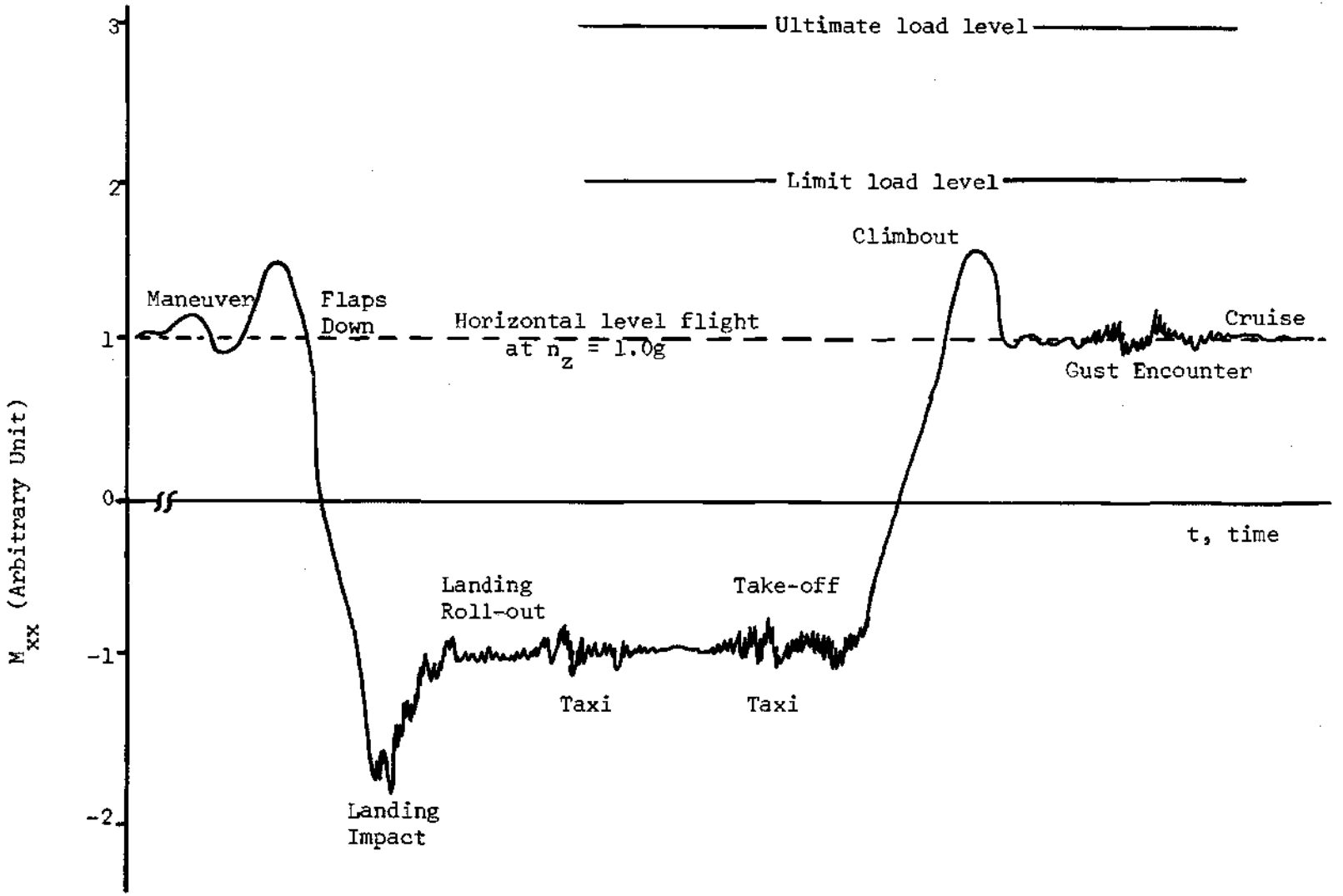

Figure 2.1 A Typical Aircraft Wing Bending Moment Record

With the removal of the airborne disturbances and the aerodynamic or velocity sensitive phases of ground operations (i.e., atmospheric gust response, landing impact, high/low speed take-off and landing roll-out), the response time history of Figure 2.1 is reduced to a sequence of time history segments with the elapsed air times preserved between the neighboring constant speed taxies and the above cited disturbances replaced by undisturbed time segments of corresponding lengths. The simplicity of this transformed sequential constant speed taxi response realization is shown in Figure 2.2.

The excitation process that generates such a response time history can be deduced from the same argument. If the geographical elevations of the runway/taxiway sites and their long wavelength unevenness resulting from the underlying topological structures of the subsoils are removed, the roughness profiles that correspond to the sample response realization of Figure 2.2 may be obtained by substituting the segmented response time histories by the respective roughnesses measured from their individual mean profiles. A representative sequence of roughnesses corresponding to the response time history of Figure 2.2 is shown in Figure 2.3. It must be remembered that in converting the runway/taxiway horizontal distances used for each constituent roughness profile, an arbitrary contracting or expanding scale factor, which is equivalent to the reciprocal of the particular constant taxi speed of a given segment, was employed. This linear transformation can be expressed as

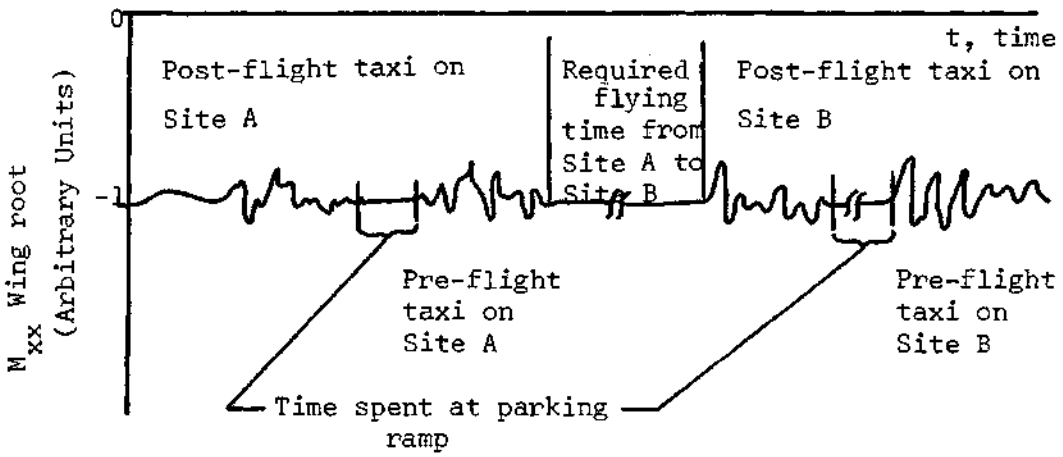

Figure 2.2 A Sequence of Taxi Events

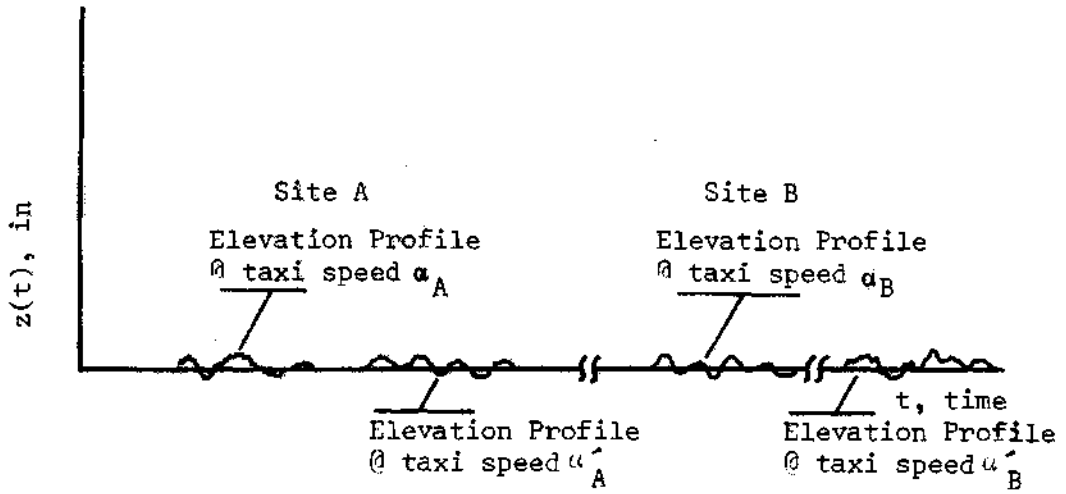

Figure 2.3 Ground Roughness Time History Corresponding to the Above Taxi Events

$$\{D_i\} = \{D(\Delta t_i)\} = \{V_i T_i\} \tag{2.1}$$

where V_i is, in a strict sense, a random variable within a given range ($v_i \geq 0$). D_i and T_i are respectively random variables depicting the horizontal distance traveled and the incremental taxi time within a given time segment for the constant speed taxies (i.e., $T_i \varepsilon \Delta t_i$).

In anticipation of using the random pulses representation, and with the awareness of the complex, if not unwieldy, notations required, it will be advantageous to relax the restriction on V_i being random. From an engineering viewpoint, the range of V_i and D_i are fairly limited for existing airplanes and airports. It is conservative to say that V_i is in the interval (10 kts, 100 kts) and D_i is in the interval (2,000 ft., 10,000 ft.). The most adverse combination of these values gives the segmented taxi time Δt_i in the interval (20 seconds, 600 seconds). Bearing in mind that the service life of the present generation of airplanes is in the order of 5,000 hours for a fighter and 50,000 hours for a commercial airliner, and allowing the shortest service life (5,000 hours) to be the total time of a given realization, it is found that the longest taxi time (600 seconds) per flight is a mere 1/30,000th of the total time. It is therefore insignificant to consider the contracting or expanding of a particular constant speed taxi segment. It is also found that the flying time for a short-haul flight and an intercontinental flight is 35 minutes and 10 hours, respectively. Thus, the criterion for the spacing of the composite roughness time history similar to that of Figure 2.3 is established, since the spacing will be

the flight time. A typical realization experienced by a given aircraft with the composite roughness of the taxi segments stretched is illustrated with the range of the spacings (i.e., the flight times) shown in Figure 2.4.

Generation of Composite Roughnesses Time Histories

The task of obtaining a complete description of the composite roughnesses will be materialized, if the vast amount of the existing power spectral density (PSD) data on runway/taxiway roughnesses together with the utilization and mission profile of a given aircraft and/or types of aircraft are furnished by the procuring governmental agency or the commercial airline operator to the airframe manufacturers for the analysis pertaining to the design of a prospective aircraft. The same information may also be derived from a systematic compilation of existing fleet operations in the manner of monitoring closely the daily utilization of each aircraft within the fleet of different types of airplanes for an extensive observation period. The procedure will be expounded fully with the schematic diagram in Figure 2.5 for an ensemble of airplanes and/or types of airplanes operating on assorted roughnesses for a finite time period. Each realization is generated in the same fashion as that of Figure 2.4 with the exception that each roughness is contracted to a point on the time axis and the height of each stroke represents the relative roughness amplitude, and the superscript (i) denotes a member aircraft in a fleet or a given type of aircraft in existence which resembles the new aircraft in their operational characteristics.

Range of variations for w_j, Δt_j, T_j, and T_n:

$$35 \text{ min} \leq w_j \leq 600 \text{ min}$$

$$25 \text{ sec} \leq \Delta t_j \leq 600 \text{ sec}$$

$$5{,}000 \text{ hr} \leq T_n \leq 50{,}000 \text{ hr}$$

$$0 < T_1 < T_2 < T_3 < \ldots T_n$$

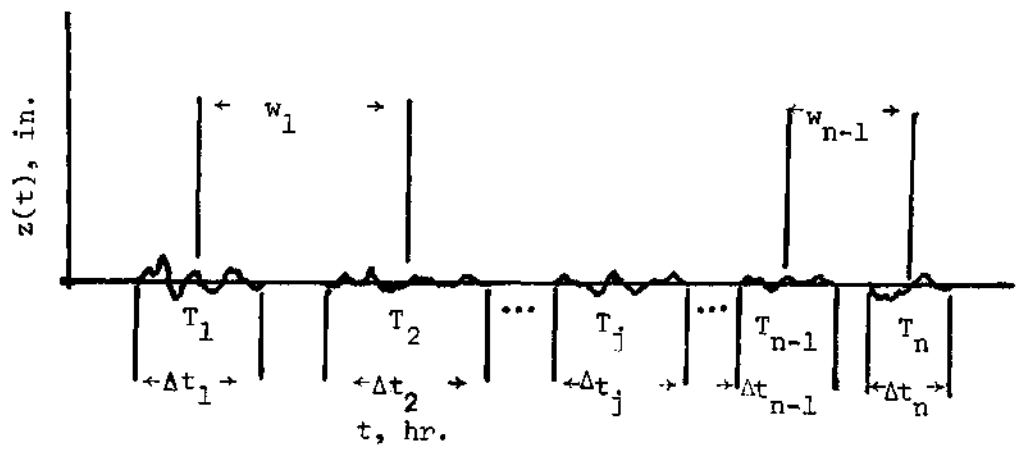

Figure 2.4 A Typical Composite of Roughnesses with Flying Time Spacing

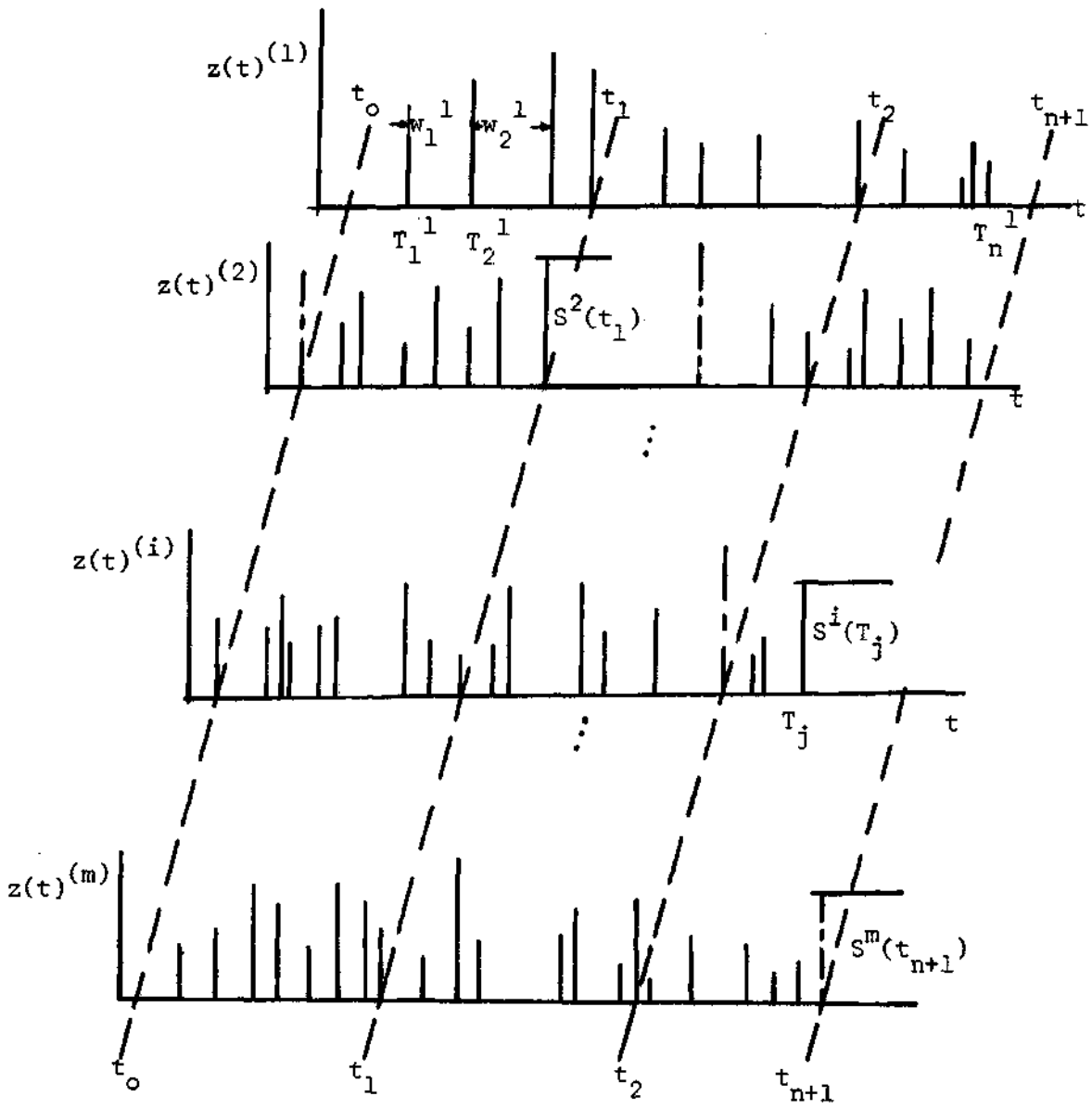

——— = $S^i(T_j) = S_j^{(i)}(t)$ of Equation (2.8)

——·—— = $S^m(t_{n+1})$ = Zero strength, m=1,2...i...

Figure 2.5 An Ensemble of Composite Roughness Records

From the preceding paragraph, it is understood that the power spectral densities of the roughnesses of the probable taxi sites are given a priori. It is further postulated that all the roughness power spectral densities are expressed in spacial frequencies, that is,

$$\Omega = \omega / V_{TAXI} \tag{2.2}$$

Hence, the Wiener-Khintchine relations for a given runway/taxiway become:

$$\Phi_{zz}(\Omega) = \frac{1}{2\pi} \int_{-\infty}^{\infty} R_{zz}(\lambda) e^{-j\Omega\lambda} d\lambda \tag{2.3a}$$

$$R_{zz}(\lambda) = \int_{-\infty}^{\infty} \Phi_{zz}(\Omega) e^{j\Omega\lambda} d\Omega \tag{2.3b}$$

where λ is the lag distance and may be expressed as

$$\lambda = V_{TAXI} \cdot \tau \tag{2.4}$$

with V_{TAXI} equal to a given constant α and τ being the dummy variable for the lag time of the temporal power spectral density, or to be more specific,

$$\Phi_{zz}(\omega)\Big|_{V_{TAXI}=\alpha} = \frac{1}{2\pi} \int_{-\infty}^{\infty} R_{zz}(\tau)\Big|_{V_{TAXI}=\alpha} e^{-j\omega\tau} d\tau \tag{2.5a}$$

$$R_{zz}(\tau)\Big|_{V_{TAXI}=\alpha} = \int_{-\infty}^{\infty} \Phi_{zz}(\omega)\Big|_{V_{TAXI}=\alpha} e^{j\omega\tau} d\omega \qquad (2.5b)$$

A sample roughness spectrum and its autocorrelation function is shown in Figure 2.6.

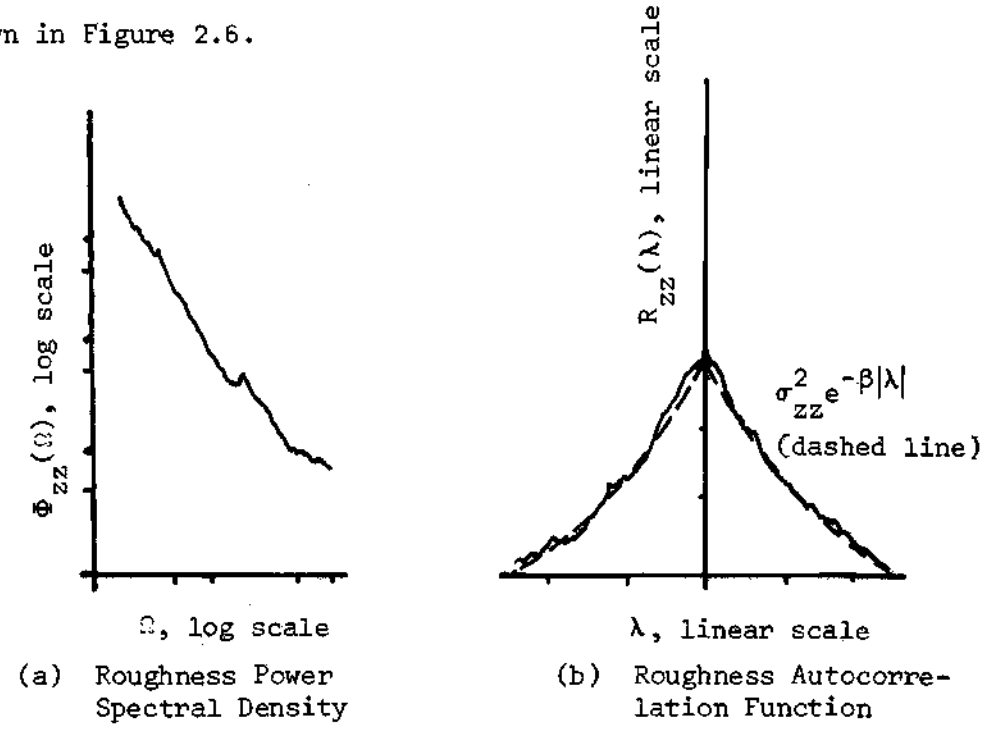

(a) Roughness Power Spectral Density

(b) Roughness Autocorrelation Function

Figure 2.6 A Typical Roughness Power Spectral Density and Its Autocorrelation Function

Most of the roughness autocorrelations can be approximated by

$$R_{zz}(\lambda) = \sigma^2_{zz} e^{-\beta|\lambda|}, \quad \sigma^2_{zz} > 0, \quad \beta > 0 \qquad (2.6)$$

where β is a given shaping factor, and σ^2_{zz} is the roughness variance of the given runway. From Equations (2.4) and (2.6), it is clear that for a given runway at a given taxi speed α

$$R_{zz}(\lambda) = \sigma_{zz}^2 e^{-\beta|\lambda|} = \sigma_{zz}^2 e^{-\alpha\beta|\tau|} = R_{zz}(\tau)\Big|_{V_{TAXI}=\alpha} \tag{2.7}$$

At this stage, two quantities will be defined to fulfill the formulation of the composite roughness description of a given realization. Let

$$S_j^{(i)}(t) = \sigma_{zz}^{(i)}(T_j) e^{-\frac{\alpha_j\beta_j}{2}|t-T_j^{(i)}|} = \sigma_{zz}^{(i)}(T_j) e^{-\gamma_j|t-T_j^{(i)}|}, \tag{2.8}$$

where

$$t_o \leq T_j^{(i)} \leq t_{n+1}, \quad i=1,2,3\cdots m, \quad j=1,2,3\cdots n$$

$S_j^{(i)}(t)$ equals the roughness strength function for a time interval Δt_j

$n(t)$ equals the arrival rate of taxi events and may be represented by the following integral

$$n = \int_{t_j}^{t_k} n(\tau)d\tau, \quad t_o \leq t_j < t_k \leq t_{n+1} \tag{2.9}$$

where n is the number of taxi events in the time interval (t_j, t_k). It is noted that t_o and t_{n+1} is chosen without any loss of generality as the first and last taxi time of an ensemble (see Figure 2.5). If zero roughness strength is permitted for the null event in which no taxi operation has been encountered, then t_o and t_{n+1} can take on values of $(-\infty)$ and $(+\infty)$, respectively.

Source of Nonstationarity in Arrival Rate

With the roughness strength function and the arrival rate of taxi events thus defined, it is revealed that a given composite roughness record is a truly nonstationary phenomenon. The nonstationarity arises from the time dependent expressions of Equations (2.8) and (2.9) for the roughness strength function and the arrival rate of taxi events, respectively.

A more than cursory understanding of the nonstationary behavior of the roughness strength function and the arrival rate of taxi events may be obtained by investigating the underlying probability distributions of the two quantities. The physical construction of a sample composite roughness as shown in Figure 2.4 will justify the assumptions required for the definition of the distributions. It is convenient to start with the distribution of the arrival rate of taxi events, and it is assumed that:

(i) The number of taxi events occurring in any finite collection of non-overlapping time intervals Δt_j, $j=0,1,2\cdots n+1$ form a set of independent random variables $\{N\}$, and $|\omega: N(\omega) = n|$ exists where n has the same meaning as expressed in Equation (2.9).

(ii) For a sufficiently small time interval

$$\Delta t_j \xrightarrow{L} \varepsilon \quad \Delta t_j = \delta t_j, \quad j=0\cdots n+1,$$

the probability of one taxi event encountered is given by $n(t_j)\,\delta t_j$, where $n(t_j)$ is identical to the $n(\tau)$ of Equation (2.9).

(iii) If δt_j is sufficiently small, the probability that more than one taxi event will take place in the interval is small (i.e., of order $O(\delta t_j)$. This is obvious from the fact that all known flying time (W_j) is of the order O(min) rather than O(sec).

If {N} denotes n of Equation (2.9) with $t_j = t_o$ and $t_k = t \leq t_{n+1}$, then the probability of having exactly n taxi events in the interval (t_o,t) can be expressed as

$$P_{\{N\}}(n,t) = \frac{1}{n!}\left[\int_{t_o}^{t} n(\tau)d\tau\right]^n e^{\left[\int_{t_o}^{t} n(\tau)d\tau\right]} \qquad (2.10)$$

This result is obtained by Laning and Battin [36] with the assumptions (i) through (iii) cast in the nomenclatures of random electron emission from the filament of a vacuum tube. It is seen from Equations (2.9) and (2.10) that the arrival rate of taxi events is a continuous function of time in the interval (t_o,t_{n+1}) and for two given times, say t_1 and t_2 in Figure 2.5, n(t) will take on different values, hence it is nonstationary. Lin [34] has applied this nonhomogeneous Poisson distribution and a stationary (constant) strength to study the nonstationary response of a linear system subjected to sequences of randolm pulses. It is the method presented therein together with the modification of allowing the strength to be simultaneously time dependent as shown by Equation (2.8) that leads to the derivation of a rational nonstationary roughness power spectral density.

Before the nonstationarity of the roughness strength function is demonstrated, it is fruitful to gain more insight on the selection of a

nonhomogeneous arrival rate instead of the homogeneous (constant) arrival rate. The difference will be clear by observing two sequences of roughness strength functions presented in Figure 2.7.

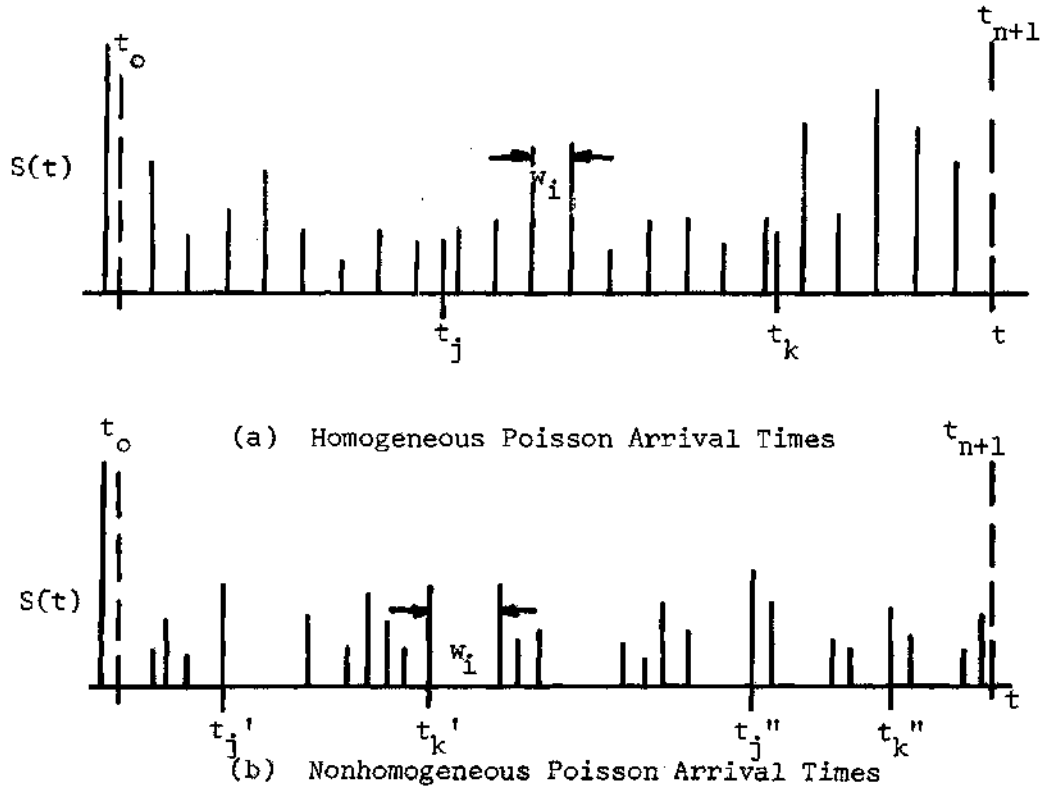

Figure 2.7 A Comparison of Arrival Rates

Figure 2.7(a) has the following properties:

(i) The number of taxi events is uniformly distributed in the interval (t_o, t_{n+1}), hence

$$n(t) = \frac{N}{t_{n+1} - t_o} = \nu$$

where N is the total number of taxi events in the interval (t_o, t_{n+1}).

(ii) The number of taxi events in the interval (t_j, t_k) is given by

$$n(t_j,t_k) = \nu \int_{t_j}^{t_k} d\tau = \nu(t_k - t_j) = \nu \int_{t_j+h}^{t_{k+h}} d\tau = n(t_j+h, t_k+h)$$

for $t_o \le t_j < t_k \le t_{n+1}$, $h \ge 0$.

Figure 2.7b has the following properties:

$$\text{(i)} \quad n(t_j',t_k') = \int_{t_j'}^{t_k'} \nu(\tau)d\tau \quad \text{for} \quad t_o \le t_j' < t_k' \le t_{n+1}$$

and

$$n(t_j'',t_k'') = \int_{t_j''}^{t_k''} \nu(\tau)d\tau \quad \text{for} \quad t_o \le t_j'' < t_k'' \le t_{n+1}$$

$$\text{(ii)} \quad n(t_j',t_k') = n(t_j'',t_k'') \text{ if and only if } t_j' = t_j'',\ t_k' = t_k''.$$

It can be easily seen that the flying times (W_j) would not follow such a regular pattern as shown in Figure 2.7(a) even if the given realization belonged to a scheduled commercial airline operation. There are always chance delays due to unforeseen weather conditions or other human factors involved in any predetermined flight operations, and deterministic scheduling may be considered highly improbable if not impossible. A probabilistically realizable record therefore must contain the inherent nonhomogeneous pattern as shown in Figure 2.7(b).

Source of Nonstationarity in Roughness Strength Function

The nonstationarity of the roughness strength function is studied by different goals of analyses. The approaches to tackle the individual categories are delineated in the following subparagraphs.

(a) Design Criteria Development for New Aircraft

The requirement for this analysis is pertaining to the acquisition of a representative composite roughness record which may approximately encompass the totality of all possible taxi site roughnesses accessible to all types of airplanes whose operational characteristics are being incorporated in the new design. The method of assessing such an "averaged" record is equivalent to calculating the instantaneous ensemble average over the finite collection of composite roughnesses of available types of airplanes. Let $\{Z^{(i)}(t)\}$, i=1,2,3$\cdots$m be the composite roughness records of "m" types of existing aircraft as shown in Figure 2.5. It is now asserted that m is fairly large such that the mathematical expectation of the roughness strength may be calculated as:

$$E[S(t)] = \lim_{m\to\infty} \frac{1}{m} \int_0^{\infty} \sum_{i=1}^{m} sp_S^{(i)}(s,t)ds \qquad (2.11a)$$

$$\approx \lim_{m\to\infty} \frac{1}{m} \sum_{i=1}^{m} \int_0^{\infty} sp_S^{(i)}(s,t)ds$$

$$= \lim_{m\to\infty} \frac{1}{m} \sum_{i=1}^{m} \varepsilon[S^{(i)}(t)] \quad \text{for } i=1,2\cdots m \text{ and } t_o \le t \le t_{n+1}$$

where $p_S^{(i)}(s,t)$ is the time dependent probability density function for the magnitude of the roughness strength functions for aircraft type "i". It must be remembered again that the approximation in Equation (2.11a) is meaningful if, and only if, the zero roughness strength for a null event of no taxi operation at time t is permitted.

(b) Fatigue Life Evaluation for Fleet Operations

The main feature for this analysis is that the ensemble of composite roughness records is taken from one type of aircraft and the mathematical expectation can be reduced from Equation (2.11a) in the following manner:

$$\varepsilon[S(t)] = \int_0^\infty s p_S(s,t) ds \qquad (2.11b)$$

where the superscript (i) is dropped from the probability density function due to the fact that the type is unique.

It is interesting to note that both of the expected roughness strength functions as expressed in Equations (2.11a) and (2.11b) are still time dependent. This is expected since the probability density function for the magnitudes of the roughness strength functions are time dependent, or nonstationary. In view of this and observing the fact that the roughness strength functions as defined by Equation (2.8) does contain random variables α_i, β_i to denote a taxi event on a given runway at a given speed, it is felt that to assume the magnitudes of the roughness strength functions to be purely random will not deviate much from the physical reality. If this assumption is employed, then

the higher order density functions may be expressed by the product of first order densities as shown in the following:

$$p_n(s,t,\cdots t_n) = \prod_{i=1}^{n} p_1(s,t_i) \qquad (2.12)$$

for $t_o < t_i < t_{n+1}$, $i=1,2,3\cdots n$.

Single Record Representation of an Ensemble

With the nonstationarities in both the arrival rate of taxi events and the roughness strength functions established, it is now possible to replace the ensemble of composite roughness records by a single expected composite roughness record for either analysis (a) or analysis (b). Figure 2.8 gives the scheme for the collapsing of the ensemble. Analysis (b) consists of averaging over only one type, say type (i), by using Equation (2.11b). It is depicted by the dashed box or sequence AB, whereas analysis (a) requires a further averaging over all the $\varepsilon[Z^{(i)}(t)]$'s by employing Equation (2.11a), or sequence ABC. Figure 2.9 shows a typical expected composite roughness record for each analysis. The shapes of the roughness strength function are enlarged in order to introduce detailed explanations on the actual evaluation of Equations (2.11a) and (2.11b). It is understood from Equation (2.11a) that to obtain the expected roughness strength function $E[Z(t)]$ at a given time $t = t_j$, the calculation involves a mere averaging over the types. Therefore Equation (2.11b) will suffice to serve as a sample. Equation (2.11b) states that

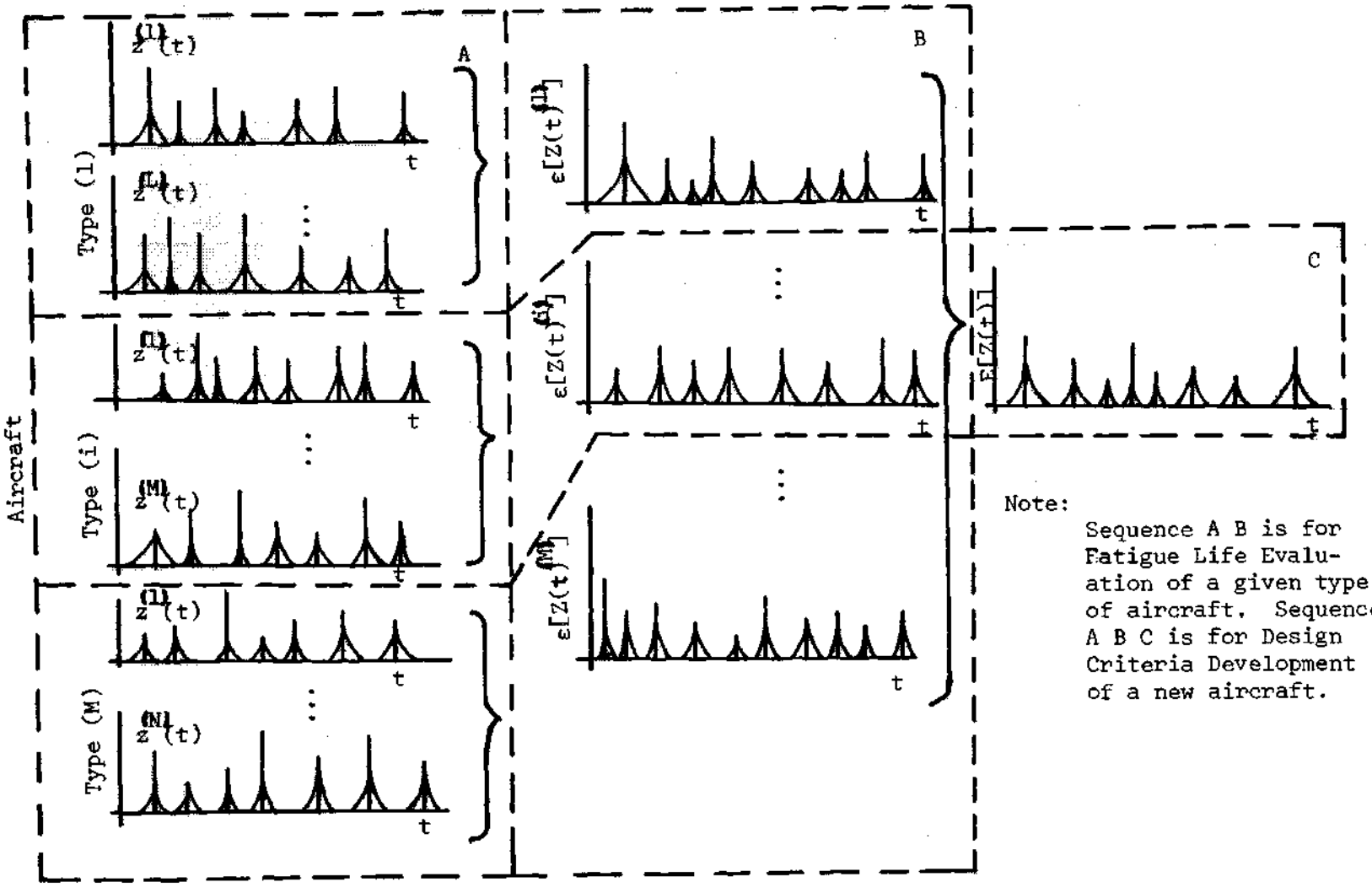

Figure 2.8 Schematic Diagram for the Collapsing of Ensembles

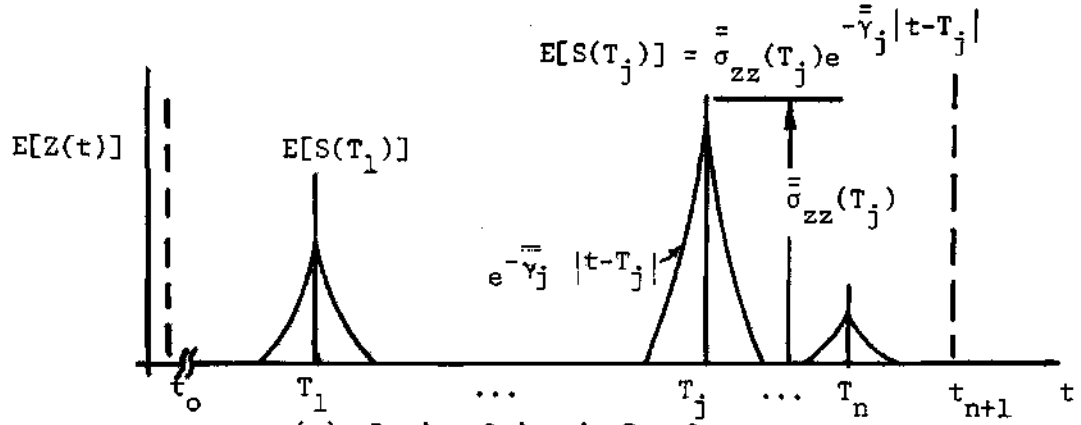

(a) Design Criteria Development

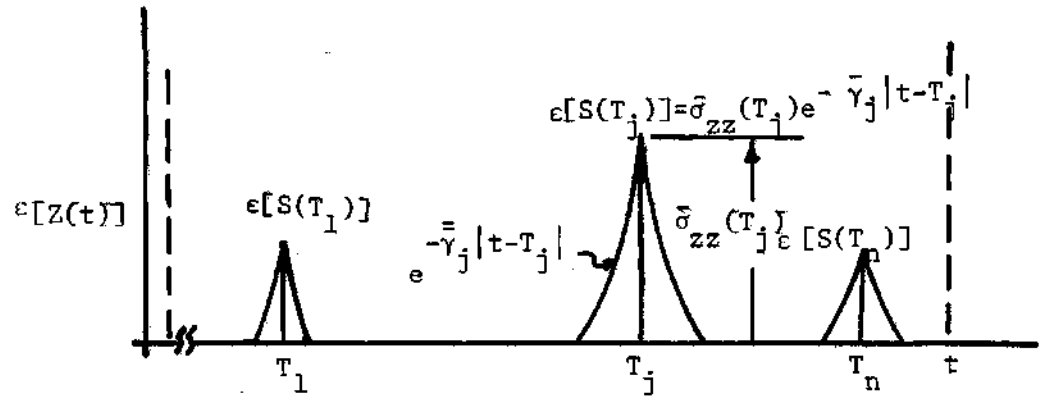

(b) Fleet Fatigue Evaluation

Figure 2.9 Typical Expected Composite Roughness Records

$$\varepsilon[S(t)] = \int_0^\infty s p_S(s,t)ds \qquad \text{(2.11b repeat)}$$

with the understanding that "s" is the magnitude of the roughness strength function at time "t". If the equation for S(t) is represented by Equation (2.8) with the subscript (i) suppressed, it will have the form as shown below

$$S_j(t) = \sigma_{zz}(T_j)e^{-\gamma_j|t-T_j|} \qquad \text{(2.8 repeat)}$$

Then it is obvious that the instantaneous magnitude is composed of two parts $\sigma_{zz}(T_j)$ and $e^{-\gamma_j|t-T_j|}$. The former is the σ_{zz} value of the roughness of a given runway for the taxi event at time T_j, the latter is a taxi speed-sensitive shaping function, if one recalls that $\gamma_j = \alpha_j\beta_j/2$ and α_j is the given taxi speed at time T_j. Hence the abbreviated probability density function $p_S(s,t)$ may be expressed in full as

$$p_S(s,t) = p(\sigma_{zz},\gamma,T_j) \quad \text{for } t = T_j \qquad (2.13)$$

If this bivariate density function is applied to Equation (2.11b), the expected roughness at time T_j will be

$$\varepsilon[S(T_j)] = \int_0^\infty\int \sigma_{zz}(T_j)e^{-\gamma|t-T_j|}p(\sigma_{zz},\gamma,T_j)d\sigma_{zz}d\gamma \qquad (2.14a)$$

However, it is noted that $\sigma_{zz}(T_j)$ is only the positive square root of the given roughness at time T_j (i.e., $\sigma_{zz}(T_j) = \sqrt{R_{zz_{T_j}}(0)}$). $R_{zz_{T_j}}(0)$ is the area under the roughness power spectral density of the runway to be traversed at time T_j. $R_{zz_{T_j}}(0)$ is a quantity independent of taxi speed as shown by setting $\tau = 0$ in Equation (2.4) to obtain $\lambda = 0$ for any taxi speed, V_{TAXI}. With the taxi speed-independent nature of $\sigma_{zz}(T_j)$ or $R_{zz_{T_j}}(0)$ established, Equation (2.13) may be written as

$$p_S(s,t) = p(\sigma_{zz},\gamma,t) = p(\sigma_{zz},t)p(\gamma,t) \tag{2.15}$$

This allows Equation (2.14a) to be expressed as

$$\varepsilon[S(T_j)] = \int_0^\infty\int \sigma_{zz}(T_j)e^{-\gamma\,|t-T_j|}p(\sigma_{zz},\gamma,T_j)d\sigma_{zz}d\gamma \tag{2.14b}$$

$$= \int_0^\infty \sigma_{zz}(T_j)p(\sigma_{zz},T_j)d\sigma_{zz} \cdot \int_0^\infty e^{-\gamma\,|t-T_j|}p(\gamma,T_j)d\gamma$$

$$= \bar{\sigma}_{zz}(T_j)e^{-\bar{\gamma}_j|t-T_j|}$$

The univariate density functions appearing in Equation (2.14b) may be obtained by the classical frequency representation for the probability distribution at time T_j from an ensemble of composite roughness records. A schematic diagram for evaluating $p(\sigma_{zz},T_j)$ is shown in Figure 2.10. It must be reminded that $\bar{\sigma}_{zz}(T_j)$ and $\bar{\gamma}_j$ as appeared in the last equality of equation (2.14b) are merely the expected values of $\sigma_{zz}(T_j)$ and $\gamma(T_j)$ respectively. Their evaluations may easily be obtained by the standard averaging procedure (i.e. calculating the centroid of Figure 2.10(b)).

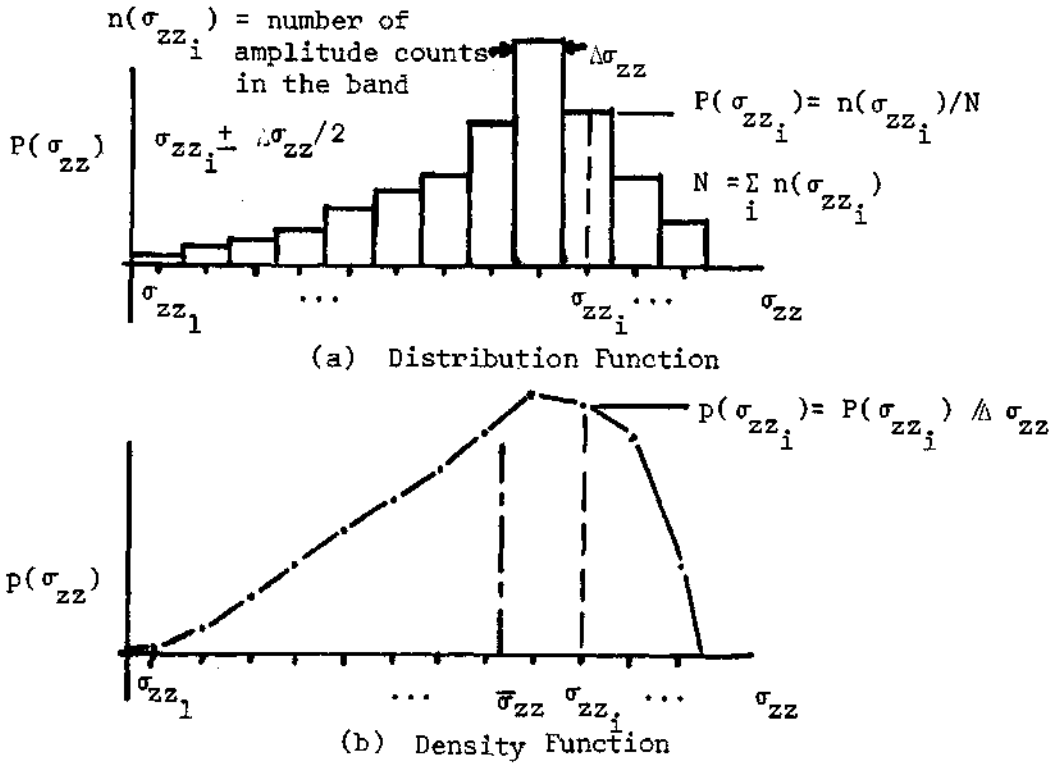

Figure 2.10 Amplitude Distribution from Frequency Counts

Stationary Strength and Nonhomogeneous Poisson Arrival Rate Pulses

Let $\varepsilon[Z(t)] = X(t)$ denote the sequence of random pulses that generates the expected composite roughness input, $\bar{\sigma}_{zz}(T_j) = \bar{\sigma}_{zz_j}$ be the purely random strength of the random pulses, and

$e^{-\bar{\gamma}_j|t-T_j|} = w_j(t-T_j)$ be the deterministic shaping functions. Then the expected composite roughness input process may be represented in the form

$$X(t) = \sum_{j=1}^{N(t)} \bar{\sigma}_{zz_j} w_j(t-T_j) \tag{2.16}$$

$$= \sum_{j=1}^{N(t_{n+1})} \bar{\sigma}_{zz_j} w_j(t-T_j)$$

where N(t) is a nonhomogeneous Poisson counting process which obeys (i) and (ii) of the discussion for Figure 2.7b and may be changed to $N(t_{n+1})$ if one remembers that $w_j(t-T_j) = 0$ for $t < T_j$ if $w_j(t-T_j)$ belongs to a physically realizable system. $\bar{\sigma}_{zz_j}$ is purely random in the sense of Equation (2.12) or $E[\bar{\sigma}_{zz_j} \bar{\sigma}_{zz_k}] = E[\bar{\sigma}_{zz_j}]E[\bar{\sigma}_{zz_k}]$ and $p(\bar{\sigma}_{zz},T_j) = p(\bar{\sigma}_{zz})$ for $j=1,2,3\cdots n$ if $p(\bar{\sigma}_{zz})$ is obtained in the following manner:

$$p(\bar{\sigma}_{zz}) = \underset{\substack{t_{n+1}\to\infty \\ t_o \to 0}}{L} \frac{1}{t_{n+1} - t_o} \int_{t_o}^{t_{n+1}} p(\bar{\sigma}_{zz},t)dt \tag{2.17}$$

$$\approx \underset{n\to\infty}{L} \frac{1}{n} \sum_{j=1}^{n} p(\bar{\sigma}_{zz},T_j)$$

It must be reminded at this stage that X(t), the expected composite roughness input process, is defined in the interval (t_o,t_{n+1}) and may be represented by a single time history, such as either Figure 2.9a or Figure 2.9b. The latter was used in deriving Equation (2.16) for sheer convenience. The extension to X(t) = E[Z(t)] is immediately obvious if one remembers the relation between $\varepsilon[S^{(i)}(t)]$ and E[S(t)] as expressed by the last equality in Equation (2.11a).

The preliminary quantities are thus totally defined within the framework of available roughness data in power spectral density form and existing aircraft operational procedures with no sacrifice in mathematical rigor. The probabilistic structure of the expected composite roughness input, X(t), which eventually leads to the generalized roughness input power spectral density may be revealed by the method of characteristic functional as proposed by Lin [34] Roberts [37] and Srinivasan, etc. [38]. The characteristic functional is defined as

$$M_{\{X\}}[\theta(t)] = E\{e^{i\int_{t_o}^{t_{n+1}} \theta(t)X(t)dt}\} \tag{2.18}$$

Substituting the second equality in Equation (2.16) into Equation (2.18),

$$M_{\{X\}}[\theta(t)] = E\{e^{i\int_{t_o}^{t_{n+1}} \theta(t) \sum_{j=1}^{N(t_{n+1})} \bar{\sigma}_{zz_j} w_j(t-T_j)dt}\} \tag{2.19}$$

$$= E\{E[e^{i\int_{t_o}^{t_{n+1}} \theta(t) \sum_{j=1}^{N(t_{n+1})} \bar{\sigma}_{zz_j} w_j(t-T_j)dt \,|\, N(t_{n+1})]\}$$

$$= \sum_{n=0}^{\infty} P_{\{N\}}(n,t_{n+1})E[e^{i\int_{t_o}^{t_{n+1}} \theta(t) \sum_{j=1}^{n} \bar{\sigma}_{zz_j} w_j(t-T_j)dt}]$$

where $E[\cdot|\cdot]$ denotes a conditional expectation, and the third equality is obtained by the relation $E\{E[X|Y]\} = E\{X\}$ (see Papoulis [39]. Remembering that $N(t_{n+1})$ is Poisson (i.e., the pulse arrival times

T_j's are independent) and the strength $\bar{\sigma}_{zz_j}$'s are independent in the sense of Equation (2.12), then

$$E[e^{i\int_{t_o}^{t_{n+1}}\theta(t)\sum_{j=1}^{n}\bar{\sigma}_{zz_j}w_j(t-T_j)dt}] \tag{2.20}$$

$$= E[\prod_{j=1}^{n} e^{i\int_{t_o}^{t_{n+1}}\theta(t)\bar{\sigma}_{zz_j}w_j(t-T_j)dt}]$$

$$= \prod_{j=1}^{n} E[e^{i\int_{t_o}^{t_{n+1}}\theta(t)\bar{\sigma}_{zz_j}w_j(t-T_j)dt}]$$

The second equality follows from $E[XY] = E[X]E[Y]$; since the X's and Y's are independent. A typical term in the last line of Equation (2.20) may be expanded as

$$E[e^{i\int_{t_o}^{t_{n+1}}\theta(t)\bar{\sigma}_{zz_j}w_j(t-T_j)dt}] \tag{2.21}$$

$$= 1 + E[\sum_{m=1}^{\infty}\frac{i^m}{m!}(\int_{t_o}^{t_{n+1}}\theta(t)\bar{\sigma}_{zz_j}w_j(t-T_j)dt)^m]$$

$$= 1 + \alpha$$

Since T_j's obey a nonhomogeneous Poisson distribution and $\bar{\sigma}_{zz_j}$'s are

mutually independent with a common density function as shown in Equation (2.17), then

$$\alpha = \sum_{m=1}^{\infty} \frac{i^m}{m!} \int_0^{\infty} \bar{\sigma}_{zz}^m p(\bar{\sigma}_{zz}) d\bar{\sigma}_{zz} \underbrace{\int_{t_o}^{t_{n+1}} \cdots \int}_{m\text{-fold}} \theta(t_1)\cdots\theta(t_m) \frac{\int_{t_o}^{t_{n+1}} w(t_1-\tau)\cdots w(t_m-\tau) n(\tau) d\tau}{\int_{t}^{t_{n+1}} n(\tau) d\tau} dt_1 \cdots dt_m \tag{2.22}$$

where $\sigma_{zz_j} = \sigma_{zz}$, $w_j(t-T_j) = w(t_m-\tau)$ for $j,m = 1,2,\ldots,n$, where $n(\tau)$ is the expected nonstationary arrival rate as shown in Equation (2.9) and must be obtained from the given record (e.g., Figure 2.9(a) or (b)). It is noted from Equation (2.22) that α is independent of T_j, and by substituting Equation (2.21) into Equation (2.20) and using the result in the last equality of Equation (2.19), the following is obtained

$$M_{\{X\}}[\theta(t)] = \sum_{n=0}^{\infty} P_{\{N\}}(n, t_{n+1})(1+\alpha)^n \tag{2.23}$$

$$= \sum_{n=0}^{\infty} \frac{1}{n!} [\int_{t_o}^{t_{n+1}} n(\tau) d\tau]^n e^{-\int_{t_o}^{t_{n+1}} n(\tau) d\tau} (1+\alpha)^n$$

$$= e^{\alpha \int_{t_o}^{t_{n+1}} n(\tau) d\tau}$$

The log-characteristic functional of X(t) is

$$\ell n\, M_{\{X\}}[\theta(t)] = \alpha \int_{t_o}^{t_{n+1}} n(\tau)d\tau \qquad (2.24)$$

$$= \sum_{m=1}^{\infty} \frac{i^m}{m!} E[\bar{\sigma}_{zz}^{\,m}] \int_{t_o}^{t_{n+1}} \cdots \int_{m\text{-fold}} \theta(t_1)\cdots\theta(t_m)$$

$$[\int_{t_o}^{t_{n+1}} w(t_1-\tau) \cdots w(t_m-\tau)n(\tau)d\tau]dt_1\cdots dt_m$$

If one recalls the log-characteristic expansion in terms of the cumulant functions of X(t)

$$\ell n\, M_{\{X\}}[\theta(t)] = \sum_{m=1}^{\infty} \frac{i^m}{m!} \int_{t_o}^{t_{n+1}} \cdots \int_{m\text{-fold}} \kappa[X(t_1)\cdots X(t_m)]\theta(t_1)\cdots\theta(t_m) \qquad (2.25)$$

$$dt_1\cdots dt_m$$

It is obvious that

$$\kappa[X(t_1)\cdots X(t_m)] = E[\bar{\sigma}_{zz}^{\,m}] \int_{t_o}^{\min(t_1\cdots t_m)} w(t_1-\tau)\cdots w(t_m-\tau) \qquad (2.26)$$

$$n(\tau)d\tau$$

where the upper limit on the integral is changed to the minimum of $t_i \cdots t_m$ in view of the fact that $w(t_j-\tau) = 0$, $j=1,2,\ldots,m$, for $t_j<\tau$. The mean function and covariance function of $X(t)$ can easily be obtained by using Equation (2.26) with $m=1$ and $m=2$, respectively. They are

$$\mu_{XX}(t) = E[\bar{\sigma}_{zz}] \int_{t_o}^{t} w(t-\tau)n(\tau)d\tau \qquad (2.27a)$$

$$\kappa_{XX}(t_1,t_2) = E[\bar{\sigma}_{zz}^2] \int_{t_o}^{\min(t_1,t_2)} w(t_1-\tau)w(t_2-\tau)n(\tau)d\tau \qquad (2.27b)$$

Nonstationary Strength and Correlated Arrival Time Pulses

Before the generalized roughness power spectral density is calculated from the double Fourier Transform of the covariance function or the second order correlation function of $X(t)$, it is pertinent to review some of the assumptions employed for the derivations of Equations (2.16) through (2.27) so that some limitations may be relaxed.

An immediately noticeable restriction, whose removal is much desired, is that the arrival time of taxi events is Poisson. It is realized that in spite of the varying flying time, two successive taxi events are not truly independent in view of the fact that one taxi event is prior to the flight and the remaining taxi event belongs to the post-flight docking and passenger/cargo discharge. The independent arrival time is approximately true for military and/or

unscheduled operations, but it is not quite acceptable for commercial airline operations where near deterministic scheduling prevail and the arrival times of taxi events are almost interdependent if one agrees that the flying time spent in approach, holding and descent is only a minor portion of the total flying time. Lin [34] has introduced a general procedure that employs the theory of random points developed by Stratonovich. It permits one to evaluate the m^{th} cumulant function of a random process X(t) in terms of the cumulant functions of a sequence of random points which are governed by the distribution functions (they are not the same as the probability distribution functions) of various orders: $f_1(t)$, $f_2(t_1,t_2)$ $\cdots$. These distribution functions are, in turn, related to a special generating functional. If such a generating functional can be obtained from the given record or by a physical approach related to the given record, then the problem of allowing $N(t_{n+1})$ to be a generalized counting process in Equation (2.16) is solved.

Again, following the procedure of Lin [34] , the distribution functions of a sequence of random points on a time axis are related to a generating functional by the following expansion:

$$L_T[v(t)] = 1 + \sum_{m=1}^{\infty} \frac{1}{m!} \int_T \cdots \int f_m(t_1 \cdots t_m) v(t_1) \cdots v(t_m) \quad (2.28)$$

$$dt_1 \cdots dt_m$$

where the generating functional is defined as

$$L_T[v(t)] = E\{\prod_{j=1}^{N(T)} [1+v(t_j)]\} \tag{2.29}$$

The function v(t) belongs to a class for which the generating functional exists. Expand Equation (2.18) into a series and let T have the interval (t_o, t_{n+1}). Then under suitable conditions

$$M_{\{X\}}[\theta(t)] = 1 + \sum_{m=1}^{\infty} \frac{i^m}{m!} \int_T \cdots \int E[X(t_1)\cdots X(t_m)] \tag{2.30}$$

$$\theta(t_1)\cdots\theta(t_m)dt_1\cdots dt_m$$

A comparison of Equations (2.28) and (2.30) reveals that the distribution functions are analogous to the moment functions of a random process X(t). Then it is logical also to compare the log-generating functional which has the form

$$\ell n\ L_T[v(t)] = \sum_{m=1}^{\infty} \frac{1}{m!} \int_T \cdots \int g_m(t_1\cdots t_m)\, v(t_1)\cdots v(t_m) \tag{2.31}$$

$$dt_1\cdots dt_m$$

with the log-characteristic functional of X(t), which has the expansion

$$\ell n\ M_{\{X\}}[\theta(t)] = \sum_{m=1}^{\infty} \frac{i^m}{m!} \int_T \cdots \int \kappa[X(t_1)\cdots X(t_m)] \tag{2.32}$$

$$\theta(t_1)\cdots\theta(t_m)dt_1\cdots dt_m$$

It is noticed that $g_m(t_1 \cdots t_m)$ is analogous to the m^{th} cumulant function of the random process X(t) and may be conveniently defined as the m^{th} cumulant function of a sequence of random points. Remebering that the relations between the cumulant functions and moment functions of X(t) may be expressed as

$$\kappa[X(t)] = E[X(t)] = \mu_X(t)$$

$$\kappa[X(t_1)X(t_2)] = E\{[X(t)-\mu_X(t_1)][X(t_2)-\mu_X(t_2)]\}$$

$$\kappa[X(t_1)X(t_2)X(t_3)] = E\{[X(t_1)-\mu_X(t_1)][X(t_2)-\mu_X(t_3)][X(t_3)-\mu_X(t_3)]\}$$

$$\cdots$$

$$\kappa[X(t_1)\cdots X(t_m)] = E\{[X(t_1)-\mu_X(t_1)]\cdots[X(t_m)-\mu_X(t_m)]\} \qquad (2.33)^*$$

$$= E[X(t_1)\cdots X(t_m)]-m\mu_X(t_1)E[X(t_2)\cdots X(t_m)]$$

$$+ \cdots + (-1)^k \binom{m}{k} \mu_X(t_1)\cdots\mu_X(t_k)$$

$$E[X(t_{k+1})\cdots X(t_m)]$$

$$+ \cdots + (-1)^m \mu_X(t_1)\cdots\mu_X(t_m)$$

---

*See Cramer [40] for the special case $t_1 = t_2 = \cdots = t_m = t$.

It is easily deduced that the relations between the cumulant functions and distribution functions of a sequence of random points are

$$g_1(t) = f_1(t)$$

$$g_2(t_1,t_2) = f_2(t_1,t_2) - f_1(t_1)f_1(t_2)$$

$$g_3(t_1,t_2,t_3) = f_3(t_1,t_2,t_3) - f_2(t_1,t_2)f_1(t_3)$$

$$- f_2(t_1,t_3)f_1(t_2) - f_2(t_2,t_3)f_1(t_1)$$

$$+ 2f_1(t_1)f_1(t_2)f_1(t_3)$$

$$\cdots$$

$$g_m(t_1,\cdots,t_m) = f_m(t_1,\cdots,t_m) - mf_1(t_1)f_{m-1}(t_2,\cdots,t_m) + \cdots$$

$$+ (-1)^k \binom{m}{k} f_1(t_1)\cdots f_1(t_k)f_{m-k}(t_{k+1},\cdots,t_m)^*$$

$$+ \cdots + (-1)^m f_1(t_1)\cdots f_1(t_m) \qquad (2.34)$$

Therefore, if all the cumulant functions ($g_m(t_1,\cdots,t_m)$, $m = 1,2,\cdots$) are known from a sequence of random points, the generalized counting process will be completely determined.

---

*The factor $\binom{m}{k}$ accounts for all of the terms obtained by combining $t_1\cdots t_m$ in the sample form $\mu_X(t_1)\ldots\mu_X(t_k)E[X(t_{k+1})\ldots X(t_m)]$ of Equation (2.33) or $f_1(t_1)\ \ldots\ f_1(t_k)f_{m-k}(t_{k+1}\ldots t_m)$ of Equation (2.34).

With the generalized counting process thus characterized by the cumulant functions ($g_m(t_1,\cdots,t_m)$, m=1,2,$\cdots$) of a sequence of random, but correlated in time, points, it is possible to remove the limitation, that $N(t_{n+1})$ is Poisson, in Equation (2.16). By incorporating N(T), a generalized counting process, into Equation (2.16), it is permitted to rewrite the first equality of Equation (2.19) as

$$M_{\{X\}}[\theta(t)] = E\{e^{i\int_T \theta(t) \sum_{j=1}^{N(T)} \bar{\sigma}_{zz_j} w_j(t-T_j)dt}\} \tag{2.35}$$

$$= E\{\prod_{j=1}^{N(T)} e^{i\int_T \theta(t)\bar{\sigma}_{zz_j} w_j(t-T_j)dt}\}$$

$$= E\{\prod_{j=1}^{N(T)} [1 + v(T_j)]\}$$

$$= L_T[v(T)]$$

Comparing the second equality of Equation (2.35) with Equation (2.29), it is clear that

$$M_{\{X\}}[\theta(t)] = L_T[e^{i\int_T \theta(t)\bar{\sigma}_{zz_j} w_j(t-T_j)dt} - 1] \tag{2.36}$$

$$= L_T[\sum_{\ell=1}^{\infty} \frac{i^\ell}{\ell!} \bar{\sigma}_{zz_j}{}^\ell \int\cdots\int_T \theta(t_1)\cdots\theta(t_\ell)$$

$$w_j(t_1-T_j)\cdots w_j(t_\ell-T_j)dt_1\cdots dt_\ell]$$

If logarithms are taken on both sides of Equation (2.36) and the expansions from Equation (2.32) and Equation (2.31) for $\ell nM_{\{X\}}[\theta(t)]$ and $\ell nL_T[v(T)]$, respectively, are used together with

$$E[\bar{\sigma}zz_j^{\ell}] = \int_0^{\infty} \bar{\sigma}_{zz_j}^{\ell}\, p(\bar{\sigma}_{zz},T_j)d\bar{\sigma}_{zz} \tag{2.37}$$

$$= \int_0^{\infty} \bar{\sigma}_{zz_j}^{\ell}\, \delta(\bar{\sigma}_{zz_j}-\bar{\sigma}_{zz}(T_j))d\bar{\sigma}_{zz} = \bar{\sigma}_{zz}^{\ell}(T_j)$$

Then

$$\sum_{m=1}^{\infty} \frac{i^m}{m!} \int_T\cdots\int \kappa[X(t_1)\cdots X(t_m)]\theta(t_1)\cdots\theta(t_m)dt_1\cdots dt_m \tag{2.38}$$

$$= \sum_{m=1}^{\infty} \frac{1}{m!} \int_T\cdots\int g_m(t_1,\cdots,t_m)\{\sum_{\ell=1}^{\infty} \frac{i^\ell}{\ell!}\bar{\sigma}_{zz}^{\ell}(T_1)\int_T\cdots\int \theta(t_1)\cdots\theta(t_\ell)$$

$$w_1(t_1-T_1)\cdots w_1(t_\ell-T_1)dt_1\cdots dt_\ell\}\cdots\{\sum_{\ell=1}^{\infty} \frac{i^\ell}{\ell!}\bar{\sigma}_{zz}^{\ell}(T_m)$$

$$\int_T\cdots\int \theta(t_1)\cdots\theta(t_\ell)w_m(t_1-T_m)\cdots w_m(t_\ell-T_m)dt_1\cdots dt_\ell\}dT_1\cdots dT_m$$

The cumulant functions of the random process X(t) may be obtained from Equation (2.38) by comparing the same number of integrations on the t_m's, m=1,2,$\cdots$, on both sides of the equation. In particular, the mean and covariance functions of X(t) are given by

$$\kappa_1[X(t)] = E[X(t)] = \mu_X(t) = \int_{t_o}^{t_{n+1}} \bar{\sigma}_{zz}(\tau)w(t-\tau)g_1(\tau)d\tau \qquad (2.39a)$$

and

$$\kappa_2[X(t_1)X(t_2)] = \kappa_{XX}(t_1,t_2) \qquad (2.39b)$$

$$= \int_{t_o}^{t_{n+1}} \bar{\sigma}_{zz}(\tau)w_1(t_1-\tau)w_1(t_2-\tau)g_1(\tau)d\tau$$

$$+ \int_{t_o}^{t_{n+1}} \int \bar{\sigma}_{zz}(\tau_1)\bar{\sigma}_{zz}(\tau_2)w_1(t_1-\tau_1)w_2(t_2-\tau_2)g_2(\tau_1,\tau_2)d\tau_1 d\tau_2$$

where integration over T of Equation (2.38) is replaced by its interval (t_o,t_{n+1}) in both Equations (2.39a) and (2.39b). Substitutions of $t = t_1$, $\tau = T_1$, and $w_1(t_1-T_1) = w(t-\tau)$ were used in Equation (2.39a). $\tau_1 = T_1$, $\tau_2 = T_2$ were used in Equation (2.39b).

At this point, it is interesting to note that the limitation of $\bar{\sigma}_{zz_j} = \bar{\sigma}_{zz}(T_j)$, $j=1,\cdots,n$ being mutually independent and possessing the same distribution as shown in Equation (2.17) is also removed by the generalized counting process and through Equation (2.37). This becomes obvious if one allows the generalized counting process to be Poisson, then

$$g_1(\tau) = f_1(\tau) = \lambda(\tau) \qquad (2.40)$$

$$g_2(\tau_1,\tau_2) = f_2(\tau_1,\tau_2) - f_1(\tau_1)f_1(\tau_2) = \lambda(\tau_1)\lambda(\tau_2) - \lambda(\tau_1)\lambda(\tau_2) = 0$$

Equations (2.40) follows from the fact that the distribution functions $(f_1(t), f_2(t_1,t_2)\cdots)$ of a sequence of random points are simply the product densities of various orders of some point processes (see Bartlett [41], and Srinivasan, etc. [38]) and when the points are uncorrelated, $f_m(t_1,\cdots,t_m) = \prod_{j=1}^{m} f_1(t_j)$ becomes the general expression for all product densities. Substituting Equation (2.40) into Equations (2.39a) and (2.39b), the mean and covariance functions of X(t) with a Poisson counting process become

$$\kappa_1[X(t)] = E[X(t)] = \mu_X(t) = \int_{t_o}^{t_{n+1}} \bar{\sigma}_{zz}(\tau) w(t-\tau)\lambda(\tau)d\tau \qquad (2.41a)$$

and

$$\kappa_2[X(t_1)X(t_2)] = \kappa_{XX}(t_1,t_2) \qquad (2.41b)$$

$$= \int_{t_o}^{t_{n+1}} \bar{\sigma}_{zz}^{\,2}(\tau) w_1(t_1-\tau) w_1(t_2-\tau)\lambda(\tau)d\tau$$

Comparing Equations (2.27a), (2.27b) with (2.41a), (2.41b), respectively, it is seen that the strength function $\bar{\sigma}_{zz}(\tau)$ is no longer time independent or stationary (i.e., $\bar{\sigma}_{zz}(\tau) \neq E[\bar{\sigma}_{zz}] = c_1$ and $\bar{\sigma}_{zz}^{\,2}(\tau) = E[\bar{\sigma}_{zz}^{\,2}] = c_2$). This is not unexpected in the light of Equation (2.17) where a pseudo-ergodic density function was obtained for $p(\bar{\sigma}_{zz},t)$ in anticipation to render α independent of T_j in Equation (2.22). The reasoning behind such a drastic move will become clear if one remembers

that, in a strict sense, α of Equation (2.22) must be expressed as

$$\alpha = \sum_{m=1}^{\infty} \frac{i^m}{m!} \int_0^{\infty} \bar{\sigma}_{zz}{}^m \, p(\bar{\sigma}_{zz}, T_j) d\bar{\sigma}_{zz} \int_{t_o}^{t_{n+1}} \cdots \int \theta(t_1) \cdots \theta(t_m) \tag{2.42}$$

$$\frac{\int_{t_o}^{t_{n+1}} w_j(t_1-\tau) \cdots w_j(t_m-\tau) \lambda(\tau) d\tau}{\int_{t_o}^{t_{n+1}} \lambda(\tau) d\tau} dt_1 \cdots dt_m = \alpha_j$$

If the substitution of Equation (2.42) into Equations (2.21) and (2.19) is made, the characteristic function of X(t) will have the expansion

$$M_{\{X\}}[\theta(t)] = \sum_{n=0}^{\infty} P_{\{N\}}(n, t_{n+1}) E\left[e^{i \int_{t_o}^{t_{n+1}} \theta(t) \sum_{j=1}^{n} \bar{\sigma}_{zz_j} w_j(t-T_j) dt}\right]$$

$$= \sum_{n=0}^{\infty} P_{\{N\}}(n, t_{n+1}) \prod_{j=1}^{n} (1+\alpha_j) \tag{2.43}$$

Any attempt to reduce the last equality of Equation (2.43) into an exponential form

$$\left(e^{\alpha \int_{t_o}^{t_{n+1}} \lambda(\tau) d\tau}\right)$$

is quite impossible from the fact that $\prod_{j=1}^{n} (1+\alpha_j) = (1+\alpha)^n$ if, and only if, $\alpha_1 = \alpha_2 = \cdots = \alpha_n = \alpha$, or α must be independent of T_j.

Physical Significance of the Restrictions

The less general X(t) with nonhomogeneous Poisson distributed taxi event arrival time and mutually independent, identically distributed strength is not totally unacceptable from an engineering viewpoint. A physical approach toward the understanding of the time averaging process on the time-dependent density functions as shown in Equation (2.17) will prove that, for certain fleet operations, the time-independent strength density function analysis is more advantageous to use than the stringent time-dependent strength density function analysis. Figure 2.11 illustrates the criteria for the choice of the most suitable combinations of arrival rate and strength distribution.

Case (a) is representative of the single record composite roughnesses for design criteria analysis. Due to the two-time averaging (see Figure 2.8), it is natural that the strength of the roughness strength function has been stabilized quite some and the individual time-independent strength density functions will be close to that obtained from Equation (2.17). The arrival rate will be more irregular in view of the fact that many aircrafts from different types were involved. It is therefore reasonable to assume that ergodic (stationary) strength distribution and nonhomogeneous Poisson arrival rate will suffice.

Case (b) is best demonstrated by the single record composite roughness for fatigue life evaluation based on fleet operations. The averaging is done over an ensemble of one type, hence the different

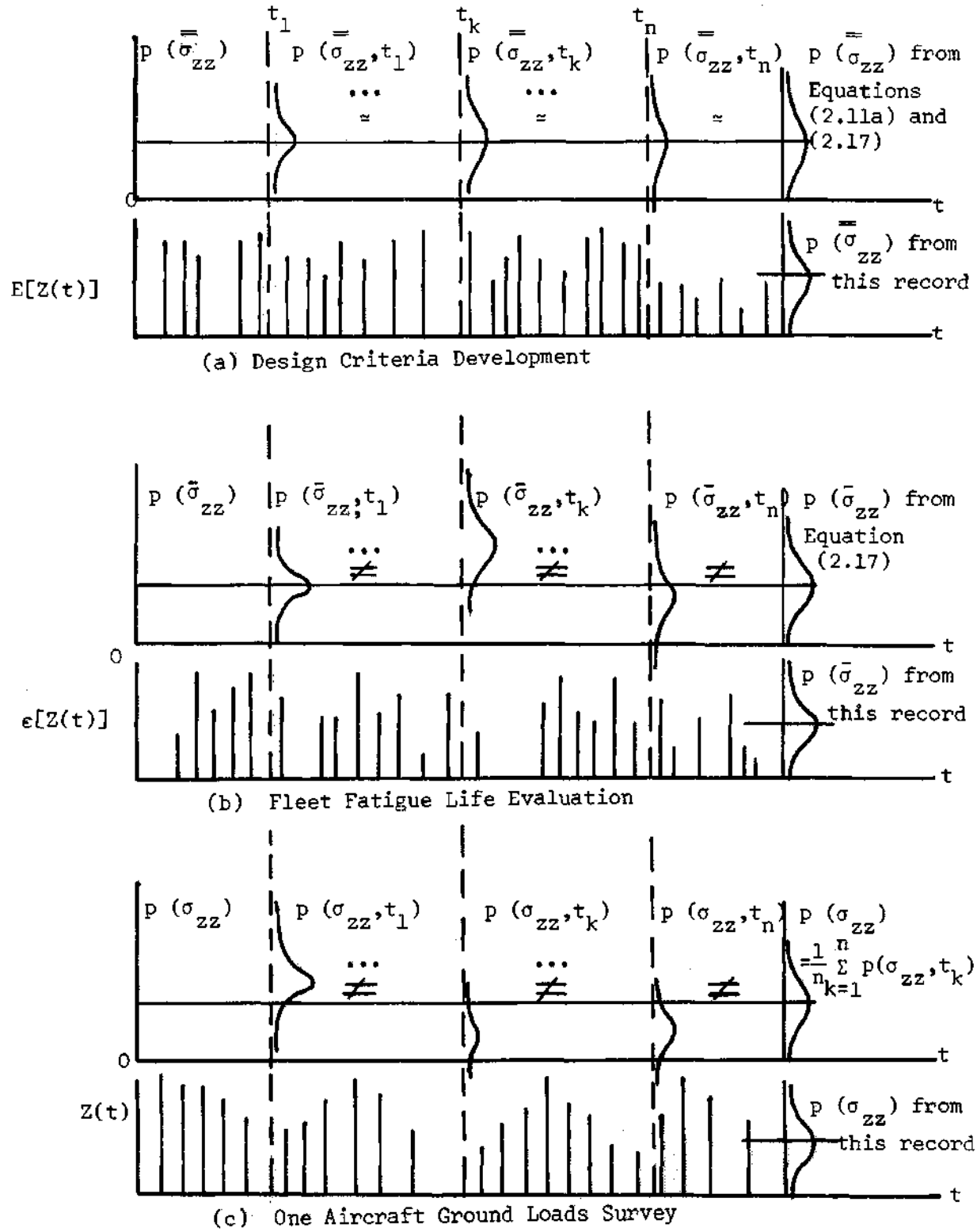

Figure 2.11 Criteria For Arrival Rate and Strength Distribution

levels of strength for the roughness strength functions are inherently present and sensitive to time in the sense that the time-independent strength density function as derived from Equation (2.17) will not be a representative strength density function at any given time. Due to the large number of aircrafts in the ensemble, the arrival rates are quite irregular. Thus, the realistic choice of strength distribution and arrival rate will be nonstationary and nonhomogeneous Poisson, respectively.

Case (c) exemplifies the single time history of a given aircraft that performs prototype flight testing or a commercial airliner that flies scheduled revenue flights on predetermined routes. It is understood that such airplanes do have some built-in periodicity in the taxi sites and flying time. The levels of strength of the roughness strength functions are selected, if not deterministic, and the arrival rates are also correlated and interdependent. A logical choice for the strength distribution and arrival rate for the present case will unequivocally be nonstationary and correlated, respectively.

Comparisons of the Generalized Results

Published Special Cases

With the cumulant functions, and therefore mean and variance functions, for the single record composite roughnesses solidly defined in Equations (2.27), (2.39), and (2.41), it is expedient to compare the findings contained herein with the results in the publications cited in page 30. It is understood that the present model

$$X(t) = \sum_{j=1}^{N(t_{n+1})} \bar{\sigma}_{zz_j} w_j(t-T_j)$$

represents a sequence of random pulses with either stationary or nonstationary impulse strength ($E[\bar{\sigma}_{zz}]$ or $\bar{\sigma}_{zz}(\tau)$) and nonstationary impulse arrival rate which is either nonhomogeneous Poisson distributed or correlated random points. $w_j(t-T_j)$'s are shaping functions and may be regarded as impulse response functions $h(t,T_j)$. Only mean and covariance functions are of the most interest if the goal is to establish the generalized power spectral density of the composite roughnesses, it is therefore sufficient to compare these two quantities.

Equations (2.27a) and (2.27b) are the mean and covariance functions of a sequence of mutually independent, identically distributed strength pulses with a nonhomogeneous Poisson arrival rate. Lin [34] has shown in his Equation (18) that $\kappa[X(t_1)\cdots X(t_m)] = E[Y^m] \int_T h(t_1,\tau)\cdots\lambda(t_m,\tau)\lambda(\tau)d\tau$ (18). For m=1 and 2, the results are exactly the same as Equations (2.27a) and (2.27b) if one substitutes $E[Y^m] = E[\bar{\sigma}_{zz}{}^m]$, $h(t_m,\tau) = w_j(t_m-\tau)$ and $\lambda(\tau) = n(\tau)$.

Equations (2.41a) and (2.41b) are, respectively, the mean and covariance functions for a sequence of random pulses with nonstationary strength and nonhomogeneous Poisson arrival rate. Equations (13) and (24) of Roberts [37] are given by

$$E[Y(t)] \int_{t_1}^{t_2} h(t,\tau)\overline{a(\tau)}\nu(\tau)d\tau \qquad (13)$$

and

$$w_{YY}(t',t'') = \int_{t_1}^{t_2} h(t',\tau)h(t'',\tau)\overline{a^2(\tau)}\nu(\tau)d\tau \qquad (24)$$

If $E[Y(t)] = E[X(t)]$, $t_1 = t_o$, $t_2 = t_{n+1}$, $h(t,\tau) = w(t-\tau)$, $\overline{a(\tau)} = \bar{\sigma}_{zz}(\tau)$ and $\nu(\tau) = \lambda(\tau)$ are substituted in (13), Equation (2.41a) is identical to (13). If $w_{YY}(t',t'') = \kappa_{XX}(t_1,t_2)$, $t_1 = t_o$, $t_2 = t_{n+1}$, $h(t',\tau) = w_1(t_1,\tau)$, $h(t'',\tau) = w_1(t_2,\tau)$ and $\nu(\tau) = \lambda(\tau)$ are substituted in (24), then Equation (2.41b) is the same as (24).

Equations (2.39a) and (2.39b) are the mean and covariance functions for a sequence of random pulses with nonstationary strength and correlated arrival rate defined by the cumulant functions $(g_1(\tau), g_2(\tau_1,\tau_2)\cdots)$ of a sequence of random points. Srinivasan, etc. [38] have demonstrated by using some general methods of point processes and product densities to obtain the mean and covariance functions in Equations (16) and (24) of [38], respectively. They are

$$\varepsilon\{Y(t)\} = \int_0^t f_1(\tau)h(t-\tau)\varepsilon\{a(\tau)\}d\tau \qquad (16)$$

where

$$f_1(\tau) = g_1(\tau) \qquad (20)$$

and

$$\mathrm{Cov}[Y(t_1)Y(t_2)] = \int_0^{t_1}\int_0^{t_2} h(t_1-\tau_1)h(t_2-\tau_2)g_2(\tau_1,\tau_2) \qquad (24)$$

$$\varepsilon\{R(\tau_1)\}\varepsilon\{a(\tau_2)\}d\tau_1 d\tau_2$$

$$+ \int_0^{\min(t_1,t_2)} h(t_1-\tau)h(t_2-\tau)g_1(\tau)\varepsilon\{a^2(\tau)\}d\tau$$

It is clear that if $\varepsilon\{Y(t)\} = E[X(t)]$, $0 = t_o$, $t = t_{n+1}$, $h(t-\tau) = w(t-\tau)$, then Equation (16) and Equation (2.39a) is the same. If $Cov[Y(t_1)Y(t_2)] = \kappa[X(t_1)X(t_2)]$, $0 = t_o$, $t_1 = t_{n+1} = t_2$, $h(t_i-\tau_i) = w_i(t_i-\ _i)$ for i=1, 2, $\varepsilon\{a(\tau_1)\} = \bar{\sigma}_{zz}(\tau_1)$, and $\varepsilon\{a(\tau_2)\} = \bar{\sigma}_{zz}(\tau_2)$, then Equation (24) is identical to (2.39b), $g_1(\tau)$ and $g_2(\tau_1,\tau_2)$ are the first and second cumulant functions of a sequence of correlated random points in both sets of Equations (16), (24), and (2.39a), (2.39b).

Standard One Runway, One Constant Speed Case

In view of the complexity of the mean and covariance functions as shown in Equations (2.39a) and (2.39b), it is of interest to substantiate the validity of the limiting case where only one runway roughness is present. It is therefore asserted that Equation (2.16) now is reduced to

$$X(t) = \sum_{j=1}^{N(t_{n+1})} \bar{\sigma}_{zz_j} w_j(t-T_j) \qquad (2.44)$$

$$= \tilde{\sigma}_{zz_j} w_1(t-T_1) = Z_1(t)$$

The last line in Equation (2.44) is obtained by setting $\bar{\sigma}_{zz_j} = 0$ for j=2,3,4,$\cdots$,n.

The analogous mean and covariance functions for Equation (2.44) are obtained from Equations (2.39a) and (2.39b), respectively, by the following development.

$$\kappa_1[X(t)] = \int_{t_o}^{t_{n+1}} \bar{\sigma}_{z_1 z_1}(\tau) w_1(t-\tau) g_1(\tau)\, \delta(\tau - T_1)\, d\tau \qquad (2.45a)$$

$$= \bar{\sigma}_{z_1 z_1}(T_1) w_1(t-T_1) g_1(T_1) = \kappa_1[Z_1(t)]$$

$$\kappa_2[X(t_1)X(t_2)] = \int_{t_o}^{t_{n+1}} \bar{\sigma}_{z_1 z_1}^2(\tau) w_1(t_1-\tau) w_1(t_2-\tau) g_1(\tau) \delta(\tau - T_1)\, d\tau$$

$$+ \int_{t_o}^{t_{n+1}} \int \bar{\sigma}_{z_1 z_1}(\tau_1) \bar{\sigma}_{z_1 z_1}(\tau_2) w_1(t_1-\tau_1) w_1(t_2-\tau_2)^* \qquad (2.45b)$$

$$\delta(\tau_1 - T_2)\, \delta(\tau_2 - T_1)\, d\tau_1 d\tau_2$$

$$= \bar{\sigma}_{z_1 z_1}^2(T_1) w_1(t_1-T_1) w_1(t_2-T_1)[g_1(T_1) + g_2(T_1, T_1)]$$

$$= \kappa_2[Z_1(t_1) Z_1(t_2)]$$

---

*The substitution of $w_2(t_2-\tau_2) = w_1(t_2-\tau_2)$ was used. Since $w_1(t_1-\tau_1) = e^{-\gamma_1 |t_1-\tau_1|} = e^{-\alpha_1 \beta_1/2 |t_1-\tau_1|}$ and $w_2(t_2-\tau_2) = e^{-\gamma_2 |t_2-\tau_2|} = e^{-\alpha_2 \beta_1/2 |t_2-\tau_2|} = w_1(t_2-\tau_2)$ still specify two different shaping functions, no inconsistency with Equation (2.39b) has occurred. It is physically impossible to have a $w_2(t_2-\tau_2) = e^{-\alpha_2 \beta_2/2 |t_2-\tau_2|}$ as β_1 is the shaping factor of a single given runway. (See page 15, Equation (2.6).)

Due to the fact that there is only one arrival at T_1, the counting process can be considered Poisson, hence

$$g_1(T_1) = f_1(T_1) = \lambda(T_1) = 1 \tag{2.46a}$$

$$g_2(T_1,T_1) = f_2(T_1,T_1) - f_1^2(T_1) = f_1^2(T_1) - f_1^2(T_1) = 0 \tag{2.46b}$$

Substitute Equation (2.46) into Equation (2.45a) and (2.45b); the mean and covariance functions of $Z_1(t)$ are given by

$$\kappa_1[Z_1(t)] = \bar{\sigma}_{z_1z_1}(T_1)w_1(t-T_1) \tag{2.47a}$$

$$\kappa_2[Z_1(t_1)Z(t_2)] = \bar{\sigma}_{z_1z_1}{}^2(T_1)w_1(t_1-T_1)w_1(t_2-T_1) \tag{2.47b}$$

From the shape of the shaping function (see page 26), $w_1(t_i-T_1) = e^{-\gamma_1|t_i-T_1|}$, i=1,2, it is apparent that Equation (2.47b) is only meaningful when $|t_2-t_1|$ is small or t_2 is close to T_1, otherwise $w_1(t_2-T_1)$ will approach zero and $\kappa_2[Z_1(t_1)Z_2(t_2)]$ will vanish. To anticipate the fact that the autocorrelation function of $Z_1(t)$ will resemble that of the standard one runway, one constant taxi speed approach of Equations (2.5a) and (2.5b), it is assumed that $Z_1(t)$ is also weakly stationary in the sense that

$$\kappa_1[Z_1(t_1)] = \bar{\sigma}_{z_1z_1}(T_1)w_1(t_1-T_1) = \lim_{t_2\to t_1} \kappa_1[Z_1(t_2)] \tag{2.48}$$

and the autocorrelation function of $Z_1(t)$ is allowed to be expressed as

$$R_{z_1z_1}(t_1,t_2) = \kappa_2[Z_1(t_1)Z_1(t_2)] + \kappa_1[Z_1[Z_1(t_1)]\kappa_1[Z_1(t_2)] \quad (2.49)$$

$$= \kappa_2[Z_1(t_1)Z_1(t_2)] + \{\kappa_1[Z_1(t_1)]\}^2$$

$$= \bar{\sigma}^2_{z_1z_1}(T_1)w_1(t_1-T_1)w_1(t_2-T_1) + \{\bar{\sigma}_{z_1z_1}(T_1)w_1(t_1-T_1)\}^2$$

In view of the presence of t_1 and t_2 as separate entities in Equation (2.49) rather than $R_{z_1z_1}(t_2-t_1)$, it is necessary to use the double Fourier transform technique for a generalized (nonstationary) power spectral density and then reduce that to the ordinary (stationary) power spectral density by limiting $\omega_1 = \omega_2$ (see Roberts [42]) in the generalized one. The generalized power spectral density is defined as

$$\Phi_{XX}(\omega_1,\omega_2) = \frac{1}{(2\pi)^2}\int_{-\infty}^{\infty}\int \kappa_2[X(t_1)X(t_2)]e^{-j(\omega_1t_1-\omega_2t_2)}dt_1dt_2 \quad (2.50a)$$

(See Bendat, etc. [43]),

or

$$S_{XX}(\omega_1,\omega_2) = \frac{1}{(2\pi)^2}\int_{-\infty}^{\infty}\int R_{XX}(t_1,t_2)e^{j(\omega_1t_1-\omega_2t_2)}dt_1dt_2 \quad (2.50b)$$

(See Roberts [42]), by different authors, and Equations (2.50a), and

(2.50b) only differ in a sign reversal and the different quantities to be transformed ($\kappa_2[X(t_1)X(t_2)] = \kappa_{XX}(t_1,t_2)$, if $\kappa_1[X(t_1)] = \kappa_1[X(t_2)] = 0$). They will render no ambiguity in the following development. Applying Equation (2.50b) to Equation (2.49), the generalized power spectral density for a one runway, one constant taxi speed $Z_1(t)$ is given by

$$S_{Z_1Z_1}(\omega_1,\omega_2) = \frac{\bar{\sigma}_{z_1z_1}^2(T_1)}{(2\pi)^2}\{\int_{-\infty}^{\infty}\int w_1(t_1-T_1)w_1(t_2-T_1)e^{j(\omega_1t_1-\omega_2t_2)}dt_1dt_2$$

$$+ \int_{-\infty}^{\infty}\int w_1^2(t_1-T_1)e^{j(\omega_1t_1-\omega_2t_2)}dt_1dt_2\} \qquad (2.51)$$

$$= \bar{\sigma}_{z_1z_1}^2(T_1)[W_1^*(\omega_1)W_1(\omega_2) + W_1^{*2}(\omega_1)e^{j\omega_1T_1}\delta(\omega_2)] \qquad (2.51)$$

where

$$W_k(\omega_i) = \frac{1}{2\pi}\int_{-\infty}^{\infty} w_k(t_i)e^{-j\omega_it_i}\,dt_i, \quad \begin{matrix} i=1,2 \\ k=1 \end{matrix} \qquad (2.52)$$

and $\delta(\omega_2) = W_1(\omega_2)$ for $w_1(t_2) = 1$. (See Davenport and Root [44].) The ordinary power spectral density of the above may be obtained by substituting $\omega_1 = \omega_2 = \omega$ into Equation (2.51), hence

$$S_{Z_1Z_1}(\omega) = S_{Z_1Z_1}(\omega,\omega) = \bar{\sigma}_{z_1z_1}^2(T_1)[|W_1(\omega)|^2 + W_1^{*2}(\omega)e^{j\omega T_1}\delta(\omega)] \qquad (2.53a)$$

It is noticed that the term with the $\delta(\omega)$ is merely the non-zero mean

of the roughness $Z_1(t)$ and the ordinary power spectral density for $\omega > 0$ is expressed by

$$\Phi_{Z_1Z_1}(\omega) = \bar{\sigma}_{z_1z_1}(T_1)|W_1(\omega)|^2 = S_{Z_1Z_1}(\omega), \quad \omega > 0 \qquad (2.53b)$$

Equation (2.53b) is exactly the same as Equation (2.5a), if one recognizes that

$$R_{zz}(\tau)\Big|_{V_{TAXI}=\alpha} = \sigma_{zz}^2 e^{-\alpha\beta|\tau|} \qquad (2.7 \text{ Repeat})$$

and

$$\text{Cov}_{z_1z_1}(\tau) = \underset{t_2-t_1=\tau\to 0}{L} \kappa_2[Z_1(t_1)Z_1(t_2)] \qquad (2.54)$$

$$= \underset{\tau\to 0}{L} \bar{\sigma}_{z_1z_1}^2(T_1)w_1(t_1-T_2)w_1(t_1+\tau-T_2)$$

$$= \bar{\sigma}_{z_1z_1}^2(T_1)e^{-2\gamma_1|t_1-T_1|}{}^{*}$$

$$= \bar{\sigma}_{z_1z_1}^2(T_1)e^{-\alpha_1\beta_1|t_1-T_1|}$$

---

*If the maintenance of constant speed were impossible and at t_1 and t_2, the respective taxi speeds would be α_1 and α_2 but for $t_2 \to t_1$ physically the two constant taxi speeds α_1 and α_2 must become α_1^2 and the following development is valid:

are identical.

Equation (2.54) is the limiting case of the covariance function of Equation (2.47b) with t_2 approaching t_1. T_1 is only a parameter to indicate the starting point of the (single runway roughness, $Z_1(t)$) composite roughness record X(t). The validity of comparing $R_{zz}(\tau)$ with $\kappa_2[Z_1(t_1)Z_1(t_2)]$ without subtracting the square of the mean roughness from $R_{zz}(\tau)$ is due to the fact that

$$R_{zz}(\tau) = \kappa_2[Z(t)Z(t+\tau)] + \kappa_1[Z(t)]\kappa_1[Z(t+\tau)]$$

and $\kappa_1[Z(t)] = \kappa_1[Z(t+\tau)] = 0$ from the assumption stated on page 8 that the mean roughnesses for all taxi sites were removed.

Generalized and Ordinary Power Spectral Densities of a Composite Roughness Record

The generalized power spectral density for a composite roughness record X(t) as shown in Equation (2.16) may be obtained by using either

---

$$\lim_{\tau\to 0} \bar{\sigma}_{z_1z_1}^2(T_1)e^{-\gamma_1|t_1-\tau_2| - \gamma_2|t_1+\tau-T_1|}$$

$$= \lim_{\tau\to 0} \bar{\sigma}_{z_1z_1}^2(T_1)e^{-\gamma_1|t_1-T_1| - \gamma_2|t_1-T_1+\tau|}$$

$$\approx \bar{\sigma}_{z_1z_1}^2(T_1)e^{-(\gamma_1+\gamma_2)|t_1-T_1|}$$

$$= \lim_{\alpha_2\to\alpha_1} \bar{\sigma}_{z_1z_1}^2(T_1)e^{-2\gamma_1|t_1-T_1|}$$

as $\gamma_1 = \alpha_1\beta_1$ and $\gamma_2 = \alpha_2\beta_1$ (see footnote, page 50).

Equation (2.50a) or (2.50b) with the following mean and covariance functions

$$\kappa_1[X(t)] = \int_{t_o}^{t_{n+1}} \sum_{j=1}^{N(t_{n+1})} \delta(\tau-T_j)\bar{\sigma}_{zz}(\tau)w_j(t-\tau)g_1(\tau)d\tau \qquad (2.55a)$$

$$= \sum_{j=1}^{N(t_{n+1})} \bar{\sigma}_{zz}(T_j)w_j(t-T_j)g_1(T_j)$$

$$\kappa_2[X(t_1)X(t_2)] = \int_{t_o}^{t_{n+1}} \sum_{j=1}^{N(t_{n+1})} \delta(\tau-T_j)\bar{\sigma}_{zz}^2(\tau)w_j(t_1-\tau)w_j(t_2-\tau)$$

$$g_1(\tau)d\tau$$

$$+ \int_{t_o}^{t_{n+1}} \int \sum_{j,k=1}^{N(t_{n+1})} \delta(\tau_1-T_j)\delta(\tau_2-T_k)\bar{\sigma}_{zz}(\tau_1)\bar{\sigma}_{zz}(\tau_2) \qquad (2.55b)$$

$$w_j(t_1-\tau_1)w_k(t_2-\tau_2)g_2(\tau_1,\tau_2)d\tau_1 d\tau_2$$

$$= \sum_{j=1}^{N(t_{n+1})} \bar{\sigma}_{zz}^2(T_j)w_j(t_1-T_j)w_j(t_2-T_j)[g_1(T_j)] +$$

$$\sum_{j,k=1}^{N(t_{n+1})} \bar{\sigma}_{zz}(T_j)\bar{\sigma}_{zz}(T_k)w_j(t_1-T_j)w_k(t_2-T_k)[g_2(T_j,T_k)]$$

where $g_1(\tau)$ and $g_2(\tau_1,\tau_2)$ are known functions from the given record. Substituting Equation (2.55b) into Equation (2.50a), the generalized power spectral density for a composite roughness record may be expressed as

$$\Phi_{XX}(\omega_1,\omega_2) = \sum_{j=1}^{N(t_{n+1})} \bar{\sigma}_{zz}^2(T_j)[g_1(T_j) + g_2(T_j,T_j)]W_j(\omega_1)W_j^*(\omega_2) \quad (2.56a)$$

$$+ \sum_{j\neq k=1}^{N(t_{n+1})} \bar{\sigma}_{zz}(T_j)\bar{\sigma}_{zz}(T_k)[g_2(T_j,T_k)]W_j(\omega_1)W_k^*(\omega_2)$$

and its ordinary power spectral density is

$$\Phi_{XX}(\omega) = \Phi_{XX}(\omega,\omega) = \sum_{j=1}^{N(t_{n+1})} \bar{\sigma}_{zz}^2(T_j)[g_1(T_j) + g_2(T_j,T_j)]|W_j(\omega)|^2$$

$$+ \sum_{j\neq k=1}^{N(t_{n+1})} \bar{\sigma}_{zz}(T_j)\bar{\sigma}_{zz}(T_k)[g_2(T_j,T_k)]W_j(\omega)\, W_k^*(\omega) \quad (2.56b)$$

where $W_j(\omega_i)$ and $W_k(\omega_i)$, $i=1,2$ is defined by setting $k=1,2,\ldots$ in Equation (2.52). If the generalized power spectral density of the composite roughness with the nonzero mean must be required, substituting Equations (2.55a), (2.55b) into Equation (2.50b), the following expression is obtained

$$S_{XX}(\omega_1,\omega_2) = \sum_{j=1}^{N(t_{n+1})} \bar{\sigma}_{zz}^2(T_j)\{[g_1(T_j) + g_2(T_j,T_j)]W_j^*(\omega_1)W_j(\omega_2) \quad (2.57a)$$

$$+ [g_1^2(T_j)]W_j^*(\omega_1)e^{j\omega_1 T_j}\,\delta(\omega_2) + \sum_{j\neq k=1}^{N(t_{n+1})} \bar{\sigma}_{zz}(T_j)$$

$$\bar{\sigma}_{zz}(T_k)[g_1(T_j)g_1(T_k) + g_2(T_j,T_k)]W_j^*(\omega_1)W_k(\omega_2)$$

and its ordinary power spectral density is given by

$$S_{XX}(\omega) = S_{XX}(\omega,\omega) = \sum_{j=1}^{N(t_{n+1})} \bar{\sigma}_{zz}^2(T_j)\{[g_1(T_j) + g_2(T_j,T_j)] \quad (2.57b)$$

$$|W_j(\omega)|^2 + [g_1(T_j)]^2 W_j^*(\omega) e^{j\omega T_j} \delta(\omega)\}$$

$$+ \sum_{j\neq k=1}^{N(t_{n+1})} \bar{\sigma}_{zz}(T_j)\bar{\sigma}_{zz}(T_k)[g_1(T_j)g_1(T_k)$$

$$+ g_2(T_j,T_k)]\, W_j^*(\omega)W_k(\omega)$$

Generalized and Ordinary Output Power Spectral Densities

If the frequency response functions for the aircraft responses in question are furnished, their output power spectral densities may be calculated from the relations

$$\Phi_{YY}(\omega_1,\omega_2) = \Phi_{XX}(\omega_1,\omega_2)H(\omega_1)H^*(\omega_2) \quad (2.58)$$

or

$$\Phi_{YY}(\omega) = \Phi_{XX}(\omega)|H(\omega)|^2$$

$S_{XX}(\omega_1,\omega_2)$ or $S_{XX}(\omega)$ may be used in lieu of $\Phi_{XX}(\omega_1,\omega_2)$ or $\Phi_{XX}(\omega)$ in Equations (2.58). However, for most response quantities, $H(0)H^*(0)$ and $|H(0)|^2$ are always zero and the evaluation of $\Phi_{YY}(0)$ or $\Phi_{YY}(0,0)$ is not warranted. Nevertheless, the $S_{XX}(\omega_1,\omega_2)$ and $S_{XX}(\omega)$ will furnish comparatively more accurate response data for the outputs that are

sensitive to very low frequencies (e.g., rigid body motions excited by long wavelength unevenness) and the selections of $\Phi_{XX}(\omega_1,\omega_1)$ and $\Phi_{XX}(\omega)$ may inadvertently introduce some unconservatism into the analysis. It is therefore advisable to calculate both $\Phi_{YY}(\omega_1,\omega_2)(\Phi_{YY}(\omega))$ and $S_{YY}(\omega_1,\omega_2)(S_{YY}(\omega))$.

CHAPTER III

DERIVATION OF FREQUENCY RESPONSE FUNCTIONS

Equations of Motion

The airplane, as shown schematically in Figure 3.1, consists of a rigid fuselage and a flexible wing. The wing is assumed to be a straight beam with a constant rectangular cross-section for the entire span. The landing gears are attached rigidly to the fuselage. The main gears have linear springs and viscous dampers in the struts. The tail gear has an inextensible strut.

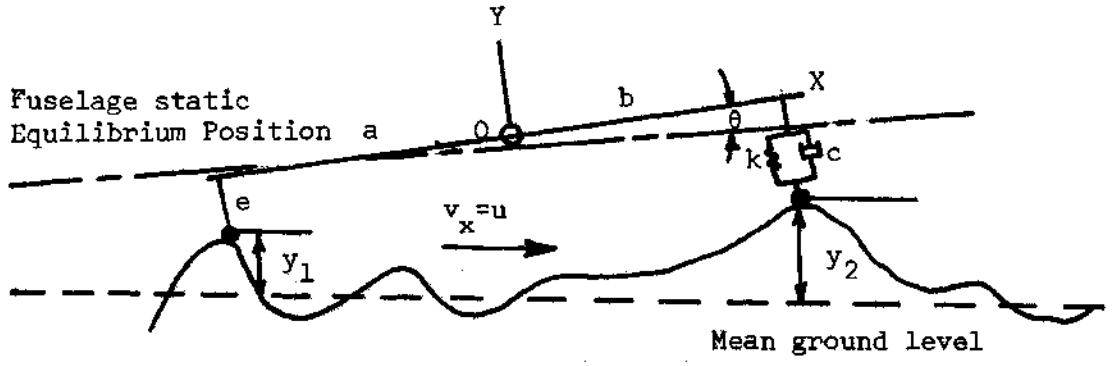

Figure 3.1 Idealized Airplane

The airplane is considered to taxi along a straight runway with a constant horizontal velocity and both the main wheels and tail wheel are assumed to remain in contact with the ground at all times. The ground profile is assumed to have no variations in the direction

perpendicular to the path. The elevations are measured from some arbitrary mean ground level; thus, the two main landing gears can be replaced by a single equivalent front gear located in the plane of symmetry (XY-plane) of the airplane. Together with the tail gear, the airplane has a bicycle gear arrangement and the dynamic responses are symmetrical about the longitudinal axis (X-axis) of the airplane.

The body axes OXYZ are embedded at the mass center of the airplane. The origin O has an instantaneous position vector $\bar{r}_o$ with respect to a fixed earth axes oxyz (see Figure 3.2). Denote the unit vectors in OXYZ coordinates and oxyz coordinates by $\bar{I},\bar{J},\bar{K}$ and $\bar{i},\bar{j},\bar{k}$, respectively, then

$$\bar{r}_o = x_1\bar{i} + y_1\bar{j} + a\bar{I} + e\bar{J} \tag{3.1}$$

Similarly, the position vector, $\bar{r}_p$, for an arbitrary point P on the wing elastic axis will become

$$\bar{r}_p = x_1\bar{i} + y_1\bar{j} + a\bar{I} + e\bar{J} + U\bar{I} + V\bar{J} + W\bar{K} \tag{3.2}$$

where U, V, and W are the displacement components of the point P in the X, Y, znd Z directions.

Let the rigid body rotation of the airplane be θ as measured from its static equilibrium position θ_o; hence, the angular velocity of the body axes OXYZ becomes

$$\bar{\omega}_o = \dot{\theta}\bar{K}$$

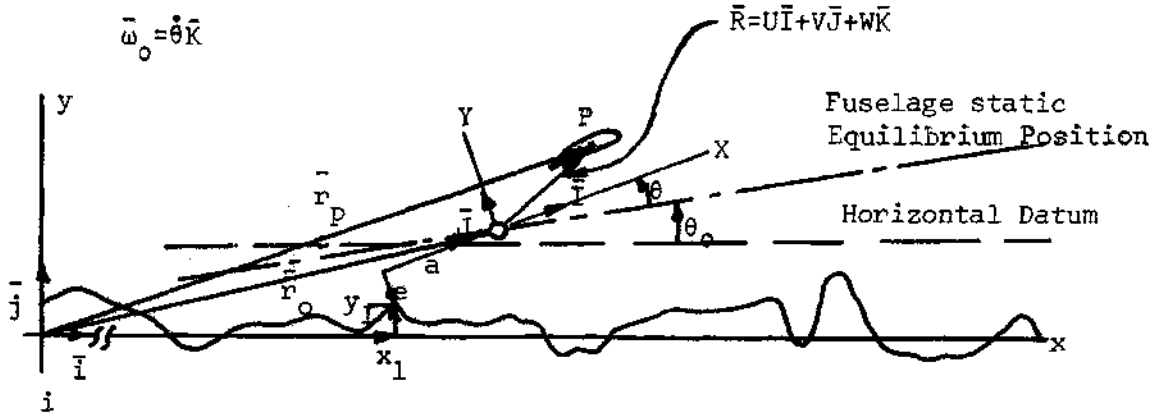

Figure 3.2 Orientations of the Coordinates

In view of the complexities of the airplane geometry, and the external constraint conditions, a logical approach to the derivation of the equations of motion will be the Lagrangean method which requires certain energy expressions. In accord with this trend of thought, the energy functions are obtained in the following.

Kinetic Energy of the Fuselage

Denote the mass of the fuselage by M_f and its mass moment of inertia about the mass center (point 0) by I_{m_f}, then the kinetic energy of the fuselage is

$$T_f = \frac{1}{2}(M_f v_o^2 + I_{m_f}\omega_o^2) \tag{3.3}$$

The v_o^2 term can be obtained by performing the dot product of $\dot{\bar{r}}_o$, the velocity vector of the mass center.*

$$\dot{\bar{r}}_o = \dot{x}_1\bar{I} + \dot{y}_1\bar{J} + \dot{\theta}\bar{k}\times(a\bar{I} + e\bar{J}) \tag{3.4}$$

$$= \dot{x}_1\bar{I} + \dot{y}_1\bar{J} + \dot{\theta}(a\bar{J} - e\bar{I})$$

$$= [\dot{x}_1 - \dot{\theta}(e\cos(\theta_o+\theta) + a\sin(\theta_o+\theta))]\bar{I}$$

$$+ [\dot{y}_1 - \dot{\theta}(e\sin(\theta_o+\theta) + a\cos(\theta_o+\theta))]\bar{J}$$

then

$$v_o^2 = \dot{\bar{r}}_o \cdot \dot{\bar{r}}_o = \dot{x}_1^2 + \dot{y}_1^2 + \dot{\theta}^2(e^2+a^2)$$

$$- 2\dot{x}_1\dot{\theta}[e\cos(\theta_o+\theta) + a\sin(\theta_o+\theta)]$$

$$+ 2\dot{y}_1\dot{\theta}[a\cos(\theta_o+\theta) - e\sin(\theta_o+\theta)]$$

and therefore Equation (3.3) becomes

$$T_f = \tfrac{1}{2}M_f\{\dot{x}_1^2 + \dot{y}_1^2 + \dot{\theta}^2(e^2+a^2) - 2\dot{x}_1\dot{\theta}[e\cos(\theta_o+\theta) \tag{3.5}$$

$$+ a\sin(\theta_o+\theta)] + 2\dot{y}_1\dot{\theta}[a\cos(\theta_o+\theta) - e\sin(\theta_o+\theta)] + \tfrac{1}{2}I_{m_f}\dot{\theta}^2$$

*See Appendix I for the transformation.

Kinetic Energy of the Wing

The wing is a continuous elastic beam and to develop its kinetic energy expression explicitly is comparatively cumbersome. However, there is a customary procedure for small oscillations [45] in which the continuous system is treated as a limiting case of some equivalent discrete system. It is this technique that enables the following development.

Firstly, the wing span is divided into n equal length segments of d each (see Figure 3.3). Assign the displacement coordinates of the individual mass centers to be U_i, V_i, and W_i; i=1,2,$\cdots$,n. Let m, I_{XX}, I_{YY} and I_{ZZ} be the mass, rotary moments of inertia and twist moment of inertia per unit length, respectively. Then, with the subscript i attached to U, V, and W in Equation (3.2), the general position vector $\bar{r}_p$ becomes

$$\bar{r}_{p_i} = x_1\bar{i} + y_1\bar{j} + (a+U_i)\bar{I} + (e+V_i)\bar{J} + W_i\bar{K} \tag{3.6}$$

and the corresponding velocity vector is

$$\bar{v}_{p_i} = \dot{\bar{r}}_{p_i} = \dot{x}_1\bar{i} + \dot{y}_1\bar{j} + \dot{U}_i\bar{I} + \dot{V}_i\bar{J} + \dot{W}_i\bar{K} + \dot{\theta}\bar{K}\times \tag{3.7}$$

$$[(\bar{a}+U_i)\bar{I} + (e+V_i)\bar{J} + W_i\bar{K}]$$

$$= [\dot{x}_1\cos(\theta_o+\theta) + \dot{y}_1\sin(\theta_o+\theta) + \dot{U}_i - \dot{\theta}(e+V_i)]\ \bar{I} +$$

$$[-\dot{x}_1 \sin(\theta_o+\theta) + \dot{y}_1 \cos(\theta_o+\theta) + \dot{V}_i + \dot{\theta}(a+U_i)]\bar{J} + \dot{W}_i\bar{K}$$

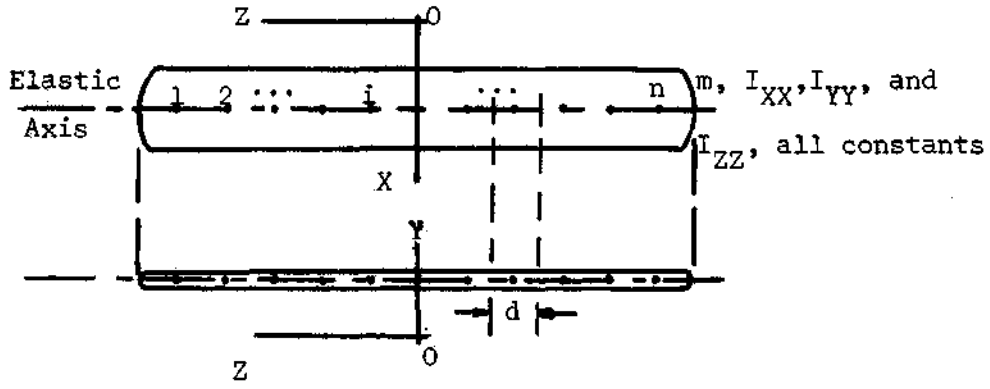

Figure 3.3 Front and Top View of the Wing

Secondly, the angular velocities associated with the rotary effect must be derived. Let ρ and ϕ denote the rotations about the OX and OY axes, respectively. From Figure 3.4, the following approximation is true for two adjacent wing segments.

$$\rho_i \simeq \text{Sin}\ \rho_i \simeq \tan \rho_i = (V_{i+1}-V_i)/d \tag{3.8}$$

and

$$\dot{\rho}_i = (\dot{V}_{i+1}-\dot{V}_i)/d \tag{3.9}$$

Figure 3.4 A Typical Deflection of the Wing Elastic Axis

Similarly,

$$\dot{\phi}_i = -(\dot{U}_{i+1}-\dot{U}_i)/d \tag{3.10}$$

It is clear, for Equations (3.10) and (3.11) to hold, the angles ρ_i and ϕ_i have to be small. These inevitably lead to a third approximation that the local twist angle is merely the sum of θ and θ_{w_i} where θ_{w_i} is the relative twist angle referenced to the wing root.

Thus, the kinetic energy for the entire wing is

$$T_w = \frac{d}{2}\sum_{i=1}^{n}[mv_{p_i}^2 + I_{XX}\dot{\rho}_i^2 + I_{YY}\dot{\phi}_i^2 + I_{ZZ}(\dot{\theta}+\dot{\theta}_{w_i})^2] \tag{3.11}$$

$$= \frac{md}{2}\sum_{i=1}^{n}\{[\dot{x}_1\,\mathrm{Cos}(\theta_o+\theta) + \dot{y}_1\,\mathrm{Sin}(\theta_o+\theta) + \dot{U}_i - \dot{\theta}(e+V_i)]^2$$

$$+ [-\dot{x}_i\mathrm{Sin}(\theta_o+\theta) + \dot{y}_1\mathrm{Cos}(\theta_o+\theta) + \dot{V}_i + \dot{\theta}(a+U_i)]^2 + \dot{W}_i^2$$

$$+ \frac{d}{2}\sum_{i=1}^{n}\{I_{XX}\left(\frac{\dot{V}_{i+1}-\dot{V}_i}{d}\right)^2 + I_{YY}\left(-\frac{\dot{U}_{i+1}-\dot{U}_i}{d}\right)^2 + I_{ZZ}(\dot{\theta}+\dot{\theta}_{w_i})^2\}$$

Potential Energy of the Fuselage

The potential energy of the fuselage is stored in the linear spring of the front gear when the airplane is disturbed from its equilibrium position. The extension or compression exerted on the spring can be visualized from Figure 3.5.

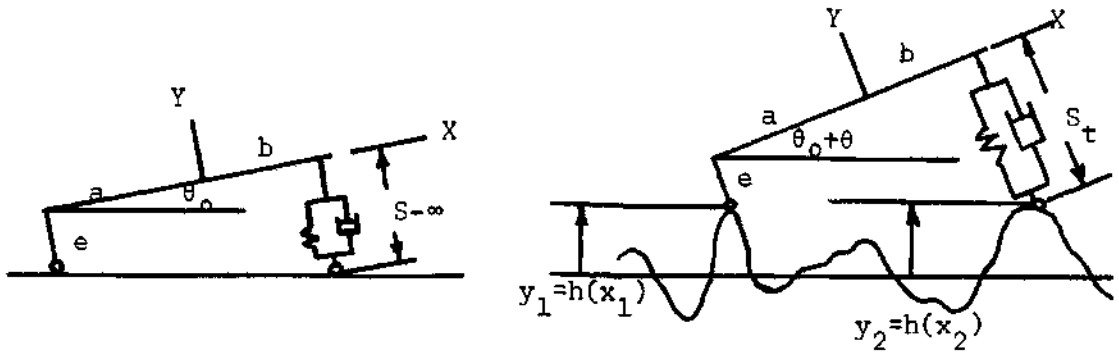

(a) Undisturbed Position (b) Disturbed Position

Figure 3.5 Instantaneous Disposition of the Airplane

In Figure 3.5(a), the airplane rests on a smooth surface and the stroke of the front gear strut is therefore

$$S_{-\infty} = e + (a+b)\tan\theta_o \tag{3.12}$$

However, after some time lapse, say at time t, the airplane is traveling along a rough surface and its instantaneous attitude is exactly as that depicted in Figure 3.5(b). Thus, the stroke becomes

$$S_t = e + (a+b)\tan(\theta_o+\theta) - \frac{y_2 - y_1}{\cos(\theta_o+\theta)} \tag{3.13}$$

from Equations (3.12) and (3.13), it is obvious that the spring displacement is

$$\Delta S = S_t - S_{-\infty} = (a+b)[\tan(\theta_o+\theta) - \tan\theta_o] - \frac{y_2 - y_1}{\cos(\theta_o+\theta)} \qquad (3.14)$$

For small θ, y_1 and y_2, the exact expression of Equation (3.14) can be reduced to

$$\Delta S \approx \frac{(a+b)\theta}{\cos^2\theta_o} - \frac{y_2 - y_1}{\cos\theta_o} \qquad (3.15)^*$$

The potential energy for the fuselage is

$$V_f = \frac{1}{2}k(\Delta S)^2 = \frac{k}{2\cos^2\theta_o}\left[\frac{(a+b)\theta}{\cos\theta_o} - (y_2-y_1)\right]^2 \qquad (3.16)$$

Potential Energy of the Wing

The potential energy of the wing is the total strain energy of the wing.** It is expressed as

$$V_W = \frac{1}{2}\int_{-L}^{L}\left[EI_{YY}\left(\frac{\partial^2 U}{\partial Z^2}\right)^2 + EI_{XX}\left(\frac{\partial^2 V}{\partial Z^2}\right)^2 + GJ\left(\frac{\partial\theta_w}{\partial z}\right)^2\right]dZ \qquad (3.17)$$

where EI_{YY}, EI_{XX}, GJ denote the bending rigidities about the OY, OX axes and torsional rigidity about the OZ-axis, respectively. To be brief, let $EI_{YY} = A$, $EI_{XX} = B$, and $GJ = C$. In anticipation of using U_i, V_i, and W_i; $i=1,2,\cdots,n$ as the generalized coordinates for the

---

*See Appendix II for the detailed derivation.

**[46] pp. 126-127 or [47] pp. 121-127.

wing, Equation (3.17) is converted to the equivalent discrete system by the finite difference approximations [48], therefore Equation (3.17) becomes

$$V_w = \frac{d}{2} \sum_{i=2}^{n} A\left(\frac{U_{i+1} + U_{i-1} - 2U_i}{d^2}\right)^2 + B\left(\frac{V_{i+1} + V_{i-1} - 2V_i}{d^2}\right)^2 \quad (3.18)$$

$$+ \frac{d}{2} \sum_{i=1}^{n} C\left(\frac{\theta_{w_{i+1}} - \theta_{w_i}}{d}\right)^2$$

Dissipation Function

It is further assumed that the only existing dissipative force is that of the viscous damping in the front gear strut. The internal friction within the strut gives a negligible Colomb damping. The wing will contribute no dissipative energy both in the sense of structural* and aerodynamic damping. Hence, the dissipation function is

$$F_c = \frac{1}{2} c (\dot{\overline{\Delta S}})^2 = \frac{c}{2 \cos^2\theta_o}[(a+b)\dot{\theta}/\cos\theta_o - \dot{y}_2 + \dot{y}_1]^2 \quad (3.19)$$

Lagrange's Equation and the Generalized Coordinates

The generalized coordinates for the airplane consist of the quantities below:

---

*[46] Indicates that the damping coefficient, g, for metal aircraft is between .02 and .08 and g is approximately 2ζ where ζ is the conventional viscous damping ratio.

x_1, y_1, y_2 and θ specify the displacements of the fuselage. U_i, V_i, W_i and θ_{w_i} designate the linear and angular displacements for the wing. Let q_j denote the generalized coordinates then for j=1,2,3,$\cdots$,4+4n

$$q_1 = x_1,\ q_2 = y_1,\ q_3 = y_2,\ q_4 = \theta; \tag{3.20}$$

$$q_5 = U_1,\ q_6 = U_2 \cdots q_{4+n} = U_n$$

$$q_{5+n} = V_1,\ q_{6+n} = V_2 \cdots q_{4+2n} = V_n$$

$$q_{5+2n} = W_1,\ q_{6+2n} = W_2 \cdots q_{4+3n} = W_n$$

$$q_{5+3n} = \theta_{w_1},\ q_{6+3n} = \theta_{w_2} \cdots q_{4+4n} = \theta_{w_n}$$

Recall the constraint condition requires that the wheels remain in contact with the rough ground, and denote the abscisas of y_1 and y_2 by x_1 and x_2, respectively (see Figure 3.5(b)), then

$$x_2 = x_1 + \frac{a + b}{\mathrm{Cos}(\theta_o+\theta)} - (y_2-y_1)\tan(\theta_o+\theta) \tag{3.21}$$

Again, remembering the small θ, y_1, y_2 assumption, Equation (3.21) is reduced to the following:

$$x_2 = x_1 + \frac{(a+b)(1+\theta\tan\theta_o)}{\mathrm{Cos}\ \theta_o} - (y_2-y_1)\tan\ \theta_o \tag{3.22}$$

The equations of constraints for y_1, y_2 and x_1 are

$$y_1 = h(x_1) \tag{3.23a}$$

$$y_2 = h(x_2) \tag{3.23b}$$

$$v_x = u \tag{3.23c}$$

where $h(x_1)$ is some known function (deterministic or random) for the ground profile, and u is the forward velocity of the airplane at point 0.

In view of the situation, the Lagrange equations for this treatise will have the form*

$$\frac{d}{dt}\frac{\partial L}{\partial \dot{q}_j} - \frac{\partial L}{\partial q_j} + \frac{\partial F}{\partial \dot{q}_j} = \sum_k \lambda_k a_{kj}, \quad \begin{matrix} j=1,2,\cdots,4+4n \\ k=1,2,3 \end{matrix} \tag{3.24}$$

where $L = T - V$, and F is the dissipation function, and the λ_k's can be obtained from Equation (3.24), together with

$$\sum_j a_{kj} dq_j + a_{kt} dt = 0 \tag{3.25}$$

and

$$\sum_j \frac{\partial f_k}{\partial q_j} dq_j + \frac{\partial f_k}{\partial t} dt = 0 \tag{3.26}$$

---

*See [45] pp. 14-22 and pp. 38-42.

with $f_k = f(q_1, q_2, \cdots, q_{4+4n}, t) = 0$, some functions to be constructed from the constraint equations.

From Equations (3.23a-3.23c), it is clear that k=1,2,3 for the λ_k's, and Equations (3.25) and (3.26) show that the coefficients have the following relations

$$a_{kj} = \frac{\partial f_k}{\partial q_j}, \quad a_{kt} = \frac{\partial f_k}{\partial t} \tag{3.27}$$

As an example, Equation (3.23a) is used to illustrate the procedure.

$$f_1 = y_1 - h(x_1) = 0 \tag{3.28}$$

substitute Equation (3.28) into Equation (3.26), the result becomes

$$dy_1 - \frac{\partial h}{\partial x_1} dx_1 = 0 \tag{3.29}$$

which clearly identifies

$$a_{11} = a_{1x_1} = -\frac{\partial h}{\partial x_1}, \quad a_{12} = a_{1y_1} = 1, \quad \text{and} \quad a_{1t} = 0 \tag{3.30}$$

similarly,

$$f_2 = y_2 - h(x_2) = y_2 - h(x_1, y_1, y_2, \theta) = 0 \tag{3.31}$$

gives:

$$a_{21} = a_{2x_1} = -\frac{\partial h}{\partial x_2}$$

$$a_{22} = a_{2y_1} = -\frac{\partial h}{\partial x_2}\tan\theta_o \qquad (3.32)$$

$$a_{23} = a_{2y_2} = +\frac{\partial h}{\partial x_2}\tan\theta_o + 1$$

$$a_{24} = a_{2\theta} = -\frac{\partial h}{\partial x_2}\,\frac{(a+b)}{\text{Cos }\theta_o}\tan\theta_o$$

for $f_3 = 0$ Equation (3.23c) specifies that $v_x=u$, from Equation (3.4) and identify the x component by u then

$$\dot{x}_1 - \dot{\theta}[e\ \text{Cos}(\theta_o+\theta) + a\ \text{Sin}(\theta_o+\theta)] - u = 0 \qquad (3.33a)$$

or

$$dx_1 - d\theta[e\ \text{Cos}(\theta_o+\theta) + a\ \text{Sin}(\theta_o+\theta)] - udt = 0 \qquad (3.33b)$$

which gives

$$a_{31} = a_{3x_1} = 1 \qquad (3.34)$$

$$a_{34} = a_{3\theta} = -[e\ \text{Cos}(\theta_o+\theta) + a\ \text{Sin}(\theta_o+\theta)]$$

$$a_{3t} = -u$$

From Equations (3.5, 3.11, 3.16, 3.18, and 3.19) the kinematic energy, potential energy, and dissipation functions for the airplane are, respectively,

$$T = T_f + T_w \tag{3.35}$$

$$V = V_f + V_w$$

$$F = F_c$$

After some work,* the Lagrange equations in the form of Equation (3.24) are obtained for the x, y_1, y_2, θ , U, V, W, and θ_w coordinates. These equations are shown below.

$$M[\ddot{x}_1 - \ddot{\theta}(e \cos \theta_o + a \sin \theta_o)] + m[\cos \theta_o \int_{-L}^{L} \ddot{U} dz - \sin \theta_o \int_{-L}^{L} \ddot{V} dz]$$

$$= \lambda_1 \frac{\partial h}{\partial x_1} - \lambda_2 \frac{\partial h}{\partial x_2} + \lambda_3 \tag{3.36}$$

$$M[\ddot{y}_1 + \ddot{\theta}(a \cos \theta_o - e \sin \theta_o)] + m[\sin \theta_o \int_{-L}^{L} \ddot{U} dz + \cos \theta_o \int_{-L}^{L} \ddot{V} dZ]$$

$$+ \frac{1}{\cos^2 \theta_o} \left\{ k \left[\frac{(a+b)\theta}{\cos \theta_o} + y_1 - y_2 \right] + c \left[\frac{(a+b)\dot{\theta}}{\cos \theta_o} + \dot{y}_1 - \dot{y}_2 \right] \right)$$

---

*See Appendix III for the differentiations and linearizations.

$$= \lambda_1 - \lambda_2 \frac{\partial h}{\partial x_2} \tan \theta_o \tag{3.37}$$

$$- \frac{1}{\cos^2\theta_o} \left(k\left[\frac{(a+b)\theta}{\cos \theta_o} + y_1 - y_2\right] + c\left[\frac{(a+b)\dot{\theta}}{\cos \theta_o} + \dot{y}_1 - \dot{y}_2\right]\right) \tag{3.38}$$

$$= \lambda_2\left(\frac{\partial h}{\partial x_2} \tan \theta_o + 1\right)$$

$$[Ma^2 + (m_f - m_w)e^2 + I_{m_f} + 2LI_{ZZ}]\ddot{\theta} - M[\ddot{x}_1(e \cos \theta_o + a \sin \theta_o) \tag{3.39}$$

$$- \ddot{y}_1(a \cos \theta_o - e \sin \theta_o)] + m[a \int_{-L}^{L} \ddot{V} dZ - e \int_{-L}^{L} \ddot{U} dZ]$$

$$+ I_{ZZ} \int_{-L}^{L} \ddot{\theta}_w dZ + \frac{1}{\cos^2\theta_o} \left(k\left[\frac{(a+b)\theta}{\cos \theta_o} + y_1 - y_2\right] + c\left[\frac{(a+b)\dot{\theta}}{\cos \theta_o} + \dot{y}_1 - \dot{y}_2\right]\right)$$

$$= - \lambda_2 \frac{\partial h}{\partial x_2} \frac{(a+b)\tan \theta_o}{\cos \theta_o} - \lambda_3(e \cos \theta_o + a \sin \theta_o)$$

$$A \frac{\partial^4 U}{\partial z^4} - I_{YY} \frac{\partial^4 U}{\partial t^2 \partial Z^2} + m(\ddot{x}_1 \cos \theta_o + \ddot{y}_1 \sin \theta_o + \ddot{U} - \ddot{\theta} e) = 0 \tag{3.40}$$

$$B \frac{\partial^4 V}{\partial Z^4} - I_{XX} \frac{\partial^4 V}{\partial t^2 \partial Z^2} + m(- \ddot{x}_1 \sin \theta_o + \ddot{y}_1 \cos \theta_o + \ddot{V} + \ddot{\theta} a) = 0 \tag{3.41}$$

$$\ddot{W} = 0 \tag{3.42}$$

$$c \frac{\partial^2 \theta_w}{\partial Z^2} - I_{ZZ}(\ddot{\theta}+\ddot{\theta}_w) = 0 \qquad (3.43)$$

where $m_w = 2Lm$ = mass of the wing

$M = m_f + m_w$ = total mass of the airplane and the i's are dropped from these equations as they have been converted back to a continuous system.

Equations (3.36-43) are the linearized equations of motion of the airplane. The sole assumption so far employed in their derivations is that of small oscillations. However, from an engineering viewpoint, further simplifications are allowed through the dimensions of the wing section. It is recognized that $A >> B(EI_{YY} >> EI_{XX})$, $C >> B(GJ >> EI_{XX})$, $A >> I_{YY}$, $B >> I_{XX}$, $C >> I_{ZZ}$ and $e \to 0$. Thus Equations (3.40, 3.41, and 3.43) are reduced to

$$\frac{\partial^4 U}{\partial Z^4} = 0 \qquad (3.44)$$

$$B \frac{\partial^4 V}{\partial Z^4} + m(-\ddot{x}_1 \text{ Sin } \theta_o + \ddot{y}_1 \text{ Cos } \theta_o + \ddot{\theta}a + \ddot{V}) = 0 \qquad (3.45)$$

$$\frac{\partial^2 \theta_w}{\partial Z^2} = 0 \qquad (3.46)$$

From the initial and boundary conditions for Equations (3.44 and 3.46), it is found that U and θ_w are identically zero. Hence, a significant reduction in the wing motion results. The only nontrivial equation is that of V.

Equations (3.36, 3.37, 3.38, and 3.39) are combined into one through the aid of the λ's and the physical structure of the ground profiles. It is acceptable to assume that $\frac{\partial h}{\partial x_1}$ and $\frac{\partial h}{\partial x_2}$ are of the order of y_1, y_2 and θ, so that the quadratic terms are negligible,* which leads to

$$(Ma^2 \cos^2 \theta_o + I_{m_f} + 2LI_{ZZ})\ddot{\theta} + c\frac{(a+b)^2}{\cos^4 \theta_o}\dot{\theta} + k\frac{(a+b)^2}{\cos^4 \theta_o}\theta \qquad (3.47)$$

$$+ ma \cos^2 \theta_o \int_{-L}^{L} \ddot{V} dZ = -Ma \cos \theta_o \ddot{y}_1 - \frac{a+b}{\cos^3 \theta_o}[c(\dot{y}_1 - \dot{y}_2)$$

$$+ k(y_1 - y_2)]$$

From Equations (3.45) and (3.47), it is obvious that V and θ are coupled and they cannot be solved independently. Equation (3.45) is rearranged below

$$B\frac{\partial^4 V}{\partial Z^4} + m\ddot{V} = m(\ddot{x}_1 \sin \theta_o - \ddot{y}_1 \cos \theta_o - \ddot{\theta}a) \qquad (3.48)$$

It is readily identified that the above is the differential equation of a vibrating beam with a somewhat complicated forcing function. However, the right-hand side can be simplified by using Equation (3.33a). If Equation (3.33a) is differentiated with respect to time, the following

---

*See [23] for some typical runway roughnesses and also see Appendix II.

is obtained

$$\ddot{x}_1 - \ddot{\theta}a \text{ Sin } \theta_o = 0 \tag{3.49}$$

Thus, Equation (3.48) becomes

$$B\frac{\partial^4 V}{\partial Z^4} + m\ddot{v} = m[\ddot{\theta}a(\text{Sin}^2\ \theta_o - 1) - \ddot{y}_1 \text{ Cos } \theta_o] \tag{3.48a}$$

$$= m[\ddot{\theta}a \text{ Cos}^2\ \theta_o - \ddot{y}_1 \text{ Cos } \theta_o]$$

The solution of Equation (3.48a) consists of two parts: (i) The homogeneous (free vibration) solution, and (ii) the particular (forced vibration) solution. Since Equation (3.48a) is a separable partial differential equation, the form of the complimentary V will be

$$V_c(Z,t) = \sum_{n=1}^{\infty} f_n(Z)e^{-j\omega_n t} \tag{3.50}$$

substitute Equation (3.50) into the left-hand side of Equation (3.49) and let the right-hand side = 0 yields

$$\sum_{n=1}^{\infty} e^{-j\omega_n t}[-m\omega_n^2 f_n(Z) + Bf_n^{IV}(Z)] = 0 \tag{3.51}$$

Let $m\omega_n^2/B = \lambda_n^4$ and recognize that $e^{-j\omega_n t} \neq 0$. Then

$$f_n^{IV}(Z) - \lambda_n^4 f_n(Z) = 0 \tag{3.52}$$

$f_n(Z)$ has the solution in the form of the following

$$f_n(Z) = A_1 \text{ Cos } \lambda_n Z + A_2 \text{ Sin } \lambda_n Z + A_3 \text{ Cosh } \lambda_n Z + A_4 \text{ Sinh } \lambda_n Z \tag{3.53}$$

The boundary conditions for Equation (3.52) are

$$f_n(0) = 0 \tag{3.54a}$$

$$f_n'(0) = 0 \tag{3.54b}$$

$$f_n''(L) = 0 \tag{3.54c}$$

$$f_n'''(L) = 0 \tag{3.54d}$$

Equations (3.54a) and (3.54b) give

$$A_1 + A_3 = 0 \tag{3.55a}$$

$$A_2 + A_4 = 0 \tag{3.55b}$$

Equations (3.54c) and (3.54d) require

$$-A_1\lambda_n^2\text{Cos }\lambda_nL - A_2\lambda_n^2\text{Sin }\lambda_nL + A_3\lambda_n^2\text{Cosh }\lambda_nL + A_4\lambda_h^2\text{Sinh }\lambda_nL = 0 \qquad (3.55c)$$

$$A_1\lambda_n^3\text{Sin }\lambda_nL - A_2\lambda_n^3\text{Cos }\lambda_nL + A_3\,\lambda_n^3\text{Sinh }\lambda_nL \qquad (3.55d)$$

$$+ A_4\lambda_n^3\text{Cosh }\lambda_nL = 0$$

combine Equations (3.55a - d) yields two equations

$$A_1(\text{Cos }\lambda_nL + \text{Cosh }\lambda_nL) + A_2(\text{Sin }\lambda_nL + \text{Sinh }\lambda_nL) = 0 \qquad (3.56a)$$

$$A_1(\text{Sin }\lambda_nL - \text{Sinh }\lambda_nL) - A_2(\text{Cos }\lambda_nL + \text{Cosh }\lambda_nL) = 0 \qquad (3.56b)$$

for A_1 and $A_2 \neq 0$, the following must hold

$$\begin{vmatrix} (\text{Cos }\lambda_nL + \text{Cosh }\lambda_nL) & (\text{Sin }\lambda_nL + \text{Sinh }\lambda_nL) \\ (\text{Sin }\lambda_nL - \text{Sinh }\lambda_nL) & -(\text{Cos }\lambda_nL + \text{Cosh }\lambda_nL) \end{vmatrix} = 0 \qquad (3.57)$$

or

$$(\text{Cos }\lambda_nL + \text{Cosh }\lambda_nL)^2 + \text{Sin}^2\,\lambda_nL - \text{Sinh}^2\lambda_nL = 0$$

$$\text{Cos}^2\lambda_nL + 2\,\text{Cos }\lambda_nL\,\text{Cosh }\lambda_nL + \text{Cosh}^2\,\lambda_nL + \text{Sin}^2\,\lambda_nL - \text{Sinh}^2\lambda_nL = 0$$

$$2 \text{ Cos } \lambda_n L \text{ Cosh } \lambda_n L = -2$$

or

$$\text{Cos } \lambda_n L = \frac{-1}{\text{Cosh } \lambda_n L} \tag{3.58}$$

Equation (3.58) can be solved graphically for values of $\lambda_1, \lambda_2, \cdots$ and all $f_n(Z)$ will be obtainable.

To solve the forced vibration part, it is assumed that the particular V will have the form

$$V_p(Z,t) = \sum_{n=1}^{\infty} f_n(Z) c_n(t) \tag{3.59}$$

and the forcing function is

$$-m(\ddot{\theta} a \text{ Cos}^2\theta_o + \ddot{y}_1 \text{ Cos } \theta_o) = \sum_{n=1}^{\infty} f_n(Z) A_n(t) \tag{3.60}$$

substituting Equations (3.59) and (3.60) into Equation (3.49) gives

$$\sum_{n=1}^{\infty} m\ddot{c}_n(t) f_n(Z) + B c_n(t) \lambda_n^4 f_n(Z) = \sum_{n=1}^{\infty} A_n(t) f_n(Z) \tag{3.61}$$

or

$$\ddot{c}_n(t) + \omega_n^2 c_n(t) = A_n(t)/m \tag{3.62}$$

Remember the orthogonality condition of $f_n(Z)$ (i.e., $\int_0^L f_m(Z)f_n(Z)dZ = 0$, $m \neq n$) and let

$$\int_0^L f_n^2(Z)dZ = \frac{1}{B_n} \tag{3.63}$$

$A_n(t)$ is readily obtained from Equation (3.60) and

$$A_n(t) = -mB_n(\ddot{\theta}(t)a\,\mathrm{Cos}^2\theta_o + \ddot{y}_1(t)\mathrm{Cos}\,\theta_o)\int_0^L f_n(Z)dZ \tag{3.64}$$

The solution of Equation (3.62) has the form

$$c_n(t) = c_1\,\mathrm{Sin}\,\omega_n t + c_2\,\mathrm{Cos}\,\omega_n t + \frac{1}{m}\int_0^t h_n(t,\tau)A_n(\tau)d\tau \tag{3.65}$$

The initial conditions for V are

$$V(Z,0) = \dot{V}(Z,0) = 0, \text{ or } c_n(0) = \dot{c}_n(0) = 0 \tag{3.66}$$

Therefore $c_1 = c_2 = 0$ and

$$c_n(t) = \frac{1}{m}\int_0^t h_n(t,\tau)A_n(\tau)d\tau \tag{3.67}$$

where $h_n(t,\tau)$ = the impulse response (weighting) function

$$= \frac{1}{\omega_n} \text{Sin } \omega_n(t-\tau) \quad * \tag{3.68}$$

From Equations (3.67), (3.64), and (3.59), the solution for $V_p(Z,t)$ is

$$V_p(Z,t) \sum_{n=1}^{\infty} - \frac{B_n}{\omega_n} \int_0^t \text{Sin } \omega_n(t-\tau)[\ddot{y}_1 \text{ Cos } \theta_o + a \text{ Cos}^2 \theta_o] \int_0^L f_n(Z)dZ$$

$$d\tau \; f_n(Z)$$

$$= \sum_{n=1}^{\infty} - \frac{B_n}{\omega_n} \int_0^t \text{Sin } \omega_n(t-\tau)[\ddot{y}_1(\tau) \text{ Cos } \theta_o + \ddot{\theta}(\tau)a \text{ Cos}^2 \theta_o]d\tau \tag{3.69}$$

$$\int_0^L f_n(Z)dZ \; f_n(Z)$$

The solution of V is therefore

$$V(z,t) = \sum_{n=1}^{\infty} [e^{-j\omega_n t} - \frac{B_n}{\omega_n} \int_0^L f_n(Z)dZ \int_0^t \text{Sin } \omega_n(t-\tau) \tag{3.70}$$

$$[\ddot{y}_1(\tau) \text{ Cos } \theta_o + \ddot{\theta}(\tau)a \text{ Cos}^2\theta_o]d\tau]f_n(Z)$$

$\ddot{V}(Z,t)$ can be obtained by applying the Leibnitz rule to Equation (3.70). After some work, the following is obtained

$$\ddot{V}(Z,t) = \sum_{n=1}^{\infty} \{-\omega_n^2 e^{-j\omega_n t} + \frac{B_n}{\omega_n} \int_0^L f_n(Z)dZ[\omega_n^2 \int_0^t \text{Sin } \omega_n(t-\tau) \tag{3.71}$$

---

*See Appendix IV for derivation.

$$(\ddot{y}_1(\tau)\ \mathrm{Cos}\ \theta_o + \ddot{\theta}(\tau)a\ \mathrm{Cos}^2\theta_o)d\tau - (\ddot{y}_1(t)\ \mathrm{Cos}\ \theta_o +$$

$$\ddot{\theta}(t)a\ \mathrm{Cos}^2\ \theta_o)]\}f_n(Z)$$

Let

$$\left.\begin{aligned} Ma^2\mathrm{Cos}^2\theta_o + I_{m_f} + 2LI_{ZZ} &= a_2 \\ c(a+b)^2/\mathrm{Cos}^4\theta_o &= a_1 \\ k(a+b)^2/\mathrm{Cos}^4\theta_o &= a_0 \\ Ma\ \mathrm{Cos}\ \theta_o &= b_2 \\ c(a+b)/\mathrm{Cos}^3\ \theta_o &= b_1 \\ k(a+b)/\mathrm{Cos}^3\theta_o &= b_0 \end{aligned}\right\} \qquad (3.72)$$

Then Equation (3.47) becomes

$$a_2\ddot{\theta} + a_1\dot{\theta} + a_o\theta + ma\ \mathrm{Cos}^2\theta_o \int_{-L}^{L} \ddot{V}dZ \qquad (3.73)$$

$$= -b_2\ddot{y}_1 - b_1(\dot{y}_1-\dot{y}_2) - b_o(y_1-y_2)$$

Since the boundary conditions of V are for symmetric modes. The $f_n(Z)$'s are all symmetric, hence

$$\int_{-L}^{L} f_n(Z)dZ = 2\int_{0}^{L} f_n(Z)dZ \tag{3.74}$$

and let

$$2ma\ \mathrm{Cos}^2\theta_o\ \omega_n^2 \int_0^L f_n(Z)dZ = g_n$$

$$2ma\ \mathrm{Cos}^2\ \theta_o B_n[\int_0^L f_n(Z)dZ]^2/\omega_n = d_n$$

Then Equation (3.73) becomes

$$a_2\ddot{\theta} + a_1\dot{\theta} + a_o\theta = \sum_{n=1}^{\infty} g_n e^{-j\omega_n t} - d_n[\omega_n^2 \int_0^t \mathrm{Sin}\ \omega_n(t-\tau) \tag{3.75}$$

$$(\ddot{y}_1(\tau)\ \mathrm{Cos}\ \theta_o + \ddot{\theta}(\tau)a\ \mathrm{Cos}^2\theta_o)d\tau - (\ddot{y}_1(t)\mathrm{Cos}\ \theta_o$$

$$+ \ddot{\theta}(t)a\ \mathrm{Cos}^2\theta_o)] - b_2\ddot{y}_1 - b_1(\dot{y}_1-\dot{y}_2) - b_o(y_1-y_2)$$

Rearranging terms, Equation (3.75) becomes

$$(a_2 + \sum_{n=1}^{\infty} d_n a\ \mathrm{Cos}^2\theta_o)\ddot{\theta} + a_1\dot{\theta} + a_o\theta \tag{3.76}$$

$$= (\sum_{n=1}^{\infty} d_n\ \mathrm{Cos}\ \theta_o - b_2)\ddot{y}_1 - b_1(\dot{y}_1-\dot{y}_2) - b_o(y_1-y_2)$$

$$+ \sum_{n=1}^{\infty} \{g_n e^{-j\omega_n t} - d_n \omega_n^2 [\int_0^t \text{Sin } \omega_n(t-\tau)(\ddot{y}_1(\tau)\text{Cos } \theta_o$$

$$+ \ddot{\theta}(\tau) a \text{ Cos}^2 \theta_o) d\tau]\}$$

Equation (3.76) is the integro-differential equation for the rotation of the airplane. The forcing functions y_1 and y_2 are specified by a stochastic process $\{h(x)\}$ where $h(x)$'s are deterministic functions of the ground profiles. To elaborate the point further, y_1 is chosen to take on the values of $h^{(i)}(x_1)$, a given ground profile, hence

$$y_1 = h^{(i)}(x_1) \tag{3.77}$$

where x_1 is the abscissa of the tail wheel and is obtained from the solution of Equation (3.33a) and the initial conditions

$$x_1(0) = 0 \tag{3.78a}$$

and

$$\theta(0) = \Theta_o = \text{a random variable} \tag{3.78b}$$

Equation (3.78a) implies that the airplane starts to traverse the given profile at the origin of the profile, and Equation (3.78b) specifies

the airplane has an arbitrary inclination θ_o at t = 0.

From Equations (3.33a), (3.78a), and (3.78b), x_1 is obtained. It is

$$x_1(t) = ut + a \text{ Sin } \theta_o(\theta(t)-\theta_o) \tag{3.79}$$

Therefore

$$y_1 = h^{(i)}(x_1) = h^{(i)}[x_1(\theta,\theta_0;ut)]$$

or y_1 is a function of the random variables θ, θ_o.

Thus, Equation (3.76) must be solved by special methods. Since it is a linear system, the power spectral method will be a convenient one to use.

Derivation of the Transfer Function

It is well known that there are three methods [49] to obtain the output response of a linear system. They are outputs produced by special types of inputs. The terminology is somewhat confusing as a result of the fact that various engineering disciplines tend to adhere to their own usages. In view of this situation, it is essential to define the terms that are fundamental in the following passages. The three modes of description of the system are listed below.

(i) The impulse response function* (or the weighting function)

---

*These terms are mostly used by non-electrical engineering personnel and are comparatively standard to dynamics or vibrations engineers.

is the output produced by a unit impulse input and is related to the output produced by a step input.

(ii) The mechanical admittance* or the frequency response function relates a sinusoidal input to the output that it produces.

(iii) The transfer function* or the system function relates the complex amplitudes of the output and input. It is a generalization of (ii). The mathematical formulations of these functions and their relations to each other are presented without proof** in the following:

(i) Let $y(t)$ = the output response of a linear time-invariant system.

$x(t)$ = the input forcing function to the same system.

$h(t-\tau)$ = the impulse response function of the same system.

Then

$$y(t) = \int_{-\infty}^{t} x(\tau)h(t-\tau)d\tau = \int_{-\infty}^{t} x(t-\tau)h(\tau)d\tau \qquad (3.80a)$$

and

$$y(t) = h(t) \qquad (3.80b)$$

when $x(t-\tau) = \delta(t-\tau)$.

---

*This term is mostly used by non-electrical engineering personnel and is comparatively standard to dynamics or vibrations engineers.

**See [47,50].

(ii) Let $Y(j\omega)$ = the output response of a linear time-invariant system.

$X(j\omega)$ = the input forcing function to the same system.

$H(j\omega)$ = the frequency response function of the same system.

Then

$$Y(j\omega) = H(j\omega)X(j\omega)$$

and

$$Y(j\omega) = H(j\omega)$$

when

$$X(j\omega) = e^{j\omega t}$$

also $X(j\omega)Y(j\omega)$ and $H(j\omega)$ are merely the Fourier transforms of $x(t)$, $y(t)$ and $h(t)$ of (i), respectively. For example

$$X(j\omega) = \frac{1}{2\pi}\int_{-\infty}^{\infty} x(t)e^{-j\omega t}dt \qquad (3.81a)$$

$$X(t) = \int_{-\infty}^{\infty} X(j\omega)e^{+j\omega t}d\omega \qquad (3.81b)$$

(iii) Let $Y(s)$ = the Laplace transform of the output response of a linear time-invariant system.

X(s) = the Laplace transform of the input forcing function to the same system.

T(s) = the Laplace transform of the impulse response function of the same system; or more simply

$$T(s) = Y(s)/X(s)$$

For example

$$T(s) = \int_0^\infty h(t)e^{-st}dt \tag{3.82}$$

and if $x(t) = \delta(t)$ then from the definition of Laplace transform

$$X(s) = \int_0^\infty \delta(t)e^{-st}dt = 1$$

and $y(t) = \int_{-\infty}^{t} \delta(\tau)h(t-\tau)d\tau = h(t)$ from the first integral of Equation (3.80a) from which $Y(s) = \int_0^\infty y(t)e^{-st}dt = \int_0^\infty h(t)e^{-st}dt = T(s)/1$. Thus it is shown that transfer function and frequency response are quite similar in nature. In fact, it is well known that the frequency response function and the transfer function are identical for a physically realizable system (i.e., a system with $h(t) = 0$ for $t<0$). This is obvious from the Fourier transform (see Equation (3.81a)) of $h(t)$ for

$$H(j\omega) = \int_{-\infty}^{\infty} h(t)e^{-j\omega t}dt = \int_0^\infty h(t)e^{-j\omega t}dt \quad \text{if} \quad h(t) = 0 \text{ for } t<0$$

If $j\omega$ equals s, the above is exactly the same as Equation (3.82). In order to obtain the transfer function for θ, we apply the Laplace transform to Equation (3.76). However, before this step is carried out, the initial conditions on $y_1(t)$, $y_2(t)$ and $\theta(t)$ must be defined.

It is understood that $y_1(t)$ and $y_2(t)$ are the ground profiles defined in the temporal domain (see Equation (3.79)) and hence for a particular set of realizations of $y_1(t)$, $y_2(t)$ and $\theta(t)$ the following time traces are typical.

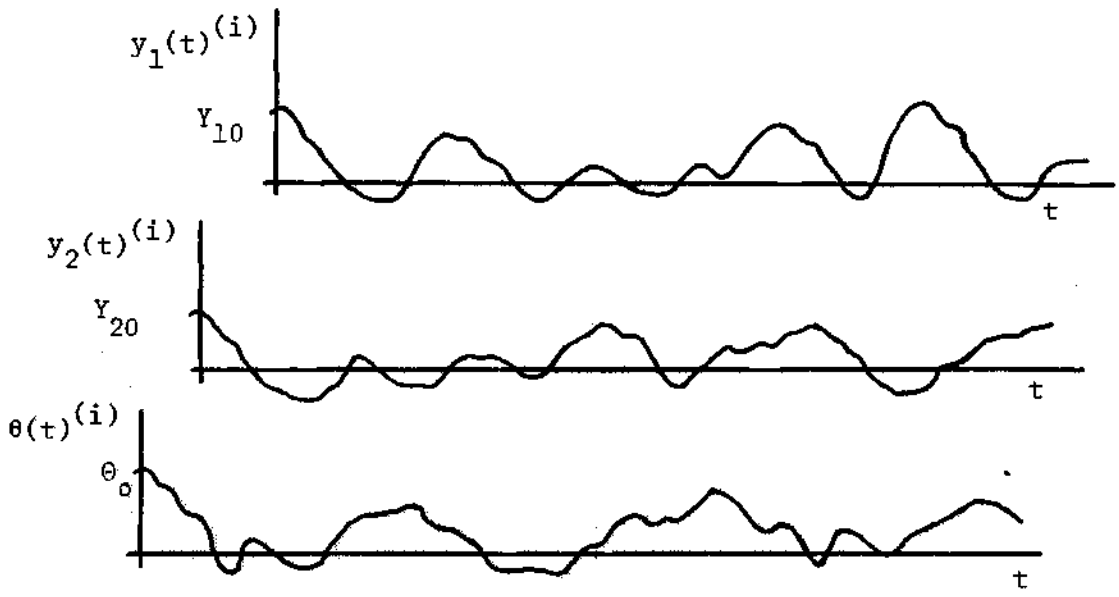

Figure 3.6. A Typical Set of Time Histories

Thus, it is permissible to assign

$$y_1(0) = Y_{10}, \qquad y_2(0) = Y_{20}, \qquad \text{and} \qquad \theta(0) = \theta_o \tag{3.83}$$

where Y_{10}, Y_{20}, θ_o are three random variables specifying the position of the airplane at t = 0. The initial conditions for $\dot{y}_1$, $\dot{y}_2$, and $\dot{\theta}$ are those for the airplane at rest or

$$\dot{y}_1(0) = \dot{y}_2(0) = \theta(0) = 0 \tag{3.84}$$

Taking the Laplace transform of Equation (3.76) and denoting $L\{\theta\}$ by Θ, $L\{y_1\}$ by Y_1 and $L\{y_2\}$ by Y_2 together with Equations (3.83) and (3.84), the following is obtained.

$$(a_2 + \sum_{n=1}^{\infty} d_n a \cos^2\theta_o)(s^2\Theta - s\theta_o) + a_1(s\Theta - \theta_o) + a_o\Theta \tag{3.85}$$

$$= (\sum_{n=1}^{\infty} d_n \cos\theta_o - b_2)(s^2Y_1 - sY_{10}) - b_1(sY_1 - Y_{10} - sY_2 + Y_{20})$$

$$- b_o(Y_1 - Y_2) + \sum_{n=1}^{\infty} \{g_n \frac{1}{sj\omega_n} - d_n\omega_n^2[\cos\theta_o \left(\frac{s^2Y_1 - sY_{10}}{s^2 + s_n^2}\right)$$

$$+ a\cos^2\theta_o \left(\frac{s^2\theta - s\theta_o}{s^2 + \omega_n^2}\right)$$

Anticipating to use the frequency response function rather than the transfer function, the variable "s" is changed into $j\omega$. The part that $h(t) = 0$, $t<0$ has not rendered any difficulty, since it is clear that the airplane will have no response of any kind prior to taxiing on a rough surface.

Carrying out the substitution and rearranging of the terms, Equation (3.85) becomes

$$\{-\omega^2[a_2 + \sum_{n=1}^{\infty} d_n a \cos^2\theta_o(1+\omega_n^2/\omega_n^2-\omega^2)] + j\omega a_1 + a_o\}\theta$$

$$= \{j\omega[a_2 + \sum_{n=1}^{\infty} d_n a \cos^2\theta_o(1 + \omega_n^2/\omega_n^2-\omega^2)] + a_1\}\theta_o$$

$$+ \{-\omega^2[\sum_{n=1}^{\infty} d_n \cos\theta_o(1 - \omega_n^2/\omega_n^2-\omega^2) - b_2] - j\omega b_1 - b_o\}Y_1$$

$$- j\omega[\sum_{n=1}^{\infty} d_n \cos\theta_o(1 - \omega_n^2/\omega_n^2-\omega^2) - b_2] - b_1\}Y_{10}$$

$$+ \{j\omega b_1 + b_o\}Y_2 - b_1 Y_{20} + \sum_{n=1}^{\infty} \{g_n/j(\omega-\omega_n)\}1 \qquad (3.86)$$

It is immediately observed that the linear system is not the ordinary single-input system, but a multiple-input system. Nevertheless, the frequency response is still applicable by virtue of the superposition principle of linear systems.* It is asserted that the output response will have the form

$$\theta(t) = \sum_{n=1}^{6} \theta_n(t)$$

where $\theta_1(t) = \theta_{\theta_o}(t)$ = output due to θ_o input

---

*See [44], p. 178.

$\theta_2(t) = \theta_{Y_1}(t)$ = output due to Y_1 input

$\theta_3(t) = \theta_{Y_{10}}(t)$ = output due to Y_{10} input

$\theta_4(t) = \theta_{Y_2}(t)$ = output due to Y_2 input

$\theta_5(t) = \theta_{Y_{20}}(t)$ = output due to Y_{20} input, and

$\theta_6(t) = \theta_1(t)$ = output due to unit input.

It is further defined that the nth frequency response function is

$$H_n(j\omega) = \Theta_n(j\omega)/F_n(j\omega) \tag{3.87}$$

where $n = 1,2,\cdots,6$ and

$$F_1(j\omega) = \Theta_o$$

$$F_2(j\omega) = Y_1(j\omega)$$

$$\vdots$$

$$F_6(j\omega) = 1(j\omega) = \frac{1}{2\pi} \int_{-\infty}^{\infty} 1e^{-j\omega t}\, dt = \delta(\omega)$$

Hence the six frequency response functions are

$$H_1(j\omega) = H_{\theta_o}(j\omega) = \frac{j\omega[a_2 + \sum_{n=1}^{\infty} d_n a \cos^2\theta_o(1+\omega_n^2/\omega_n^2-\omega^2)] + a_1}{-\omega^2[a_2 + \sum_{n=1}^{\infty} d_n a \cos^2\theta_o(1+\omega_n^2/\omega_n^2-\omega^2) + j\omega a_1 + a_o}$$

$$= \frac{j\omega[a_2 + \sum_{n=1}^{\infty} d_n a \cos^2\theta_o(1+\omega_n^2/\omega_n^2-\omega^2)] + a_1}{D} \quad (3.87a)$$

$$H_2(j\omega) = H_{Y_1}(j\omega) = \frac{-\omega^2[\sum_{n=1}^{\infty} d_n \cos\theta_o(1-\omega_n^2/\omega_n^2-\omega^2) - b_2] - j\omega b_1 - b_o}{D} \quad (3.87b)$$

$$H_3(j\omega) = H_{Y_{1O}}(j\omega) = \frac{-j\omega[\sum_{n=1}^{\infty} d_n \cos\theta_o(1-\omega_n^2/\omega_n^2-\omega^2) - b_2] + b_1}{D} \quad (3.87c)$$

$$H_4(j\omega) = H_{Y_2}(j\omega) = \frac{j\omega b_1 + b_o}{D} \quad (3.87d)$$

$$H_5(j\omega) = H_{Y_{2O}}(j\omega) = \frac{-b_1}{D} \quad (3.87e)$$

and

$$H_6(j\omega) = H_1(j\omega) = \frac{\sum_{n=1}^{\infty} g_n/j(\omega-\omega_n)}{D} \quad (3.87f)$$

With the frequency response functions obtained, the output power spectrum $\Phi_{\theta\theta}(\omega)$ can be expressed in terms of Equations (3.87a-f) and

the power and cross spectra of the input forcing functions. If $\Phi_{mn}(\omega)$ denotes the cross spectra when $m \neq n$ and the power spectra when $m=n$ then

$$\Phi_{\theta\theta}(\omega) \approx \sum_{m,n=1}^{6} H_m(j\omega)H_n^*(j\omega)\Phi_{mn}(\omega) \qquad (3.88)$$

If it is assumed that only Y_1 and Y_2 are correlated (see page 70), Y_1, Y_2, Y_{10}, Y_{20}, and θ_o all have zero means, and $H_6(j\omega)$ is the transient response (see page 78) that dies out as t increases, Equation (3.88) is reduced to

$$\Phi_{\theta\theta}(\omega) = |H_{Y_1}(j\omega)|^2\Phi_{Y_1Y_1}(\omega) + |H_{Y_2}(j\omega)|^2\Phi_{Y_2Y_2}(\omega) \qquad (3.89a)$$

$$+ H_{Y_1}(j\omega)H_{Y_2}^*(j\omega)\Phi_{Y_1Y_2}(\omega) + H_{Y_2}(j\omega)H_{Y_1}^*(j\omega)\Phi_{Y_2Y_1}(\omega)$$

Remembering from Equation (3.77) that $y_1 = h^{(i)}(x_1)$ and $y_2 = h^{(i)}(x_2)$ and in view of the complex relations of x_1 and x_2 are expressed by Equations (3.21) and (3.22), some engineering judgement must be allowed to reduce the cumbersome dependence of x_2 on θ, y_1, y_2 and θ_o. It is reasonable to assume that, for transport type aircraft, θ_o is small (i.e., Sin $\theta_o \approx$ tan $\theta_o \approx 0$, Cos $\theta_o \approx 1$) and the product terms of Equation (3.22) will be much smaller than x_1, or a + b. The following approximation for Equations (3.22) is permitted.

$$x_2 \simeq x_1 + (a+b) \tag{3.90}$$

The same assumption will reduce Equation (3.79) to

$$x_1(t) = ut \tag{3.91}$$

and therefore

$$x_2(t) = ut + (a+b) \tag{3.92}$$

For a given profile $y_1 = h^{(i)}(x_1)$ and $y_2 = h^{(i)}(x_2)$, both y_1 and y_2 can be transformed to

$$y_1 = Z^{(i)}(t) \tag{3.93}$$

$$y_2 = Z^{(i)}(t+c) \qquad c = a + b/u \tag{3.93b}$$

by a linear transformation governed by Equations (3.91) and (3.92). At this stage, it must be reminded that $h^{(i)}(x)$ is only a member function of $\{h(x)\}$ which is a stochastic process describing a collection of runway/taxiway roughnesses, at different constant taxi speeds (see page 86, and Chapter II, pages 9, 12). It is therefore expedient to write

$$Y_1 = \{Z^{(i)}(t)\} \tag{3.94a}$$

$$Y_2 = \{Z^{(i)}(t+c)\} \tag{3.94b}$$

In order to avoid the distinction between the covariance functions and autocorrelation functions of the given roughnesses, it is assumed that

$$E[Y_1] = E[Y_2] = E[X^{(i)}(t)] = E[Z^{(i)}(t+c)] = 0 \tag{3.95}$$

This assumption will not introduce any discrepancies for frequencies larger than zero and it is a general practice in the aeronautical field to remove linear and/or lower order trends to reduce contaminations from long wavelength unevenness. If this is done, the autocorrelation functions and covariance functions of Y_1 and Y_2 will be given by

$$R_{Y_1Y_1}(\tau) = E[Z^{(i)}(t)Z^{(i)}(t+\tau)] \tag{3.96a}$$

$$= \kappa_2[Z^{(i)}(t)Z^{(i)}(t+\tau)]$$

$$R_{Y_2Y_2}(\tau) = E[Z^{(i)}(t+c)Z^{(i)}(t+c+\tau)] \tag{3.96b}$$

$$= \kappa_2[Z^{(i)}(t+c)Z^{(i)}(t+c+\tau)]$$

if $Z^{(i)}(t)$ is also assumed weakly stationary. From Equations (3.96a) and (3.96b), it is obvious that $R_{Y_1Y_1}(\tau) = R_{Y_2Y_2}(\tau)$ since a stationary

time history is insensitive to a translation in time origin. There is no problem in removing the weakly stationary assumption and it can be achieved by simply replacing t by t_1, $t+\tau$ by t_2 in Equations (3.96a) and (3.96b), therefore

$$R_{Y_1Y_1}(t_1,t_2) = E[Z^{(i)}(t_1)Z^{(i)}(t_2)]$$

$$= \kappa_2[Z^{(i)}(t_1)Z^{(i)}(t_2)] \tag{3.97a}$$

$$R_{Y_2Y_2}(t_1,t_2) = E[Z^{(i)}(t_1+c)Z_1{}^{(i)}(t_2+c)]$$

$$= \kappa_2[Z^{(i)}(t_1+c)Z^{(i)}(t_2+c)] \tag{3.97b}$$

The ordinary and generalized power spectra of Y_1 and Y_2 are obtained by the single and double Fourier transforms, respectively. They are

$$\Phi_{Y_1Y_1}(\omega) = \frac{1}{2\pi}\int_{-\infty}^{\infty} R_{Y_1Y_1}(\tau)e^{-j\omega\tau}\,d\tau = \Phi_{Y_2Y_2}(\omega) \tag{3.98a}$$

$$\Phi_{Y_1Y_1}(\omega_1,\omega_2) = \frac{1}{(2\pi)^2}\int_{-\infty}^{\infty}\int \kappa_2[Z^{(i)}(t_1)Z^{(i)}(t_2)]e^{-j(\omega_1t_1-\omega_2t_2)}\,dt_1dt_2 \tag{3.98b}$$

$$\Phi_{Y_2Y_2}(\omega_1,\omega_2) = \frac{1}{(2\pi)^2}\int_{-\infty}^{\infty}\int \kappa_2[Z^{(i)}(t_1+c)Z^{(i)}(t_2+c)]e^{-j(\omega_1t_1-\omega_2t_2)}\,dt_1dt_2$$

$$= e^{j(\omega_1-\omega_2)c}\,\Phi_{Y_1Y_1}(\omega_1,\omega_2) \tag{3.98c}$$

The cross-correlation functions for Y_1 and Y_2 are expressed as

$$R_{Y_1Y_2}(\tau) = E[Z^{(i)}(t)Z^{(i)}(t+c+\tau)]$$

$$= R_{Y_1Y_1}(\tau+c) \tag{3.99a}$$

$$R_{Y_2Y_1}(\tau) = E[Z^{(i)}(t+c)Z^{(i)}(t+\tau)]$$

$$= R_{Y_1Y_1}(\tau-c) \tag{3.99b}$$

if Y_1 and Y_2 are assumed weakly stationary, and

$$R_{Y_1Y_2}(t_1,t_2) = \kappa_2[Z^{(i)}(t_1)Z^{(i)}(t_2+c)] \tag{3.99c}$$

$$R_{Y_2Y_1}(t_1,t_2) = \kappa_2[Z^{(i)}(t_1+c)Z^{(i)}(t_2)] \tag{3.99d}$$

if Y_1 and Y_2 are nonstationary. The corresponding cross-spectra for Y_1 and Y_2 are

$$\Phi_{Y_1Y_2}(\omega) = \frac{1}{2\pi}\int_{-\infty}^{\infty} R_{Y_1Y_1}(\tau+c)e^{-j\omega\tau}\,d\tau = e^{j\omega c}\,\Phi_{Y_1Y_1}(\omega) \tag{3.100a}$$

$$\Phi_{Y_2Y_1}(\omega) = \frac{1}{2\pi}\int_{-\infty}^{\infty} R_{Y_1Y_1}(\tau-c)e^{-j\omega\tau}\,d\tau = e^{-j\omega c}\Phi_{Y_1Y_1}(\omega) \tag{3.100b}$$

$$\Phi_{Y_1Y_2}(\omega_1,\omega_2) = \frac{1}{(2\pi)^2}\int_{-\infty}^{\infty}\int \kappa_2[Z^{(i)}(t_1)Z^{(i)}(t_2+c)]e^{-j(\omega_1 t_1-\omega_2 t_2)}dt_1dt_2$$

$$= \Phi_{Y_1Y_1}(\omega_1,\omega_2)e^{-j\omega_2 c} \qquad (3.100c)$$

$$\Phi_{Y_2Y_1}(\omega_1,\omega_2) = \frac{1}{(2\pi)^2}\int_{-\infty}^{\infty}\int \kappa_2[Z^{(i)}(t_1+c)Z^{(i)}(t_2)]e^{-j(\omega_1 t_1-\omega_2 t_2)}dt_1dt_2$$

$$= \Phi_{Y_1Y_1}(\omega_1,\omega_2)e^{j\omega_1 c} \qquad (3.100d)$$

Substituting Equations (3.98a), (3.100a), and (3.100b) into Equation (3.89), the output power spectrum for rotation is given by

$$\Phi_{\theta\theta}(\omega) = \{|H_{Y_1}(j\omega)|^2 + |H_{Y_2}(j\omega)|^2 + H_{Y_1}(j\omega)H^*_{Y_2}(j\omega)e^{j\omega c} \qquad (3.101a)$$

$$+ H_{Y_2}(j\omega)H^*_{Y_1}(j\omega)e^{-j\omega c}\}\Phi_{Y_1Y_1}(\omega)$$

$$= \{|H_{Y_1}(j\omega)|^2 + 2R[H_{Y_2}(j\omega)H^*_{Y_1}(j\omega)e^{-j\omega c}]$$

$$+ |H_{Y_2}(j\omega)|^2\}\Phi_{Y_1Y_1}(\omega)$$

The generalized output power spectrum for rotation is given by

$$\Phi_{\theta\theta}(\omega_1,\omega_2) = H_{Y_1}(\omega_1)H^*_{Y_1}(\omega_2)\Phi_{Y_1Y_1}(\omega_1,\omega_2) + H_{Y_2}(\omega_1)H^*_{Y_2}(\omega_2)$$

$$\Phi_{Y_2Y_2}(\omega_1,\omega_2) + H_{Y_1}(\omega_1)H^*_{Y_2}(\omega_2)\Phi_{Y_1Y_2}(\omega_1,\omega_2) +$$

$$H_{Y_2}(\omega_1)H^*_{Y_1}(\omega_2)\Phi_{Y_2Y_1}(\omega_1,\omega_2) \tag{3.89b}$$

Substituting Equations (3.98b), (3.98c), (3.100c) and (3.100d) into Equation (3.89b), the generalized output spectrum for rotation may be expressed as

$$\begin{aligned}\Phi_{\theta\theta}(\omega_1,\omega_2) = \{&H_{Y_1}(\omega_1)H^*_{Y_1}(\omega_2) + H_{Y_2}(\omega_1)H^*_{Y_2}(\omega_2)e^{j(\omega_1-\omega_2)c} \\ &+ H_{Y_1}(\omega_1)H^*_{Y_2}(\omega_2)e^{-j\omega_2 c} + H_{Y_2}(\omega_1)H^*_{Y_1}(\omega_3)e^{j\omega_1 c} \\ &\cdot \Phi_{Y_1Y_1}(\omega_1,\omega_2)\end{aligned} \tag{3.101b}$$

where $\Phi_{Y_1Y_1}(\omega)$ or $\Phi_{Y_1Y_1}(\omega_1,\omega_2)$ is the roughness spectrum derived in Chapter II, or Equations (2.56a,b; 2.57a,b).

CHAPTER IV

SUMMARY AND CONCLUSIONS

This study presents a new method of assessing aircraft dynamic loads resulting from ground operations based on existing roughness power spectral densities and given operational characteristics or mission profiles of the aircraft. A summary of the important aspects of the findings is given below. It is followed by a discussion of the conclusions which can be drawn fruitfully from the present investigation.

Summary

The major advantage of the present method is its universal adaptability to analyses of different natures. (See pp. 44-55). It is unified in the sense that the methodology requires no modification in its formulation to accommodate either stochastic or deterministic roughness profiles. The basis for this versatility lies in the fact that the shaping function $w_j(t-T_j)$ is completely general. (See page 28.)

For a deterministic runway, it is always possible to match the profile by both bumps and dips of known form (e. g., $\mathrm{Sin}[\pi(t-T_j)/a_j]$ $1 - \mathrm{Cos}\,[\pi(t-T_j)/a_j]$ etc.) with known strength A_j at each uneven locality. The assessment of arrival times for the bumps and dips is inconsequential, since they are derived a priori from the known record

(see page 35) in the form of time history Z(t) or a roughness profile $h^{(i)}(x)$. The cumulant functions of random points of Equations (2.34) are always obtainable from combinatorial analysis of the given record or complexion and its product densities from Equations (14) and (15) of Srinivasan, etc. [38]. For a one runway constant speed taxi analysis, Equation (2.53a), (2.53b), or (2.54) may be employed to calculate the input roughness spectrum which will have exactly the same result as obtained by Equation (2.3a) or (2.5a). It is interesting to note that Equations (2.56b) and (2.57b) are also applicable in obtaining the same result by the mere fact that $\bar{\sigma}^{-2}_{zz}(T_j) \neq 0$ for one and only one value of T_j.

Finally, it must be remembered that quantities appeared in Equations (2.56b) and (2.57b) are all available either from the existing roughness power spectral densities or the given record. The method requires no additional profile measuring or data collecting on the roughnesses, there might be some slight reprocessing of the power spectral densities in the event that the autocorrelation functions of the constituent roughnesses are not furnished together with the power spectral densities.

Conclusions

Due to the immense scheme of data compilation (see Figure 2.8), it is not possible at this phase of the study to present any numerical results upon which quantitative comparisons and conclusions can be drawn. However, some salient features that are not revealed in the

past are brought to light through this general approach with considerably less restrictions.

The central results for the composite roughness input spectrum is given by Equations (2.56a), (2.56b), (2.57a) and (2.57b). They have shown that a roughness input spectrum approach employing a narrow-band stationary Gaussian process yields an acceptable load exceedance curve expressed as (see Rich, etc. [51])

$$M(y) = \sum_{j=1}^{n} \frac{t_j}{t_T} N_{oj} e^{-y^2/2\sigma_{yj}^2} \frac{t_j}{t_T}, \quad \sum_{j=1}^{n} t_j = t_T \tag{4.1}$$

where the σ_{yj}'s are obtained from one runway with n discrete taxi speed segments at t_j seconds per segment, or given by Firebaugh [52] as

$$N(y) = \sum_{n=1}^{4} 2N_o TP_n e^{-(y/sR_n)} \tag{4.2}$$

where $R_n = \sigma_y/\sigma_{h_n}$ with σ_{h_n}'s equal to 0.2 in., 0.28 in., 0.41 in., and 0.57 in. for P_n's of 0.50, 0.32, 0.15, and 0.03, respectively. Equation (4.2) employs four types of roughnesses obtained empirically from 64 runways and 115 roughness power spectra (some of the runways are surveyed along the center line as well as lines parallel to the center line). The reason behind this inadvertent agreement is that the term $[g_1(T_j) + g_2(T_j,T_j)]$ in the single summation of Equations (2.56a), (2.56b), (2.57a), and (2.57b) are usually much larger than the terms

$[g_2(T_j,T_k)]$ or $[g_1(T_j) \cdot g_1(T_k) + g_2(T_j,T_k)]$ in the double summation of the respective equations if the T_j's and T_k's are not strongly correlated. This statement may be verified easily by assuming the arrival times being nonhomogeneous Poisson (see Equation (2.40)), then

$$[g_1(T_j) + g_2(T_j,T_j)] = g_1(T_j) = \lambda(T_j)$$

$$[g_2(T_j,T_k)] = 0$$

$$[g_1(T_j)g_1(T_k) + g_2(T_j,T_k)] = \lambda(T_j)\lambda(T_k) \qquad (4.3)$$

It is seen that $\lambda(T_j)\lambda(T_k) << \lambda(T_j)$, for $\lambda(T_k)$ and $\lambda(T_j) << 1$ so that the double summation is negligible if the arrival times are uncorrelated or T_j's and T_k's are far apart. This indicates that approximations of the kind expressed by Equations (4.1) and (4.2) are only valid for operations with mutually independent taxi events and the expressions from Equations (2.56a), (2.56b), (2.57a) and (2.57b) are the exact solutions with the interactions between different roughnesses included.

The output spectrum for the rotation θ is expressed by Equations (3.101a) and (3.101b). It is obvious that taxi speed does affect the transfer function through the terms

$$2\Re[H_{Y_2}(j\omega)H^*_{Y_1}(j\omega)e^{-j\omega c}]$$

in Equation (3.101a) and

$$[H_{Y_1}(\omega_1)H^*_{Y_2}(\omega_2)e^{-j\omega_2 c} + H_{Y_2}(\omega_1)H^*_{Y_1}(\omega_2)e^{-j\omega_1 c}$$

$$+ H_{Y_2}(\omega_1)H^*_{Y_2}(\omega_2)e^{j(\omega_1-\omega_2)c}]$$

in Equation (3.101b) since c = a+b/u where u is the taxi speed. This exemplifies the reason why the experimental transfer functions of [10,11,12,13,14] are not taxi speed insensitive. It is interesting to note that, for the stationary case of Equation (3.101a), the term

$$2R[H_{Y_2}(j\omega)H^*_{Y_1}(j\omega)e^{-j\omega c}]$$

tends to contribute more to the transfer function magnitudes for all frequencies as the taxi speed increases (i.e., $\lim_{c\to 0} e^{-j\omega c} = 1$). This is exactly the trend shown in Figures 14 and 19 of [13,14], respectively. The behavior of the transfer function in the generalized output spectrum is not clear since there are no existing double frequency transfer functions for aircraft responses. There are published data on single degree of freedom mass spring system (see [37,38,42]) but their comparisons to aircraft responses may not be readily seen.

In passing, it is also worth noting that the composite roughness spectra as represented by Equations (2.56a), (2.56b), (2.57a) and (2.57b) are the only existing analytical forms describing runway roughnesses by the variances ($\bar{\sigma}_{zz}$'s) of the constituent runways (see [51]) as well as the only existing roughness representation including

the interactions between runways (or bumps, etc.). It is therefore strongly felt that the results of this study are of significant importance in the advancement of power spectral methods in the aeronautical field.

APPENDICES

APPENDIX I

TRANSFORMATION OF AXES

The Eulerian angles are used as the parameters of transformation as proposed by Goldstein,* and following his notations, the transformation matrix [A] has the form given by

$$[A] = \begin{bmatrix} \text{Cos}\psi'\text{Cos}\phi' - \text{Cos}\theta'\text{Sin}\phi'\text{Sin}\psi' & \text{Cos}\psi'\text{Sin}\phi' + \text{Cos}\theta'\text{Cos}\phi'\text{Sin}\psi' & \text{Sin}\psi'\text{Sin}\theta' \\ -\text{Sin}\psi'\text{Cos}\phi' - \text{Cos}\theta'\text{Sin}\phi'\text{Cos}\psi' & -\text{Sin}\psi'\text{Sin}\phi' + \text{Cos}\theta'\text{Cos}\phi'\text{Cos}\psi' & \text{Cos}\psi'\text{Sin}\theta' \\ \text{Sin}\theta'\text{Sin}\phi' & -\text{Sin}\theta'\text{Cos}\phi' & \text{Cos}\theta' \end{bmatrix} \quad \text{(I-1)}$$

For the transformation of o-xyz axes to O-XYZ axes, let $\phi' = \theta_o + \theta$, $\theta' = \psi' = 0$, then Equation (I-1) becomes

$$[A^{XYZ}_{xyz}] = \begin{bmatrix} \text{Cos}(\theta_o+\theta) & \text{Sin}(\theta_o+\theta) & 0 \\ -\text{Sin}(\theta_o+\theta) & \text{Cos}(\theta_o+\theta) & 0 \\ 0 & 0 & 1 \end{bmatrix} \quad \text{(I-2)}$$

Therefore, the rotational transformation of the unit vectors $\bar{I}$, $\bar{J}$, $\bar{K}$ of the O-XYZ axes are obtained from the following multiplication.

$$\begin{Bmatrix} \bar{I} \\ \bar{J} \\ \bar{K} \end{Bmatrix} = \begin{bmatrix} A^{XYZ}_{xyz} \end{bmatrix} \begin{Bmatrix} \bar{i} \\ \bar{j} \\ \bar{k} \end{Bmatrix} \quad \text{(I-3a)}$$

---

*See [45], pp. 107-109.

or

$$\bar{I} = \cos(\theta_o+\theta)\bar{i} + \sin(\theta_o+\theta)\bar{j} \qquad \text{(I-3b)}$$

$$\bar{J} = -\sin(\theta_o+\theta)\bar{i} + \cos(\theta_o+\theta)\bar{j} \qquad \text{(I-3c)}$$

$$\bar{K} = \bar{k} \qquad \text{(I-3d)}$$

The transformation from the local axes 0_3-$X_3Y_3Z_3$ of a wing station "i" to the body axes 0-XYZ may be obtained by substituting $\phi' = \theta_{w_i}$, $\theta' = \rho_i$, and $\psi' = \psi_i$ into the inverse matrix of [A]. If this is done, the following result is obtained.

$$\begin{bmatrix} A^{XYZ} \\ X_3Y_3Z_3 \end{bmatrix} = [A]^{-1}$$

$$= \begin{bmatrix} \cos\theta_{w_i}\cos\psi_i - \cos\rho_i\sin\theta_{w_i}\sin\psi_i & -\sin\psi_i\cos\theta_{w_i} - \cos\rho_i\sin\theta_{w_i}\cos\psi_i & \sin\rho_i\sin\theta_{w_i} \\ \cos\psi_i\sin\theta_{w_i} + \cos\rho_i\cos\theta_{w_i}\sin\psi_i & -\sin\psi_i\sin\theta_{w_i} + \cos\rho_i\cos\theta_{w_i}\cos\psi_i & -\sin\rho_i\cos\theta_{w_i} \\ \sin\rho_i\sin\psi_i & \sin\rho_i\cos\psi_i & \cos\rho_i \end{bmatrix} \qquad \text{(I-4)}$$

If θ_{w_i}, ρ_i and ψ_i are assumed small (i.e., Cos x = 1, Sin x = x, for $x = \theta_{w_i}$, ρ_i, and ψ_i) and the quadratic terms $\theta_{w_i}\psi_i \cdots$ etc. are neglected, (I-4) can be reduced to

$$\begin{bmatrix} A^{XYZ}_{X_3Y_3Z_3} \end{bmatrix} = \begin{bmatrix} 1 & -\psi_i - \theta_{w_i} & 0 \\ \theta_{w_i} + \psi_i & 1 & \rho_i \\ 0 & \rho_i & 1 \end{bmatrix} \tag{I-5}$$

The angular velocity of wing station "i" may be expressed by

$$\begin{Bmatrix} \\ \Omega_{X_3Y_3Z_3} \\ \\ \end{Bmatrix} = \begin{Bmatrix} \dot{\rho}_i \bar{I}_1 \\ \dot{\phi}_i \bar{J}_2 \\ \dot{\theta}_{w_i} \bar{K}_3 \end{Bmatrix} \tag{I-6}$$

where $\dot{\rho}_i$, $\dot{\theta}_i$, $\dot{\theta}_{w_i}$ are, respectively, the rotational velocities about $OX(O_1X_1)$, $O_1Y_1(O_2Y_2)$, and O_3Z_3 axes when ρ_i, ϕ_i are small.

The angular velocities with respect to O-XYZ axes are therefore

$$\begin{Bmatrix} \\ \Omega_{XYZ} \\ \\ \end{Bmatrix} = \begin{Bmatrix} \delta_X \bar{I} \\ \omega_Y \bar{J} \\ \omega_2 \bar{K} \end{Bmatrix} = \begin{bmatrix} A^{XYZ}_{X_3Y_3Z_3} \end{bmatrix} \begin{Bmatrix} \dot{\rho}_i \bar{I}_1 \\ \dot{\phi}_i \bar{J}_2 \\ \dot{\theta}_{w_i} \bar{K}_3 \end{Bmatrix} \tag{I-7a}$$

or

$$\left.\begin{aligned} \omega_X \bar{I} &= \dot{\rho}_i \bar{I}_1 - (\psi_i + \theta_{w_i}) \dot{\phi}_i \bar{J}_2 \\ \omega_Y \bar{J} &= (\theta_{w_i} + \psi_i) \dot{\rho}_i \bar{I}_1 + \dot{\phi}_i \bar{J}_2 + \rho_i \dot{\phi}_i \bar{J}_2 \end{aligned}\right\} \tag{I-7b}$$

and

$$\omega_Z \bar{K} = \rho_i \dot{\phi}_i \bar{J}_2 + \dot{\theta}_{w_i} \bar{K}_3$$

If $\dot{\rho}_i$, $\dot{\phi}_i$, and θ_{w_i} are all small and their products with θ_{w_i}, ψ_i, and ρ_i are negligible, then Equations (I-7b) are reduced to

$$\left.\begin{aligned} \omega_X \bar{I} &= \dot{\rho}_i \bar{I}_1 \\ \omega_Y \bar{J} &= \dot{\phi}_i \bar{J}_2 \\ \omega_Z \bar{K} &= \dot{\theta}_{w_i} \bar{K}_3 \end{aligned}\right\} \qquad \text{(I-7c)}$$

To evaluate ω_X, ω_Y, and ω_Z from Equations (I-7c), one simply performs the following dot products:

$$\omega_X = \omega_X \bar{I} \cdot \bar{I} = \dot{\rho}_i \bar{I}_1 \cdot \bar{I} = \dot{\rho}_i \qquad \text{(I-8a)}$$

since, O_1-$X_1Y_1Z_1$ is only a translation of O-XYZ to each wing station "i", or $\bar{I}_1, \bar{J}_1, \bar{K}_1$ are identically $\bar{I}$, $\bar{J}$, and $\bar{K}$

$$\omega_Y = \omega_Y \bar{J} \cdot \bar{J} = \dot{\phi}_i \bar{J}_2 \cdot \bar{J} = \dot{\phi}_i (\cos \rho_i \bar{J}_1 + \sin \rho_i \bar{K}_1) \cdot \bar{J} = \dot{\phi}_i \qquad \text{(I-8b)}$$

where $\bar{J}_2 = \cos \rho_i \bar{J}_1 + \sin \rho_i \bar{K}_1$ results from a rotation ρ_i of the $O_1X_1Y_1Z_1$ axes are shown by Figure I-1.

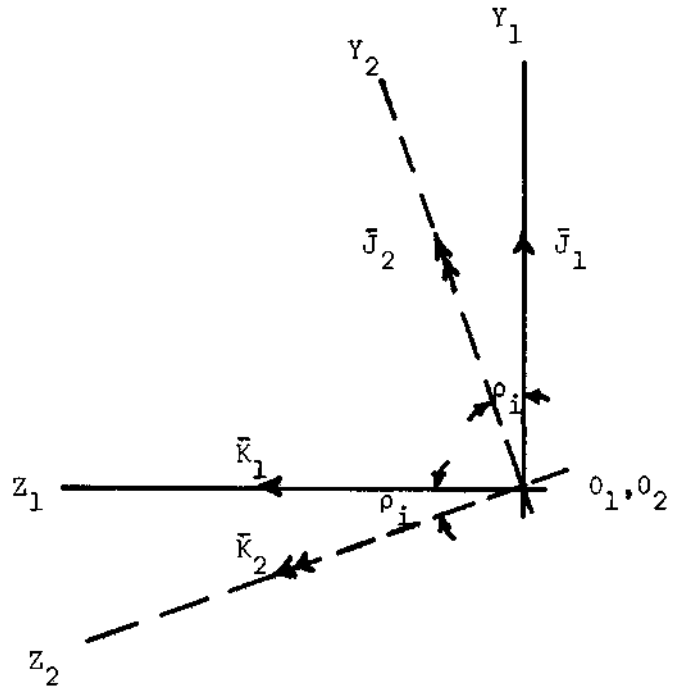

Figure I-1. Rotation of $O_2X_2Y_2Z_2$ Axes about O_1X_1

$$\omega_Z = \omega_Z \bar{K} \cdot \bar{K} = \dot{\theta}_{w_i} \bar{K}_3 \cdot \bar{K} = \dot{\theta}_{w_i} (\text{Cos } \phi_i \bar{K}_2 + \text{Sin } \phi_i \bar{I}_2) \bar{K} \qquad \text{(I-8c)}$$

$$= \dot{\theta}_{w_i} (\text{Cos } \phi_i \text{Cos } \rho_i \bar{K}_1 - \text{Cos } \phi_i \text{Sin } \rho_i \bar{J}_1 + \text{Sin } \phi_i \bar{I}_1) \bar{K}$$

$$= \dot{\theta}_{w_i} \qquad \text{(I-8c)}$$

where $\bar{K}_3 = \text{Cos } \phi_i \bar{K}_2 + \text{Sin } \phi_i \bar{I}_2$ is obtained from a rotation ϕ_i of the $O_2X_2Y_2Z_2$ axes as shown by Figure I-2.

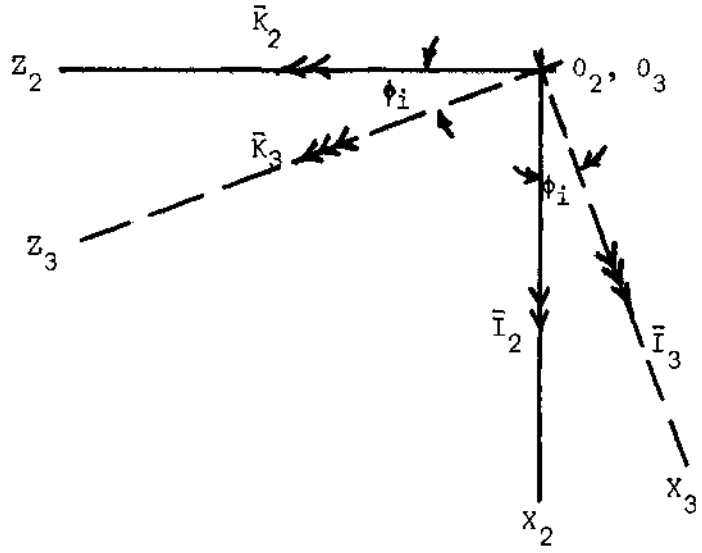

Figure I-2. Rotation of $O_3X_3Y_3Z_3$ Axes about O_2Y_2

Equations (I-8a), (I-8b), and (I-8c) are reflected in Equations (3.9), (3.10), and (3.11) of Chapter III (see pp. 65-66).

APPENDIX II

APPROXIMATION OF SOME TRIGONOMETRIC RELATIONS

Assume θ, y_1, and y_2 are all small such that the quadratic and higher order terms of their products may be neglected. The following results, then, remain valid.

$$\tan(\theta_o+\theta) \approx \frac{\theta + \tan\theta_o}{1 - \theta\tan\theta_o} = (\theta + \tan\theta_o)(1 + \theta\tan\theta_o + \cdots)$$

$$\approx (\theta + \tan\theta_o) + \theta\tan^2\theta_o = \theta(1 + \tan^2\theta_o) + \tan\theta_o$$

$$(a+b)[\tan(\theta_o+\theta) - \tan\theta_o] \approx (a+b)\theta(1+\tan^2\theta_o)$$

$$\approx \frac{(a+b)\theta}{\cos^2\theta_o} \qquad \text{(II-1)}$$

$$\frac{1}{\cos(\theta_o+\theta)} \approx \frac{1}{\cos\theta_o - \theta\sin\theta_o} = \frac{1}{\cos\theta_o(1-\theta\tan\theta_o)}$$

$$= \frac{1}{\cos\theta_o}(1 + \theta\tan\theta_o + \cdots)$$

$$\approx \frac{(1+\theta\tan\theta_o)}{\cos\theta_o}$$

$$\frac{(y_2-y_1)}{\cos(\theta_o+\theta)} \approx \frac{(y_2-y_1)(1+\theta\tan\theta_o)}{\cos\theta_o} \approx \frac{y_2-y_1}{\cos\theta_o} \qquad \text{(II-2)}$$

APPENDIX III

DIFFERENTIATION AND LINEARIZATION OF THE LAGRANGIANS AND DISSIPATION FUNCTIONS

The Lagrange's equations for $q_1 = x_1$ is obtained from the following development.

$$\frac{\partial L}{\partial \dot{q}_1} = \frac{\partial T}{\partial \dot{x}_1} = m_f[\dot{x}_1 - \dot{\theta}(e\cos\theta_o + a\sin\theta_o)] +$$

$$md \sum_{i=1}^{n} \{[\dot{x}_1\cos\theta_o + \dot{y}_1\sin\theta_o + \dot{U}_i - \dot{\theta}(e+V_i)]\cos\theta_o$$

$$- [-\dot{x}\sin\theta_o + \dot{y}_1\cos\theta_o + \dot{V}_1 + \dot{\theta}(a+U_i)]\sin\theta_o\}$$

$$\frac{d}{dt}\left(\frac{\partial L}{\partial \dot{q}_1}\right) = m_f[\ddot{x}_1 - \ddot{\theta}(e\cos\theta_o + a\sin\theta_o)] + md \sum_{i=1}^{n} \{[\ddot{x}_1\cos\theta_o$$

$$+ \ddot{y}_1\sin\theta_o + \ddot{U}_i - \ddot{\theta}(e+V_i) - \dot{\theta}\dot{V}_i]\cos\theta_o - [-\ddot{x}_1\sin\theta_o$$

$$+ \ddot{y}_1\cos\theta_o + \ddot{V}_i + \ddot{\theta}(a+U_i) + \dot{\theta}\dot{U}_i]\sin\theta_o\}$$

$$\frac{\partial L}{\partial q_1} = -\frac{\partial V}{\partial x_1} = 0, \qquad \frac{\partial F}{\partial \dot{q}_1} = 0$$

Let $\underset{\substack{n\to\infty \\ d\to dZ}}{L}\ m_f + nmd = m_f + m_w = M$, then the above equations give

$$M[\ddot{x}_1 - \ddot{\theta}(e\cos\theta_o + a\sin\theta_o)] + m[\cos\theta_o \int_{-L}^{L} \ddot{U}dZ - \sin\theta_o \cdot$$

$$\int_{-L}^{L} \ddot{V}dZ] = \lambda_1 \frac{\partial h}{\partial x_1} - \lambda_2 \frac{\partial h}{\partial x_2} + \lambda_3 \qquad \text{(III-1)}$$

The Lagrange's equation for $q_2 = y_1$ is given by the following steps.

$$\frac{\partial L}{\partial \dot{q}_2} = \frac{\partial T}{\partial \dot{y}_1} = m_f[\dot{y}_1 + \dot{\theta}(a\cos\theta_o - e\sin\theta_o)] + md \sum_{i=1}^{n} \{[\dot{x}_1\cos\theta_o$$

$$+ \dot{y}_1\sin\theta_o + \dot{U}_i - \dot{\theta}(e+V_i)]\sin\theta_o + [-\dot{x}_1\sin\theta_o + \dot{y}_1\cos\theta_o$$

$$+ \dot{V}_i + \dot{\theta}(a+U_i)]\cos\theta_o\}$$

$$\frac{d}{dt}\left(\frac{\partial L}{\partial \dot{q}_2}\right) = m_f[\ddot{y}_1 + \ddot{\theta}(a\cos\theta_o - e\sin\theta_o)] + md \sum_{i=1}^{n} \{[\ddot{x}_1\cos\theta_o$$

$$+ \ddot{y}_1\sin\theta_o + \ddot{U}_i - \ddot{\theta}(e+V_i) - \dot{\theta}\dot{V}_i]\sin\theta_o + [-\ddot{x}_1\sin\theta_o$$

$$+ \ddot{y}_1\cos\theta_o + \ddot{V}_i + \ddot{\theta}(a+U_i) + \dot{\theta}\dot{U}_i]\cos\theta_o\}$$

$$\frac{\partial L}{\partial q_2} = -\frac{\partial V}{\partial y_1} = -\frac{k}{\cos^2\theta_o}\left[\frac{(a+b)\theta}{\cos\theta_o} + y_1 - y_2\right]$$

$$\frac{\partial F}{\partial \dot{q}_2} = \frac{\partial F}{\partial \dot{y}_1} = \frac{c}{\cos^2\theta_o}\left[\frac{(a+b)\dot{\theta}}{\cos\theta_o} + \dot{y}_1 - \dot{y}_2\right] \quad \text{for} \quad \underset{d\to dZ}{\underset{n\to\infty}{L}} \; m_f + nmd = M$$

these quantities give

$$M[\ddot{y}_1 + \ddot{\theta}(a\cos\theta_o - e\sin\theta_o)] + m[\sin\theta_o \int_{-L}^{L} \ddot{U}dZ + \cos\theta_o \int_{-L}^{L} \ddot{V}dZ]$$

$$+ \frac{1}{\cos^2\theta_o}\{k\left[\frac{(a+b)\theta}{\cos\theta_o} + y_1 - y_2\right] + c\left[\frac{(a+b)\dot{\theta}}{\cos\theta_o} + \dot{y}_1 - \dot{y}_2\right]\}$$

$$= \lambda_1 - \lambda_2 \frac{\partial h}{\partial x_2}\tan\theta_o \qquad \text{(II-2)}$$

The Lagrange's equation for $q_3 = y_2$ may be obtained from the following development.

$$\frac{\partial L}{\partial \dot{q}_3} = \frac{\partial T}{\partial \dot{y}_2} = 0, \quad \frac{d}{dt}\left(\frac{\partial L}{\partial \dot{q}_3}\right) = 0$$

$$\frac{\partial L}{\partial q_3} = -\frac{\partial V}{\partial y_2} = \frac{k}{\cos^2\theta_o}\left[\frac{(a+b)\theta}{\cos\theta_o} - y_2 + y_1\right]$$

$$\frac{\partial F}{\partial \dot{q}_3} = \frac{\partial F}{\partial \dot{y}_2} = \frac{-c}{\cos^2\theta_o}\left[\frac{(a+b)\dot{\theta}}{\cos\theta_o} + \dot{y}_1 - \dot{y}_2\right]$$

and these quantities give

$$-\frac{1}{\cos^2\theta_\theta}\left\{k\left[\frac{(a+b)\theta}{\cos\theta_o} + y_1 - y_2\right] + c\left[\frac{(a+b)\dot{\theta}}{\cos\theta_o} + \dot{y}_1 - \dot{y}_2\right]\right\}$$

$$= \lambda_2\left(\frac{\partial h}{\partial x_2}\tan\theta_o + 1\right) \qquad \text{(III-3)}$$

The Lagrange's equation for $q_4 = \theta$ is obtained by calculating the following quantities.

$$\frac{\partial L}{\partial \dot{q}_4} = \frac{\partial T}{\partial \dot{\theta}} = m_f[\dot{\theta}(e^2+a^2) - \dot{x}_1(e\cos\theta_o + a\sin\theta_o) + \dot{y}_1[a\cos\theta_o - e\sin\theta_o)] + I_{m_f}\dot{\theta} + md\sum_{i=1}^{n}\{-[\dot{x}_1\cos\theta_o + \dot{y}_1\sin\theta_o + \dot{U}_i - \dot{\theta}(e+V_i)]e + [-\dot{x}_1\sin\theta_o + \dot{y}_1\cos\theta_o + \dot{V}_i + \dot{\theta}(a+U_i)]a\} + I_{ZZ}d\sum_{i=1}^{n}(\dot{\theta}+\dot{\theta}_{w_i})$$

$$\frac{d}{dt}\left(\frac{\partial L}{\partial \dot{q}_4}\right) = m_f[\ddot{\theta}(a^2+e^2) - \ddot{x}_1(e\cos\theta_o + a\sin\theta_o) + \ddot{y}_1(a\cos\theta_o - e\sin\theta_o)] + I_{m_f}\ddot{\theta} + m_w[-\ddot{x}(e\cos\theta_o + a\sin\theta_o)$$

$$+ \ddot{y}_1(a\cos\theta_o - e\sin\theta_o)] + m[a\int_{-L}^{L} \ddot{V}dZ - e\int_{-L}^{L} \ddot{U}dZ]$$

$$+ I_{ZZ}(2L\ddot{\theta} + \int_{-L}^{L} \ddot{\theta}_w dZ)$$

$$\frac{\partial L}{\partial q_4} = -\frac{\partial V}{\partial \theta} = -\frac{k}{\cos^2\theta_o}\left[\frac{(a+b)\theta}{\cos\theta_o} + y_1 - y_2\right]\frac{(a+b)}{\cos\theta_o}$$

$$\frac{\partial F}{\partial \dot{q}_4} = \frac{\partial F}{\partial \dot{\theta}} = \frac{c}{\cos^2\theta_o}\left[\frac{(a+b)\dot{\theta}}{\cos\theta_o} + \dot{y}_1 - \dot{y}_2\right]\frac{(a+b)}{\cos\theta_o}$$

Let $m_f + m_w = M$; the above quantities give

$$[Ma^2 + (m_f - m_w)e^2 + I_{m_f} + 2LI_{ZZ}]\ddot{\theta} - M[\ddot{x}_1$$

$$(e\cos\theta_o + a\sin\theta_o) - \ddot{y}_1(a\cos\theta_o - e\sin\theta_o)] + m[a\int_{-L}^{L} \ddot{V}dZ$$

$$- e\int_{-L}^{L} \ddot{U}dZ] + I_{ZZ}\int_{-L}^{L} \ddot{\theta}_w dZ + \frac{1}{\cos^2\theta_o}\{k\left[\frac{(a+b)\theta}{\cos\theta_o} + y_1 - y_2\right]$$

$$+ c\left[\frac{(a+b)\dot{\theta}}{\cos\theta_o} + \dot{y}_1 - \dot{y}_2\right]\} = -\lambda_2\frac{\partial h}{\partial x_2}\frac{(a+b)\tan\theta_o}{\cos\theta_o} - \lambda_3(e\cos\theta_o$$

$$+ a\sin\theta_o) \qquad \text{(III-4)}$$

The Lagrange's equation for $q_{i+4} = U_i$, $i = 1,2,\cdots,n$ is obtained from the following development.

$$\frac{\partial L}{\partial \dot{q}_{i+4}} = \frac{\partial T}{\partial U_i} = md[\dot{x}_1 \text{Cos}\theta_o + \dot{y}_1 \text{Sin}\theta_o + \dot{U}_i - \dot{\theta}(e+U_i)]$$

$$+ d\left[\frac{(\dot{U}_i - \dot{U}_{i+1})}{d^2} I_{YY} - \frac{(\dot{U}_{i-1} - \dot{U}_i)}{d^2} I_{YY}\right]$$

$$\frac{d}{dt}\left(\frac{\partial L}{\partial \dot{U}_i}\right) = m_d[\ddot{x}_1 \text{Cos}\theta_o + \ddot{y}_1 \text{Sin}\theta_o + \ddot{U}_i - \ddot{\theta}e]$$

$$+ \frac{d}{dt}\left\{dI_{YY} \frac{1}{d^2}[(\dot{U}_i - \dot{U}_{i+1}) - (\dot{U}_{i-1} - \dot{U}_i)]\right\}$$

$$= md[\ddot{x}_1 \text{Cos}\theta_o + \ddot{y}_1 \text{Sin}\theta_o + \ddot{U}_i - \ddot{\theta}e]$$

$$+ dI_{YY} \frac{2\ddot{U}_i - \ddot{U}_{i+1} + \ddot{U}_{i-1}}{d^2}$$

$$\underset{d \to 0}{\lim} \frac{1}{d} \frac{d}{dt}\left(\frac{\partial L}{\partial \dot{U}_i}\right) = md[\ddot{x}_1 \text{Cos}\theta_o + \ddot{y}_1 \text{Sin}\theta_o + \ddot{U} - \ddot{\theta}e]$$

$$- I_{YY} \frac{\partial^4 U_i}{\partial t^2 \partial z^2} *$$

$$- \frac{\partial L}{\partial q_{i+4}} = \frac{\partial V}{\partial U_i} = dA\{(U_{i+1} + U_{i-1} - 2U_i) \cdot -2 + (U_{i+2} + U_i$$

$$- 2U_{i+1}) + (U_i + U_{i-2} - 2U_{i-1})\} \frac{1}{d^4}$$

---

*See [48], p. 242.

$$= dA \frac{(U_{i+2} - 4U_{i+1} + 6U_i - 4U_{i-1} + U_{i-2})}{d^4}$$

$$\lim_{d \to 0} \frac{1}{d} \frac{\partial V}{\partial U_i} = A \frac{\partial^4 U_i}{\partial Z^4} \quad *$$

$$\frac{\partial F}{\partial \dot{q}_{i+4}} = \frac{\partial F}{\partial U_i} = 0$$

These quantities give

$$m[\ddot{x}_1 \mathrm{Cos}\theta_o + \ddot{y}_1 \mathrm{Sin}\theta_o + \ddot{U} - \ddot{\theta} e] - I_{YY} \frac{\partial^4 U}{\partial t^2 \partial z^2} + A \frac{\partial^4 U}{\partial z^4}$$

$$= 0 \qquad \text{(III-5)}$$

where "i" is dropped in view of $d \to 0$, U becomes continuous from -L to L.

The Lagrange's equation for $q_{i+4+n} = V_i$, $i=1,2,\cdots,n$ is obtained from the following quantities:

$$\frac{\partial L}{\partial \dot{q}_{i+4+h}} = \frac{\partial T}{\partial \dot{V}_i} = md[-\dot{x}_1 \mathrm{Sin}\theta_o + \dot{y}_1 \mathrm{Cos}\theta_o + \dot{V}_i + \dot{\theta}(a + U_i)]$$

---

*See [48], p. 242.

$$+ dI_{XX} \frac{-(\dot{V}_{i+1}-\dot{V}_i) + (\dot{V}_i-\dot{V}_{i-1})}{d^2}$$

$$\frac{d}{dt}\left(\frac{\partial L}{d\dot{q}_{i+4+n}}\right) = md[-\ddot{x}_1 \sin\theta_o + \ddot{y}_1 \cos\theta_o + \ddot{U}_i + \ddot{\theta}a]$$

$$+ dI_{XX}\left(\frac{-\ddot{V}_{i+1} + 2\ddot{V}_i - \ddot{V}_{i-1}}{d^2}\right)$$

$$\underset{d\to 0}{L} \frac{1}{d}\frac{d}{dt}\left(\frac{\partial L}{\partial \dot{V}_i}\right) = m[-\ddot{x}_1 \sin\theta_o + \ddot{y}_1 \cos\theta_o + \ddot{V}_i + \ddot{\theta}a]$$

$$- I_{XX} \frac{\partial^4 V_i}{\partial^2 t \partial Z^2}$$

$$- \frac{\partial L}{q_{i+4+n}} = \frac{\partial V}{\partial V_i} = dB\{(V_{i+1}+V_{i-2}-2V_i) - 2 + (V_{i+2}+V_i$$

$$- 2V_{i+1}) + (V_i+V_{i-2}-2V_{i-1})\} \frac{1}{d^4}$$

$$\underset{d\to 0}{L} \frac{1}{d}\frac{\partial V}{\partial V_i} = B \frac{\partial^4 V_i}{\partial Z^4}$$

$$\frac{\partial F}{\partial \dot{V}_i} = 0.$$

Combining these quantities and suppressing i, the following equation is obtained.

$$m[-\ddot{x}_1 \mathrm{Sin}\theta_o + \ddot{y}_1 \mathrm{Cos}\theta_o + \ddot{V} + \ddot{\theta}a] - I_{XX} \frac{\partial^4 V}{\partial^2 t \partial Z^2} + B \frac{\partial^4 V}{\partial Z^4} = 0 \qquad \text{(III-6)}$$

The Lagrange's equation for $q_{i+4+2n} = w_i \quad i=1,2,\cdots,n$ is obtained from evaluating the quantities

$$\frac{\partial L}{\partial \dot{q}_{i+4+2h}} = \frac{\partial T}{\partial \dot{w}_i} = m d \dot{w}_i$$

$$\frac{d}{dt}\left(\frac{\partial L}{\partial \dot{w}_i}\right) = m d \ddot{w}_i$$

$$-\frac{\partial L}{\partial q_{i+4+2n}} = \frac{\partial V}{\partial w_i} = 0, \quad \frac{\partial F}{\partial \dot{q}_{i+4+2n}} = \frac{\partial F}{\partial \dot{w}_i} = 0$$

or

$$\ddot{w} = 0 \qquad \text{(III-7)}$$

The Lagrange's equation for $q_{i+4+3n} = \theta_{w_i}$, $i=1,2,\cdots,h$ is obtained from the following quantities.

$$\frac{\partial L}{\partial \dot{q}_{i+4+3n}} = \frac{\partial I}{\partial \dot{\theta}_{w_i}} = dI_{ZZ}(\dot{\theta} + \dot{\theta}_{w_i})$$

$$\frac{d}{dt}\left(\frac{\partial L}{\partial \dot{q}_{i+4+3n}}\right) = dI_{ZZ}(\ddot{\theta}+\ddot{\theta}_{w_i})$$

$$-\frac{\partial L}{\partial q_{i+4+3n}} = \frac{\partial V}{\partial \theta_{w_i}} = dC\left(\frac{(\theta_{w_{i+1}} - \theta_{w_i}) - 1 + (\theta_{w_i} - \theta_{w_{i-1}})}{d^2}\right)$$

$$\lim_{d\to 0} \frac{1}{d}\frac{\partial V}{\partial \theta_{w_i}} = -C\frac{\partial^2 \theta_{w_i}}{\partial Z^2}$$

$$\frac{\partial F}{\partial \dot{q}_{i+4+3n}} = \frac{\partial F}{\partial \theta_{w_i}} = 0,$$

therefore

$$I_{ZZ}(\ddot{\theta}+\ddot{\theta}_w) - C\frac{\partial^2 \theta_w}{\partial Z^2} = 0 \qquad \text{(III-8)}$$

APPENDIX IV

DERIVATION FOR THE IMPULSE RESPONSE FUNCTION $h_n(t,\tau)$

Let $h_n(t,\tau)$ be the impulse response function of a given undamped system, then

$$\ddot{h}_n(t,\tau) + \omega_n^2 h(t,\tau) = \delta(t-\tau)$$

or

$$\int_0^{t'} d\dot{h}_n(t,\tau) + \omega_n^2 \int_0^{t'} h(t,\tau)dt = \int_0^{t'} \delta(t-\tau)dt \qquad \text{(IV-1)}$$

It is further required that

$$\dot{h}_n(\tau,\tau) = 1 \quad \text{and} \quad h(\tau,\tau) = 0 \qquad \text{(IV-2)}$$

Equations (IV-2) and (IV-1) are always compatible for $\omega_n^2 > 0, t'>0$. Assume

$$h_n(t,\tau) = A(\tau)\text{Cos}\omega_n t + B(\tau)\text{Sin}\omega_n t \qquad \text{(IV-3)}$$

then

$$\dot{h}_n(t,\tau) = -\omega_n(A(\tau)\text{Sin}\omega_n t - B(\tau)\text{Cos}\omega_n t) \qquad \text{(IV-4)}$$

Substituting Equation (IV-2) into Equations (IV-3) and (IV-4), the following has to hold

$$\left.\begin{aligned} A(\tau)\mathrm{Cos}\omega_n\tau + B(\tau)\mathrm{Sin}\omega_n\tau &= 0 \\ A(\tau)\mathrm{Sin}\omega_n\tau - B(\tau)\mathrm{Cos}\omega_n\tau &= -1/\omega_n \end{aligned}\right\} \qquad \text{(IV-5)}$$

which give

$$A(\tau) = \frac{\begin{vmatrix} 0 & \mathrm{Sin}\omega_n\tau \\ -\frac{1}{\omega_n} & \mathrm{Cos}\omega_n\tau \end{vmatrix}}{\begin{vmatrix} \mathrm{Cos}\omega_n\tau & \mathrm{Sin}\omega_n\tau \\ \mathrm{Sin}\omega_n\tau & -\mathrm{Cos}\omega_n\tau \end{vmatrix}} = -\frac{1}{\omega_n}\,\mathrm{Sin}\;\omega_n\tau$$

$$B(\tau) = \frac{\begin{vmatrix} \mathrm{Cos}\omega_n\tau & 0 \\ \mathrm{Sin}\omega_n\tau & -\frac{1}{\omega_n} \end{vmatrix}}{\begin{vmatrix} \mathrm{Cos}\omega_n\tau & \mathrm{Sin}\omega_n\tau \\ \mathrm{Sin}\omega_n\tau & -\mathrm{Cos}\omega_n\tau \end{vmatrix}} = \frac{1}{\omega}\,\mathrm{Cos}\omega_n\tau$$

therefore

$$h_n(t,\tau) = \frac{1}{\omega_n}\left(-\mathrm{Sin}\omega_n\tau\mathrm{Cos}\omega_n t + \mathrm{Cos}\omega_n\tau\mathrm{Sin}\omega_n t\right)$$

$$= \frac{1}{\omega_n}\,\mathrm{Sin}\;\omega_n(t-\tau) \qquad \text{(IV-6)}$$

LITERATURE CITED

1. H. W. Liepmann, "On the Application of Statistical Concepts to the Buffeting Problem," *Journal of the Aerospace Science*, Vol. 19, No. 12, Dec., 1952, pp. 793-800.

2. H. Press and B. Mazelsky, "A Study of the Application of Power Spectral Methods of Generalized Harmonic Analysis to Gust Loads on Airplanes, *NACA TN 2853*, 1953.

3. Y. C. Fung, "Statistical Aspects of Dynamic Loads," *Journal of the Aerospace Science*, Vol. 20, No. 5, May, 1953, pp. 317-329.

4. Y. C. Fung, "The Analysis of Dynamic Stresses in Aircraft Structures During Landing as Nonstationary Random Processes," *Journal of Applied Mechanics*, Vol. 22, Trans. ASME Vol. 77, 1955, p. 449.

5. R. E. Bieber, "Missile Structural Loads by Nonstationary Statistical Methods," *Jour. of Aero. Sci.*, Vol. 28, April, 1961, pp. 284-294.

6. Y. K. Lin, "Nonstationary Response of Continuous Structures to Random Loading," *Journal of the Acoustical Society of America*, Vol. 35, No. 2, February, 1963, pp. 222-227.

7. J. L. Bogdanoff, J. E. Goldberg, and M. C. Bernard, "Response of a Simple Structure to a Random Earthquake-Type Disturbance," *Bulletin of the Seismological Society of America*, Vol. 51, 1961, p. 293.

8. E. Rosenblueth and J. I. Bustamante, "Distribution of Structural Response to Earthquakes," *American Society of Civil Engineering*, EM 3, 1962, p. 75.

9. J. H. Walls, J. C. Houbolt, and H. Press, "Some Measurements and Power Spectra of Runway Roughness," *NACA TN 3305*, 1954.

10. J. C. Houbolt, J. H. Walls, and R. F. Smiley, "On Spectral Analysis of Runway Roughness and Loads Developed During Taxiing," *NACA TN 3484*, 1955.

11. G. H. Grimes, "Development of a Method and Instrumentation for Evaluation of Runway Roughness Effect on Military Aircraft," *AGARD Report 119*, May 1957.

12. G. J. Morris and J. W. Stickle, "Response of a Light Airplane to Roughness of Unpaved Runway," *NASA TN D-510*, 1960.

13. G. J. Morris, "Response of a Jet Trainer Aircraft to Roughness of Three Runways," *NASA TN D-1203*, 1964.

14. G. J. Morris, "Response of a Turbojet and a Piston-Engine Transport Airplane to Runway Roughness," *NASA TN D-3161*, 1965.

15. W. E. Thompson, "Measurements and Power Spectra of Runway Roughness at Airports in Countries of the North Atlantic Treaty Organization," *NACA TN 4303*, 1958.

16. J. C. Houbolt, "Runway Roughness Studies in the Aeronautical Field," Proceedings ASCE, *Journal of the Air Transport Division*, Vol. 87, No. AT 1, March, 1961, pp. 11-31.

17. T. L. Coleman and A. W. Hall, "Implications of Recent Investigations on Runway Roughness Criteria," *AGARD Report 416*, January, 1963.

18. B. H. Groomes, "Sod and Matted Landing Surface Roughness Characteristics," Air Force Flight Dynamics Lab, Research and Technology Division, Wright-Patterson AFB, Ohio. Report No. FDDS-TM-64-32, January, 1964.

19. G. J. Morris and A. W. Hall, "Recent Studies of Runway Roughness," *NASA SP-83*, 1965, pp. 1-5.

20. A. W. Hall and S. Kopelson, "The Location and Simulated Repair of Roughness Areas of a Given Runway by an Analytical Method," *NASA TN D-1486*, December, 1962.

21. C. C. Tung, J. Penzien, and R. Horonjeff, "The Effect of Runway Unevenness on the Dynamic Response of Supersonic Transports," *NASA CR-119*, October, 1964.

22. H. P. Y. Hitch, "The Behavior of Aircraft on Rudimentary Airstrips," presented at the Symposium on the Noise and Loading Actions of Helicopters, *VSTOL Aircraft and Ground Effect Machines*, September, 1965, at the Institute of Sound and Vibration Research of the University of Southampton.

23. E. E. Hahn, "Design Criteria for Ground-Induced Dynamic Loads," *RTD-TDR-63-4139*, Vol. I, Vol. II, AF Flight Dynamics Laboratory, Research and Technology Division, Air Force Systems Command, Wright-Patterson AFB, Ohio, November, 1963.

24. Y. K. Lin, "Response of a Nonlinear Flat Panel to Periodic and Randomly-Varying Loadings," *J. Aerosp. Sci.*, Vol. 29, September, 1962, pp. 1029-1033.

25. T. K. Caughey, "Derivation and Application of the Fokker-Plank Equation to Discrete Nonlinear Dynamic Systems Subjected to White Random Excitation," *J. Acoust. Soc. of Am.*, Vol. 35, No. 11, November, 1963.

26. S. H. Crandall, "Perturbation Techniques for Random Vibration of Nonlinear Systems," *J. Acoust. Soc. of Am.*, Vol. 35, No. 11, Nov., 1963.

27. T. K. Caughey, "Equivalent Linearization Techniques," *J. Acoust. Soc. of Am.*, Vol. 35, No. 11, November, 1963.

28. G. R. Khabbaz, "Power Spectral Density of the Response of a Nonlinear System to Random Excitation," *J. Acoust. Soc. of Am.*, Vol. 38, 1965, pp. 847-850.

29. C. C. Tung, "The Effect of Runway Roughness on the Dynamic Response of Airplanes," *Journal of Sound and Vibration*, 5 (1): 1964-172 (1967).

30. T. K. Caughey and H. J. Stumpf, "Transient Response of a Dynamic System under Random Excitation," *Journal of Applied Mechanics*, Vol. 28, Trans. ASME, Series E, Vol. 83, 1961, p. 563.

31. B. F. Kur'yanov, "'Normalized' Spectra of Random Processes," *Soviet Physics-Acoustics*, Vol. 11, No. 2, Oct.-Dec., 1965, pp. 159-162.

32. Y. K. Lin, "Application of Nonstationary Shot Noise in the Study of System Response to a Class of Nonstationary Excitations," *J. Appl. Mech.*, Series E, Vol. 30, Dec., 1963, pp. 555-558.

33. Y. K. Lin, "On Nonstationary Shot Noise," *J. Acoust. Soc. Am.*, Vol. 36, 1964, pp. 82-84.

34. Y. K. Lin, "Nonstationary Excitation and Response on Linear Systems Treated as Sequences of Random Pulses," *J. Acoust. Soc. Am. 38(3)*, 1965, pp. 453-460.

35. J. C. Houbolt, "Interpretation and Design Application of Power Spectral Gust Response Analyses Result," *Proceedings of AIAA/ ASME Seventh Structures and Materials Conference*, Cocoa Beach, Fla., 1966, p. 83.

36. J. H. Laning, Jr. and R. H. Battin, *Random Processes Automatic Control*, McGraw-Hill, New York, 1956, pp. 63-65.

37. J. B. Roberts, "The Response of Linear Vibratory Systems to Random Impulses," *J. Sound Vib.*, 2(4), 375-390 (1965).

38. S. K. Srinivasan, R. Subramanian, and S. Kumaraswamy, "Response of Linear Vibratory Systems to Nonstationary Stochastic Impulses," *J. Sound Vib.*, 6(2), 169-179 (1967).

39. A. Papoulis, *Probability, Random Variables, and Stochastic Processes*, McGraw-Hill, New York, 1965, pp. 178-179.

40. H. Cramér, *Mathematical Methods of Statistics*, Princeton, Princeton, N. J., 1946, pp. 185-187.

41. M. S. Bartlett, *Stochastic Processes*, Cambridge University Press, 1955, pp. 78-80.

42. J. B. Roberts, "On the Harmonic Analysis of Evolutionary Random Vibration," *J. Sound Vib.*, 2(3), 336-352 (1965).

43. J. S. Bendat, L. D. Enochson, G. H. Klein, and A. G. Piersol, "Advanced Concepts of Stochastic Processes and Statistics for Flight Vehicle Vibration Estimation and Measurement," ASD-TOR-62-973, Aeronautical Systems Division, Wright-Patterson Air Force Base, 1962, pp. 4-7.

44. W. B. Davenport, Jr. and W. L. Root, *An Introduction to the Theory of Random Signals and Noise*, McGraw-Hill, New York, 1958, pp. 368.

45. H. Goldstein, *Classical Mechanics*, Addison-Wesley Publishing Co., Inc., Reading, Mass., 1959, pp. 347-350.

46. R. H. Scanlan and R. Rosenbaum, *Introduction to the Study of Aircraft Vibration and Flutter*, MacMillan Co., New York, 1962, pp. 85-88.

47. R. L. Bisplinghoff, H. Ashley, and R. L. Halfman, *Aeroelasticity*, Addison-Wesley Publishing Co., Inc., Cambridge, Mass., 1955, pp. 813-817.

48. R. N. DeG. Allen, *Relaxation Methods in Engineering and Science*, McGraw-Hill Book Co., Inc., New York, 1954, p. 241.

49. H. M. James, N. B. Nichols, and R. S. Phillips, *Theory of Servomechanisms*, McGraw-Hill Book Co., Inc., 1947, Chapter 2.

50. S. H. Crandall and W. D. Mark, *Random Vibration in Mechanical Systems*, Academic Press, New York, 1963, pp. 56-61.

51. M. J. Rich, I. J. Kenigsberg, M. H. Israel, and P. P. Cook, "Power Spectral Density Analysis of V/STOL Aircraft Structures,"

presented at the 24th Annual National Forum of the American Helicopter Society, May, 1968.

52. J. M. Firebaugh, "Estimation of Taxi Load Exceedances Using Power Spectral Methods," *Journal of Aircraft,* Vol. 5, No. 5, September-October, 1968, pp. 507-509.